이학박사 학위논문

Studies on the molecular mechanism during the acquisition of thermotolerance in *Arabidopsis*

애기 장대 고온저항성 획득에서 분자 작동원리에 대한 연구

2021년 2월

서울대학교 대학원

화학부

한신희

Studies on the molecular mechanism during the acquisition of thermotolerance in *Arabidopsis*

애기 장대 고온저항성 획득에서
분자 작동원리에 대한 연구

지도교수 박 충 모

이 논문을 이학박사 학위논문으로 제출함
2021년 01월
서울대학교 대학원
화학부
한 신 희

한신희의 박사학위논문을 인준함
2021년 1월

위 원 장 서 필 준 (인)
부 위 원 장 박 충 모 (인)
위 원 이 형 호 (인)
위 원 강 상 규 (인)
위 원 김 정 원 (인)

ABSTRACT

In nature, plants continuously exposed to unfavorable conditions. Heat is one of the major stress which affects to plant growth and development. Especially, it has been widely reported in recent decades that global warming is accelerated and widely affects to crop productivity. In this sense, it is essential that I extend understanding on molecular mechanism of thermotolerance.

Heat shock has deleterious effects on the cell by protein unfolding and unspecific aggregation. In addition, heat shock triggers disruption of the cytoskeleton that cause the loss of the correction localization of organelles and collapse of intracellular transport process. One of the detrimental effects of heat shock-induced oxidative stress in plants is genetic disturbance that is caused by the induction of DNA damages and the inhibition of DNA repair activity.

Therefore, plants possess various mechanisms to cope with damage of cells caused by heat stress. It has been previously reported that the transcription level of heat shock responsive genes in plants is increased by heat stress. The HEAT SHOCK PROTEINs (HSPs) and the HEAT SHOCK FACTORs (HSFs) are major constituents of the heat shock regulatory system in plants by controlling protein homeostasis. Secondary metabolites activate or stabilize Reactive oxygen species (ROS)-scavenging enzymes and suppresses production of ROS. In this study, I investigate how thermotolerance is affected by light priming, and how

important the DNA integrity of plants is for thermotolerance of plants.

In Chapter 1, a study on the effect of the presence of light on the thermotolerance of plants before the heat stress is described. ROS serve as critical signaling mediators in plant adaptation responses to environmental stimuli. Meanwhile, ROS biosynthesis and metabolism should be tightly regulated, because they often impose oxidative damages on biological molecules, such as DNA and proteins, and cellular structures. It is known that at high temperatures, ROS rapidly accumulate in plant tissues. Thus, a quick activation of ROS scavenging systems is necessary for thermal adaptation. However, it is largely unknown how the thermo-induced ROS detoxifying capacity is enhanced by environmental factors at the molecular level. Here, I demonstrated that environmental light primes the thermally induced ROS detoxification process for thermotolerance development in *Arabidopsis*. While the ROS detoxification capacity was markedly enhanced in light-pretreated plants at high temperatures, its enhancement was not as evident in dark-pretreated plants as in light-pretreated plants. ASCORBATE PEROXIDASE 2 (APX2) is a representative ROS scavenging enzyme that is activated under heat stress conditions. It was observed that the thermal induction of *APX2* gene was more prominent in light-pretreated plants than in dark-pretreated plants. Notably, the light-gated *APX2* gene induction was compromised in *Arabidopsis* mutants lacking the red light photoreceptor phytochrome B (phyB). Furthermore, exogenous application of the antioxidant ascorbate recovered the heat-sensitive phenotype of the *phyB* mutant. These observations indicate that light-primed ROS detoxifying capability is intimately linked with the induction of thermotolerance. I propose

that the phyB-mediated light priming of ROS detoxification is a key component of thermotolerant adaptation in plants.

In Chapter 2, I investigated how the DNA integrity of plants affects the high temperature resistance of plants. High temperature stress interferes with the folding of proteins at the cellular level of plants or disrupts the cell wall or cytoskeleton of cells. In addition, it reduces DNA integrity by modifying nucleotides or breaking DNA strands. However, it is not known how this DNA integrity affects the thermotolerance of plants. Here, I proved that thermotolerance of plants is increased by activating a mechanism that repairs DNA integrity reduced by high temperature by HIGH EXPRESSION OF OSMOTICALLY RESPONSE GENES 1 (HOS1). HOS1 protein is known as a regulatory protein that regulates plant low temperature resistance, flowering time, and circadian clock by degrading target proteins or remodeling chromatin. In this study, it was observed that the thermotolerance of HOS1 deficient plants was significantly reduced compared to that of wild-type plants. Based on this phenotype, it was confirmed that HOS1 regulates genes related to DNA repair at high temperatures. Among them, it was observed that the thermotolerance decreased in mutant plants which the RECQ2 helicase enzyme, which released the double strands of DNA, was deficient. In addition, it was confirmed that DNA was damaged by high temperature in HOS1 deficient mutant and RECQ2 deficient mutant. Through this observation, it was proven that the HOS1 protein increases the expression of RECQ2 at high temperatures to repair damaged DNA, thereby increasing thermotolerance of plants. In addition, it was demonstrated that the stability of HOS1 protein is increased by high temperature,

and that the HSFA1-HSP90 module is required to increase the stability of HOS1 protein. In conclusion, I propose a new mechanism for regulating the high temperature resistance of plants, and assert how important it is to maintain the integrity of the DNA for the thermotolerance of plants.

Key words: heat stress, ROS, APX2, primging effect, phytochrome B, thermotolerance, HOS1, RECQ2, DNA integrity, DNA repair, HSFA1, HSP90

Student number: 2016-23460

CONTENTS

ABSTRACT..... i

CONTENTS..... v

LIST OF FIGURES..... x

LIST OF TABLES..... xv

ABBREVIATIONS..... xvi

CHAPTER 1: Light primes the thermally induced detoxification of reactive oxygen species during thermotolerance development in *Arabidopsis*

INTRODUCTION

1. Plant adaptation to high temperatures..... 1

2. Linkage between temperature responses and light signalings in plants..... 2

3. Priming effects in plants..... 3

MATERIALS AND METHODS

1. Plant materials and growth..... 5

2. Thermotolerance assay..... 5

3. Measurement of chlorophyll contents..... 6

4. Light quality assay..... 7

5. Gene expression analysis..... 7

6. Fluorescence microscopy..... 8

7. Measurement of APX enzyme activity..... 8

8. Statistical analysis..... 9

RESULTS

Thermotolerance development is diurnally regulated in *Arabidopsis*..... 11

Light priming is essential for thermotolerance development..... 12

Light priming triggers ROS detoxification..... 16

Light primes the HSF-mediated ROS detoxification..... 22

Photoreceptor-mediated light signaling primes thermotolerance development 24

PhyB-mediated priming of ROS detoxification leads to induction of thermotolerance..... 38

DISCUSSION

Signaling crosstalks between light and temperature cues during thermotolerance..... 43

Photoreceptor-mediated light signaling primes thermotolerance development..

..... 44

Light-gated ROS detoxification and thermotolerance development..... 46

ACKNOWLEDGEMENTS..... 48

CHAPTER 2: HOS1 activates DNA repair systems to enhance plant thermotolerance

INTRODUCTION

MATERIALS AND METHODS

1. Plant materials and growth..... 52
2. Thermotolerance assay..... 53
3. Gene expression analysis..... 54
4. Protein stability..... 55
5. RNA sequencing..... 56
6. Comet assay..... 56
7. Chromatin immunoprecipitation (ChIP)..... 57
8. Analysis of endogenous ROS contents..... 58
9. Infrared thermography..... 59

10. Transcriptional activation activity assay..... 59

11. Yeat two-hybrid..... 60

12. Bimolecular fluorescence complementation (BiFC)..... 61

13. Trypan blue staining..... 61

14. Statistical analysis..... 62

RESULTS

HOS1 is required for the acquisition of termotolerance..... 65

DNA damage response is reduced in *hos1-3* mutant at high temperatures.. 71

HOS1 mediates the thermal induction of *RECQ2* gene during thermo-tolerance response..... 76

The HSFA1-HSP90-HOS1 module activates DNA repair response at high temperatures..... 101

DISCUSSION

ACKNOWLEDGEMENTS..... 126

REFERENCES..... 127

PUBLICATION LIST..... 140

ABSTRACT IN KOREAN..... 141

LIST OF FIGURES

Figure 1. Thermotolerance development is diurnally regulated in *Arabidopsis*.. 13

Figure 2. Light illumination prior to heat treatment is essential for thermotolerance development..... 15

Figure 3. Effects of different light-dark combinations on heat-responsive gene expression..... 17

Figure 4. Light priming enhances ROS detoxification during thermotolerance development..... 19

Figure 5. Effects of light priming on ROS accumulation..... 20

Figure 6. Measurement of APX enzyme activity..... 21

Figure 7. Light-gated ROS detoxification requires HSFs during thermo-tolerance development..... 23

Figure 8. Effects of light priming on ROS accumulation in *hsfa1 QK* mutant..... 25

Figure 9. Thermotolerance of Col-0 seedlings under different light wavelengths..... 26

Figure 10. Expression of *APX2* gene in *Arabidopsis* mutants that are defective in photoreceptors..... 28

Figure 11. Thermotolerance of *phyB* mutant seedlings..... 29

Figure 12. Levels of *APX2* transcripts in heat-treated seedlings..... 30

Figure 13. Expression of *APX* family genes in Col-0 and *phyB* mutant..... 32

Figure 14. Expression of genes related to ROS detoxification..... 33

Figure 15. ROS accumulation in heat-treated seedlings..... 34

Figure 16. Thermotolerance responses in *Arabidopsis* mutants that are defective in PIF transcription factors..... 36

Figure 17. PhyB-primed thermotolerance is functionally distinct from chloroplast-gated thermotolerance..... 37

Figure 18. PhyB-mediated light signals prime ROS detoxification during thermotolerance development..... 40

Figure 19. The effects of GSH on red light-primed thermotolerance..... 41

Figure 20. Working scheme for the light priming of thermotolerance development..... 42

Figure 21. HOS1 is required for the acquisition of thermotolerance..... 66

Figure 22. Thermotolerance phenotypes of 35S:*MYC-HOS1* transgenic plants..... 67

Figure 23. Acquired thermotolerance phenotypes of *hos1-3* mutant..... 68

Figure 24. Thermal images of heat-treated seedlings..... 69

Figure 25. Thermotolerance phenotypes of *hos1-3 pif4-101* double mutant.... 70

Figure 26. Complementation of *hos1-3* mutant..... 72

Figure 27. Transcription of *HOS1* gene in 35S:*mHOS1 hos1-3* plants..... 73

Figure 28. Thermal accumulation of reactive oxygen species (ROS)..... 74

Figure 29. Histochemical detection of hydrogen peroxide..... 75

Figure 30. Scatter plots of related gene expression values obtained by RNA sequencing analysis..... 77

Figure 31. Gene ontology analysis of HOS1-regulated genes at high temperatures..... 78

Figure 32. Thermal induction of DNA damage response genes..... 79

Figure 33. RT-qPCR analysis of selected DNA damage response genes..... 80

Figure 34. Comet assays on heat-treated *hos1-3* seedlings..... 81

Figure 35. Thermotolerance phenotypes of *recq2* mutant..... 82

Figure 36. Chlorophyll contents in DNA damage response-related mutants..... 83

Figure 37. Comet assays on *recq2* mutant..... 84

Figure 38. Thermotolerance phenotypes of *wrnexo* mutant..... 86

Figure 39. Binding of HOS1 to *RECQ2* chromatin..... 87

Figure 40. T*RECQ2* promoter sequences examined in chromatin immunoprecipitation (ChIP)-qPCR..... 88

Figure 41. Control data for ChIP-qPCR assays..... 89

Figure 42. Two histone deacetylase (HDAC)-deficient mutants, *hda6* and *hda15-1*, were included in the thermotolerance assays..... 90

Figure 43. Histone modifications at *RECQ2* chromatin..... 91

Figure 44. Histone modifications in the P3 sequence region of *RECQ2* chromatin..... 92

Figure 45. Transcriptional activation activity assays in *Arabidopsis* protoplasts..... 94

Figure 46. Thermotolerance phenotypes of *hos1-3 recq2* mutant..... 95

Figure 47. Thermotolerance phenotypes of *hos1-3 recq2* double mutant..... 96

Figure 48. Thermotolerance phenotypes of *hos1-3 RECQ2*-ox plants..... 97

Figure 49. Thermotolerance phenotypes of *hos1-3* mutant in the presence of cisplatin..... 98

Figure 50. Thermotolerance phenotypes of *recq2* mutant in the presence of cisplatin..... 99

Figure 51. Effects of mitomycin on thermotolerance..... 100

Figure 52. Cell death increases in *hos1-3* and *recq2* mutants at high temperatures..... 102

Figure 53. Transcription of heat response genes in the *hos1-3* mutant at high temperatures..... 103

Figure 54. HSP90 protein abundance in the *hos1-3* mutant..... 104

Figure 55. Thermal stabilization of HOS1..... 105

Figure 56. Effects of MG132 on HOS1 protein stability..... 106

Figure 57. Effects of high temperatures on *HOS1* transcription..... 108

Figure 58. Effects of HSP90 inhibitor on thermal accumulation of HOS1. 109

Figure 59. Effects of radicicol on the thermal accumulation of HOS1 proteins..... 110

Figure 60. Comet assays in the presence of GDA..... 111

Figure 61. Comet assays in the presence of radicicol..... 112

Figure 62. Thermal protein abundance of HOS1 in *HSP90*-RNAi plants.. 113

Figure 63. Thermotolerance phenotypes of *HSP90*-RNAi plants..... 114

Figure 64. Thermotolerance phenotypes of *hos1-3* mutant in the presence of radicicol..... 115

Figure 65. Thermal protein abundance of HOS1 in the *hsfa1* QK mutant. 116

Figure 66. Thermotolerance phenotypes of *hsfa1a*/*hsfa1b*/*hsfa1d*/*hsfa1e* quadruple knockout (*hsfa1* QK) mutant..... 117

Figure 67. Comet assays on heat-treated *hsfa1* QK mutant..... 119

Figure 68. HOS1 does not interact physically with HSP90..... 120

Figure 69. Thermotolerance phenotypes of *uvh6* mutant..... 121

Figure 70. Acquisition of thermotolerance via the HOS1-mediated activation of DNA repair response..... 122

LIST OF TABLE

Table 1. Primers used in Chapter 1 10

Table 2. Primers used in Chapter 2 63

ABBREVIATIONS

LDs	Long days
SDs	Short days
ZT	Zeitgeber time
RT-qPCR	Reverse transcription-mediated quantitative PCR
AD	GAL4 activation domain
BD	GAL4 binding domain
3-AT	3-Amino-1,2,4-triazole
CaMV	Cauliflower mosaic virus
ChIP	Chromatin immunoprecipitation
ROS	Reactive oxygen species
APX2	ASCORBATE PEROXIDASE 2
phyB	phytochrome B
GPX	glutathione peroxidase
GSH	reduced glutathione
CAT	catalase
SOD	superoxide dismutase
HSPs	HEAT SHOCK PROTEINs
PIFs	PHYTOCHROME-INTERACTING FACTORs
YUC8	YUCCA8
CRY	cryptochrome

HSFA	HEAT SHOCK FACTOR A
DCMU	3-(3,4-dichlorophenyl)-1,1-dimethylurea
DBMIB	2,5-dibromo-3-methyl-6-isopropyl-p-benzoquinone
ASC	ascorbate
H_2DCFDA	2,7-dichlorodihydrofluorescein diacetate
Col-0	Columbia-0
HSE	heat shock element
CBFs	C-repeat binding factors
FLC	FLOWERING LOCUS C
SOM	SOMNUS
HOS1	HIGH EXPRESSION OF OSMOTICALLY REPONSIVE GENES1
mHOS1	modified HOS1 protein
GDA	geldanamycin
MMC	Mitomycin C
TUB	TUBULIN
GO	Gene ontology
BiNGO	Biological Networks Gene Ontology tool
GUS	β-glucuronidase
lacZ	β-galactosidase
BiFC	Bimolecular fluorescence complementation
ANOVA	analysis of variance
DAB	3,3-diaminobenzidine
NBT	nitro blue tetrazolium

AtWRNexo	WERNER SYNDROME-LIKE EXONUCLEASE exonuclease
HDA	HISTONE DEACETYLASE
cisplatin	*cis*-diamminedichloroplatinum (II)
UVH6	ULTRAVIOLET HYPERSENSITIVE 6

CHAPTER 1

Light primes the thermally induced detoxification of reactive oxygen species during thermotolerance development in *Arabidopsis*

INTRODUCTION

1. Plant adaptation to high temperatures

Plants are continuously exposed to unfavorable environmental changes in natural habitats. Temperature is one of the major environmental factors that profoundly affect plant growth and development, metabolism and physiology, and seed productivity (Quint et al., 2016). In particular, it has been widely documented in recent decades that global warming, a gradual increase of global average temperature, and associated climate changes, such as extreme cold and heat spells in local areas, broadly influences vegetation on earth and crop productivity (Zhao et al., 2017). In this sense, it is necessary to extend our understanding on molecular mechanisms that direct plant adaptation process to thermal stresses for developing means of improving crop cultivation capacity.

Plants possess versatile protection systems to cope with high temperature stresses (Larkindale et al., 2005; Morimoto et al., 2017). One such adaptive mechanism is the coordinated regulation of reactive oxygen species (ROS) biosynthesis and metabolism, which accumulate to a high level in plants at unfavorable high temperatures (Lee et al., 2015). High-level accumulation of ROS is harmful to plant growth and survival because they cause bleaching of chlorophylls and destruction of cellular components (You and Chan, 2015; Zhao et al., 2017). It has been reported that several ROS scavenging enzymes including ascorbate peroxidase (APX), glutathione peroxidase (GPX) and catalase (CAT) function

collectively while superoxide dismutase (SOD) triggers ROS production (Mittler et al. 2004). Therefore, the balance between SOD and the ROS scavenging enzymes is crucial for maintaining appropriate ROS level. Especially ASCORBATE PEROXIDASE 2 (APX2) is one of the central ROS detoxification enzymes that function during thermotolerance development in plants (Panchuk et al., 2002). APX enzymes utilize ascorbate as an electron donor to reduce hydrogen peroxide to water (Karyotou and Donaldson, 2005), thereby reducing the risk of oxidative damages (Caverzan et al., 2012). HEAT SHOCK PROTEINs (HSPs) also contribute to the protection of plant cells from heat-induced cellular damages. They act as heat-induced molecular chaperons, which facilitate and correct protein folding, assembly, and stabilization so that protein substrates are protected from thermo-triggered denaturation (Perez et al., 2009). Consequently, overexpression of *HSP101* in *Arabidopsis* plants enhances thermotolerance (Queitsch et al., 2000).

2. Linkage between temperature responses and light signalings in plants

It is notable that temperature responses are closely linked with light signaling. In plants, light acts as a pivotal environmental signaling inducer as well as the ultimate source of photosynthesis (Lee et al., 2017). Thus, plants possess multiple photoreceptors that are capable of efficiently sensing specific ranges of light wavelengths (Lau and Deng, 2012). The phytochrome (phy) photoreceptors have two interchangeable forms, Pr and Pfr, the interconversion of which is regulated by the red to far-red light ratio in nature (Xu et al., 2015). Upon photo-activation, the phy proteins enter the nucleus, where they interact with a group of

PHYTOCHROME-INTERACTING FACTORs (PIFs) to trigger a wide range of light responses (Zhang et al., 2013). Interestingly, the phy photoreceptors also function as thermosensors: the light-activated reversion of Pfr to Pr is accelerated at warm temperatures (Jung et al., 2016; Legris et al., 2016). The blue light-sensing cryptochrome (CRY) photoreceptors are known to interact with PIF4, which is a key component of thermomorphogenesis (Ma et al., 2016). The phototropin (PHOT) photoreceptors have been initially identified as the modulator of phototropic plant growth (Zhao et al., 2013). Later, it has been proven that they also sense temperature changes to rearrange chloroplasts in the cytoplasm for optimal photosynthesis (Fujii et al., 2017). Meanwhile, it is known that thermo-induced plant growth is attenuated under UV-B light conditions (Hayes et al., 2017). In contrast, *Arabidopsis* mutants lacking the UV-B photoreceptor are still sensitive to warm temperatures. These reports signify the integration of light and temperature signals in regulating plant growth, morphogenesis, and environmental adaptation.

3. Priming effects in plants

In nature, plants utilize light information to anticipate upcoming environmental fluctuations that occur regularly in a daily basis (Gabriel and Zeier, 2008), among which diurnal rhythms of ambient temperature fluctuations have been most comprehensively studied in recent years. Of particular interest is the light gating of temperature responses (Lee et al., 2012; Dickinson et al., 2018). The transcription of genes that mediate freezing tolerance is accelerated when photoperiod is short (Lee et al., 2012). Thus, plants exhibit enhanced freezing tolerance under short

days. In addition, hypocotyl thermomorphogenesis is more prominent during the daytime under long day conditions, when temperature is typically high (Park et al., 2017). Furthermore, it has been recently reported that a retrograde chloroplast signaling gates thermotolerance response (Dickinson et al., 2018), perhaps providing a molecular link between photosynthetic activity and thermotolerance development. However, it is not clear how light signaling is associated with temperature responses at the molecular level in most cases.

In this work, I demonstrated that phyB-mediated light priming is essential for thermotolerance development in *Arabidopsis*. My data illustrate that light primes the HEAT SHOCK FACTOR A1 (HSFA1)-mediated thermal induction of *APX2* gene expression under high temperature conditions. While the *APX2* gene was induced to some extent by high temperatures in darkness, the thermal induction of the *APX2* gene was more prominent in plants that are exposed to light prior to heat treatment in a phyB-dependent manner. I also demonstrated that the light-gated *APX2* expression enhances ROS scavenging capacity and exogenous application of ascorbate is sufficient to mimic the light priming of thermotolerance. In conjunction with the direct role of HSFA1 transcription factor in inducing *APX2* transcription, it is evident that the HSFA1-mediated temperature signals and the phyB-mediated light signals converge at APX2, constituting a light priming mechanism of ROS detoxification for the induction of thermotolerance.

MATERIALS AND METHODS

1. Plant materials and growth

All *Arabidopsis thaliana* lines used were in Columbia (Col-0) background except for the quadruple *hsfa1* mutant (*QK*) (Liu et al., 2011), which was generated from both Col-0 and Ws-2 background. The *QK* mutant was kindly provided by Dr. Yee-Yung Charng. The *phyA-211*, *phyB-9*, *cry1cry2*, and the quadruple *pifq* mutants have been described previously (Wang et al., 2010; Zhang et al., 2013). The *pifq* mutant was obtained from the *Arabidopsis* Biological Resource Center (Ohio State University).

Sterilized *Arabidopsis* seeds were cold-imbibed at 4°C for 3 d in complete darkness to synchronize germination. Plants were grown on Murashige and Skoog (MS)- agar plates under long days (LDs, 16-h light and 8-h dark) with white light illumination (150 μmol $m^{-2}s^{-1}$), which was provided by fluorescent FLR40D/A tubes (Osram), in a controlled culture room set at 22°C with 60% humidity.

2. Thermotolerance assay

Seven-day-old seedlings grown on MS-agar plates under LDs were exposed to 45°C for 45 min at Zeitgeber time 8 (ZT8) in darkness and allowed to recover at 23°C for 5 d under continuous light. For light quality assay, seven-day-old seedlings were exposed to specific wavelength ranges of light for 2 h before heat treatment, as described above. For chemical treatment, seedlings were grown on

MS-agar containing 0.5 mM ascorbate (Sigma, St. Louis, USA), and 1 mM GSH (Sigma) before heat-treated, as described above. For the examination of chloroplast-gated light signaling on the induction of thermotolerance, either 30 μM DCMU (Sigma) or 50 μM DBMIB (Sigma) was exogenously applied to seven-day-old seedlings for 2 h before heat treatment (Sherameti et al. 2002).

For light-transfer and dark-transfer assays on the induction of thermotolerance, seven-day-old seedlings were preincubated for different lengths of either light period or dark period before heat treatments (45°C, 45 min) at ZT8, respectively. Presence of newly developing leaves after 5 d of recovery following heat treatment was considered as the sign of survival.

3. Measurement of chlorophyll contents

Heat-treated seedlings were allowed to recover under constant light at 23°C for 5 d. Seedlings were then harvested for the extraction of chlorophylls with 100% methanol and were incubated at 4°C for 2 h in complete darkness. Chlorophyll contents were analyzed by measuring absorbance at 650 and 660 nm using Mithras LB940 multimode microplate reader (Berthold technologies). The contents of chlorophyll *a* and chlorophyll *b* were calculated from the absorbance values at 650 and 660 nm, as described previously (Lee et al., 2015). Total chlorophyll contents indicate the sum of chlorophyll a and chlorophyll b. Relative chlorophyll contents were calculated by dividing total chlorophyll contents of heat-treated seedlings by those of seedlings treated under control conditions.

4. Light quality assay

For light quality assays, seven-day-old seedlings were exposed to white, red, blue, or far-red light for 2 h. Light intensity is 100-120 μmol m^{-2} s^{-1}. The *phyB* mutant, the *cry1 cry2* mutant, or the *phyA* mutant was included as the photoreceptor mutant in the assays using red light, blue light, or far-red light illumination, respectively. The *pifq* mutant was also included in the red light assays. At ZT8, seedlings were exposed to 45°C for 45 min in darkness. Total RNA samples were extracted from whole seedlings, and ROS quantification were performed right after heat treatment.

5. Gene expression analysis

Transcript levels were analyzed by reverse transcription-mediated quantitative real-time PCR (RT-qPCR). All RT-qPCR reactions were performed following the principles that have been proposed to guarantee reproducible and accurate measurements of transcript levels (Udvardi et al., 2008). Total RNA samples were extracted from whole seedlings, unless otherwise specified. RT-qPCR reactions were conducted in 384-well blocks with an QuantStudio 6 Flex (Life technologies) using the SYBR Green I master mix in a volume of 10 μl. The two-step thermal cycling profile employed was 15 s at 95°C for denaturation and 1min at 60-65°C for annealing and polymerization. An *eIF4A* gene (At3g13920) was included as internal control in each PCR reaction to standardize the differences in the amounts of cDNA samples used.

To ensure the reproducibility of RT-qPCR reactions, they were performed

in biological triplicates using total RNA samples prepared separately from three independent plant materials that were grown under identical conditions. The comparative $\Delta\Delta C_T$ method was employed to evaluate relative quantities of each amplified product in the samples. The threshold cycle (C_T) was automatically determined for each reaction by the system set with default parameters.

6. Fluorescence microscopy

The cell-permeant 2',7'-dichlorodihydrofluorescein diacetate (H_2DCFDA, Sigma) was used to stain ROS in plant tissues. Plant samples were incubated in 10 μM H_2DCFDA solution for 1 h at 23°C in complete darkness. It is known that the nonfluorescent H_2DCFDA is converted to the fluorescent 2',7'-dichlorofluorescein (DCF) upon chemical reactions with ROS (Zhong et al., 2009). Fluorescence microscope (Olympus) equipped with the GFP filter was used to image DCF fluorescence in whole seedling. The 5X objective lens was used, and fluorescence exposure time was set to 30 ms. The ImageJ public domain was used to quantify fluorescence intensity. Relative fluorescence analysis was performed by averaging the fluorescence of the whole leaf.

7. Measurement of APX enzyme activity

The 7-day-old seedlings grown at 23°C were preincubated with light or darkness for 2 h before 45°C treatment for 45 min. Whole seedlings were harvested for APX enzyme activity. APX enzyme activity was measured as described in the previous report (Verma and Dubey, 2003). The 2 ml reaction mixture contained

100 mM pH 7.0 potassium phosphate buffer, 500 µl of 0.2 mM ascorbic acid, 100 µl of 0.2 mM EDTA, 300 µl of 6% H_2O_2 and 100 µl of leaf extract. Leaf extract was added at the last and the decrease in absorbance was recorded at 290 nm using a UV-Vis spectrophotometer at 15 sec intervals up to 3 min. The relative enzyme activity of light-primed seedlings under mock conditions was set to 1.

8. Statistical analysis

The statistical significance between two means of measurements was determined using the one-sided Student *t*-test with *P* values of < 0.01 or < 0.05. Statistical analyses were performed using the IBM SPSS Statistics 25 software (https://www.ibm.com/).

Primers	Sequences	Usage
eIF4A-F	5′-TGACCACACAGTCTCTGCAA	RT-qPCR
eIF4A-R	5′-ACCAGGGAGACTTGTTGGAC	"
HSP70-F	5′-TGAGGCAGATGAGTTCGAGG	"
HSP70-R	5′-CTCCTGCACCACCCATATCA	"
HSP90.1-F	5′-TGCGAGGTCTGGAACAAAAG	"
HSP90.1-R	5′-ACCACCAGCTTGAGACTCCC	"
HSP101-F	5′-GGCTTGACGAGATTGTGGTG	"
HSP101-R	5′-CGGGTCATAACTCTCTGCCA	"
APX1-F	5′-CCAACCGTGAGCGAAGATTA	"
APX1-R	5′-CGTCAAACCTCATTGTTCCG	"
APX2-F	5′-TGCATTGTCTGGTGGACACA	"
APX2-R	5′-GAAGAGCCTTGTCGGTTGGT	"
APX3-F	5′-TCTCTGTGAGGGCGTGAAAG	"
APX3-R	5′-GGAACGAACACGATGTCAGG	"
APX4-F	5′-TAGCAGGACAATCAGCGGTC	"
APX4-R	5′-CAAACAATCCCCACTGACCA	"
APX5-F	5′-GCTGTATGCAAAGGACGAGGA	"
APX5-R	5′-TGCGTCACTGCTGAAGGAAT	"
APX6-F	5′-ACCTGATCCAGAAGGCAAGC	"
APX6-R	5′-TAAGGCAACAAGCTCCTGGG	"
sAPX-F	5′-TCGGTGAATCGGAGTTTCAA	"
sAPX-R	5′-GGCAGAATTTGGTGCTGAGA	"
tAPX-F	5′-TTGCCATCCCATCTTGGTTA	"
tAPX-R	5′-CAGCATGCTTAAGCTCAGCC	"
GPX1-F	5′-AACGCAGGAGGATTCTTGGG	"
GPX1-R	5′-GAAAGGGGATGTGGTGGGAG	"
GPX2-F	5′-ACAAGGAGCAAGGGTTGGAG	"
GPX2-R	5′-ACCTGGTGCAGACAGTTTGT	"
CAT1-F	5′-AAACTCGGGTGCTCCTGTCT	"
CAT1-R	5′-ACAACCCTCTCAGGAATCCG	"
CAT2-F	5′-TGCGAGAGAGCATTCAGGAC	"
CAT2-R	5′-GATACGCACTCCCAGCTGAA	"

Table 1. Primers used in Chapter 1

The primers were designed using the NCBI Primer-BLAST software (https://www.ncbi.nlm.nih.gov/tools/primer-blast/) in a way that their calculated melting temperatures are in a temperature range of 50 - 60^{o}C. F, forward primer. R, reverse primer.

RESULTS

Thermotolerance development is diurnally regulated in *Arabidopsis*

In plants, many temperature responses, such as cold and freezing tolerance, heat tolerance, and thermomorphogenesis, are rhythmic across the day/night cycle (Lee et al., 2012; Dickinson et al., 2018; Park and Park, 2018). These rhythmic behaviors enable plants to anticipate upcoming temperature changes and prepare for timely responses to temperature environments (Zhu et al., 2016). Owing to the wide-ranging effects of global warming on ecological vegetation and crop agriculture, plant thermotolerance is emerging as a key issue in the field during recent decades. It is known that phytochromes, which otherwise act as photoreceptors, sense ambient temperatures through the photochemical conversion step and its interacting partner PIF4 plays a central role in thermal adaptation (Jung et al., 2016). These observations, together with the well-known crosstalks between light and temperature signals (Park et al., 2017), suggest that thermotolerance development would be rhythmic in parallel to rhythmic light responses (Dickinson et al., 2018).

To systemically investigate the potential rhythmicity of thermotolerance induction during the day, Col-0 seedlings were exposed to heat (45^{o}C) for 45 min at different zeitgeber time (ZT) points for up to 48 h under either long days (LDs, 16-h light and 8-h dark) or constant light (Fig.1A). Heat treatments were performed in complete darkness to get rid of any indirect effects of light illumination

during heat exposure. It was found that thermotolerance development, as analyzed by measurements of survival rates and chlorophyll contents, was rhythmic under LDs, reaching the peak at noon (ZT8, ZT32) and the trough at dawn (ZT0, ZT24, ZT48) (Fig. 1B-D). This observation is consistent with the diurnal rhythmicity of thermotolerance under shortdays (SDs) in the previous report (Dickinson et al., 2018). It was notable that Col-0 seedlings were most sensitive to heat at the end of dark period, whereas they were thermo-resistant during the light period, implying that light would be important for thermotolerance.

In plants, daily rhythmicity is generally derived from either light effects or circadian effects (Schaffer et al., 2001). To examine whether the rhythmicity of thermotolerance is associated with circadian rhythms, Col-0 seedlings entrained under LDs were subjected to heat treatments under constant light (Fig. 1E). It was found that the daily rhythms of survival rate and chlorophyll contents disappeared under constant light (Fig. 1F-H). Instead, seedlings exhibited relatively high resistance to heat in the light, indicating that thermotolerance development is not circadian-gated but diurnally regulated. It was also likely that light is required for the induction of thermotolerance.

Light priming is essential for thermotolerance development

I found that the diurnal rhythms of thermotolerance development was evident with the peak at noon and the trough at dawn under LDs. Under constant light, thermotolerance was strongly induced at all ZT points tested. These observations

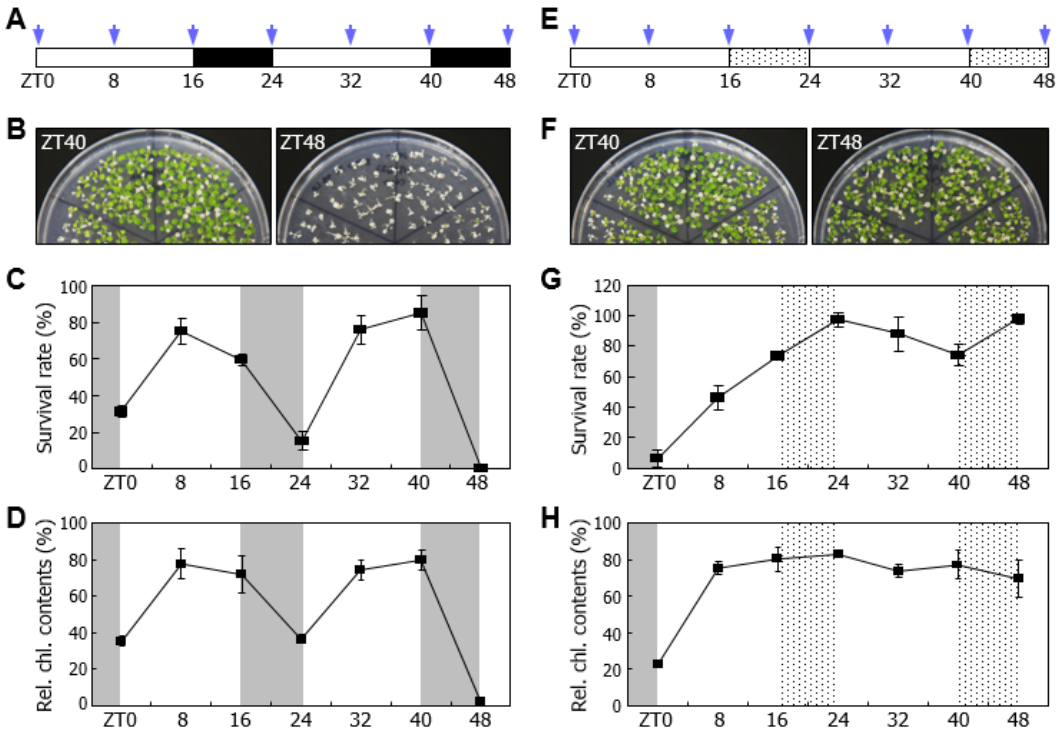

Figure 1. Thermotolerance development is diurnally regulated in *Arabidopsis*

(A-D) Thermotolerance development under long days (LDs, 16-h light and 8-h dark). Scheme of heat treatments **(A)**, thermotolerance phenotypes **(B)**, survival rates **(C)**, and relative chlorophyll contents **(D)** were analyzed. In **(A)**, arrows mark the ZT points of heat treatments. **(E-H)** Thermotolerance development under constant light. Scheme of heat treatments **(E)**, thermotolerance phenotypes **(F)**, survival rates **(G)**, and relative chlorophyll contents **(H)** were analyzed as described above. Biological triplicates, each consisting of approximately 20 seedlings, were statistically analyzed in each assay. Bars indicate standard error of the mean (SE).

suggest that light is required for the induction thermotolerance. Since heat treatments were carried out in darkness, I ruled out the possibility of direct effects of light on the induction of thermotolerance. The remaining possibility was that light priming prior to heat exposure would affect the induction of thermotolerance.

I first carried out dark-transfer experiments, in which seedlings were incubated for different lengths of dark period before heat treatment at ZT8 (Fig. 2A). It was found that survival rate and chlorophyll contents of seedlings were significantly reduced in seedlings that were after incubated in darkness for longer than 2 h (Fig. 2B, C). On the other hand, light-transfer experiment, in which seedlings preincubated for different lengths of light periods were exposed to heat treatment, revealed that light preincubation for longer than 2 h is sufficient for the enhancement of thermotolerance (Fig. 2D-F). Together, these data indicate that light preincubation for certain period of time prior to heat treatment is essential for thermotolerance development.

To confirm the requirement of light preincubation for thermotolerance, I examined the expression of temperature-responsive genes in seedlings following dark-transfer treatments. It is known that ROS rapidly accumulate in heat stress-exposed plants and production of antioxidants and ROS-scavenging enzymes underlies the induction of thermotolerance (Lee et al., 2015). For example, *APX2* gene encoding ascorbate peroxidase is quickly induced after heat exposure, and the production of APX2 enzyme is a prerequisite for thermotolerance development (Panchuk et al., 2002). Gene expression analysis by reverse transcription-mediated quantitative real-time PCR (RT-qPCR) showed that the thermal induction of the

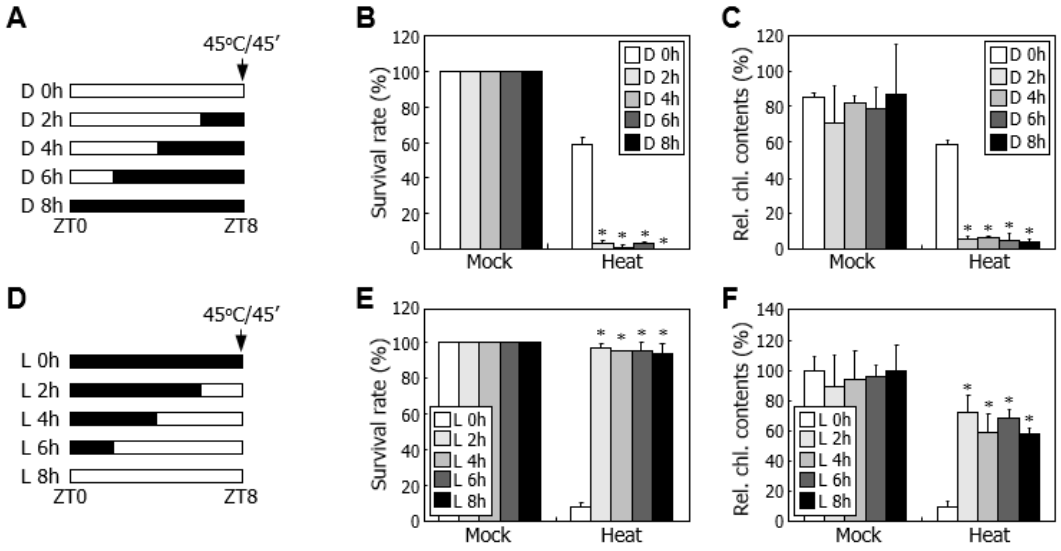

Figure 2. Light illumination prior to heat treatment is essential for thermotolerance development

Seven-day-old Col-0 seedlings grown under LDs at 23°C were then incubated in either light or darkness for up to 8 h prior to heat treatment. The heat-treated seedlings were allowed to recover under constant light at 23°C for 5 d. Biological triplicates, each consisting of ~20 seedlings, were statistically analyzed using student *t*-test (*P < 0.01, difference from 0 h). Bars indicate SE. L and D, light and dark, respectively. **(A-C)** Thermotolerance development in dark-pretreated seedlings. Scheme of heat treatments **(A)**, thermotolerance phenotypes **(B)**, and relative chlorophyll contents **(C)** were assayed. **(D-F)** Thermotolerance development in light-pretreated seedlings. Scheme of heat treatments **(D)**, thermotolerance phenotypes **(E)**, and relative chlorophyll contents **(F)** were assayed as described above.

APX2 gene was most prominent in light-preincubated seedlings but its induction was abruptly reduced in seedlings that are exposed to darkness for longer than 2 h prior to heat treatment (Fig. 3). Genes encoding HSP70 and HSP101, representative molecular chaperones functioning during thermotolerance development (Queitsch et al., 2000; Su et al., 2008), were significantly induced in the light-preincubated seedlings but their induction was largely attenuated in dark-preincubated seedlings (Fig. 3). Taken together, these observations further support that light exposure prior to heat treatment is necessary for thermotolerance enhancement.

Light priming triggers ROS detoxification

Since ROS is rapidly produced under heat stress conditions, causing thermobleaching of chlorophylls and eventual cell death (You and Chan, 2015), it is anticipated that ROS scavenging systems should be promptly activated in heat-stressed plants (Lee et al., 2015). It has been reported that light signaling is tightly associated with ROS metabolism in developing seedlings (Zhong et al., 2009). In addition, I observed that the thermal induction of *APX2* gene expression is gated by light (Fig. 3), raising a possibility that light would prime the ROS detoxification in the course of thermotolerance development.

APX enzymes catalyze the conversion of hydrogen peroxide to water using ascorbate (Caverzan et al., 2012). It is thus well-known that exogenous application of ascorbate reduces ROS accumulation in heat-stressed plants, thus enhancing thermotolerance (Lee et al., 2015). On the basis of the previous

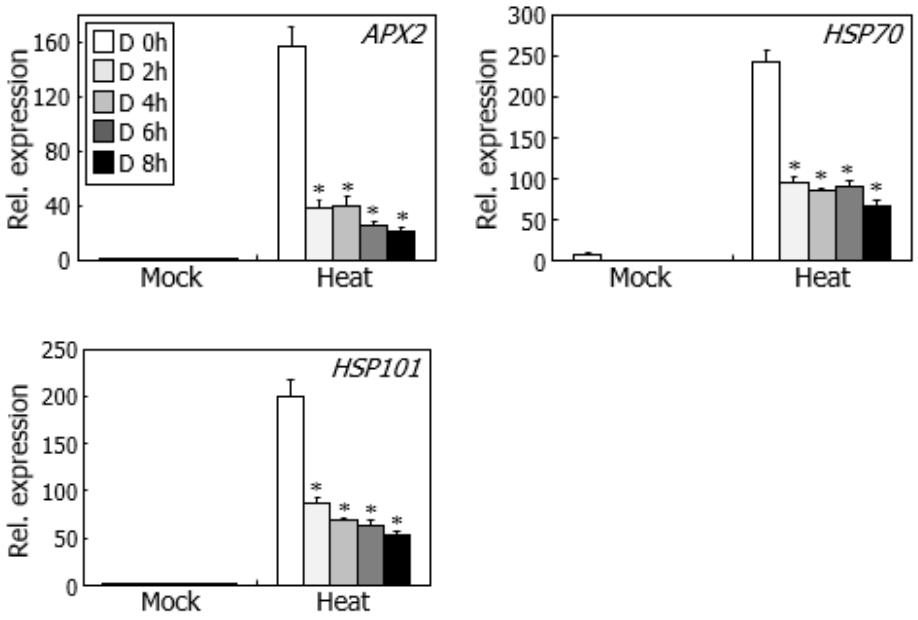

Figure 3. Effects of different light-dark combinations on heat-responsive gene expression

Seven-day-old Col-0 seedlings grown under LDs at 23°C were then incubated in either light or darkness for up to 8 h prior to heat treatment. RT-qPCR was employed for gene expression analysis. Biological triplicates were statistically analyzed (*t*-test, $*P < 0.01$).

observations, I hypothesized that APX-mediated ROS detoxification would be important for the light-gated establishment of thermotolerance. To examine this hypothesis, I analyzed the thermotolerance phenotypes of Col-0 seedlings in the presence of ascorbate. Light-preincubated seedlings were resistant to heat regardless of ascorbate application (Fig. 4A, B). In contrast, while darkness-exposed seedlings were susceptible to heat, their thermotolerance was enormously enhanced in the presence of ascorbate, supporting that light-gated ROS detoxification via APX2 underlies thermotolerance development.

Next, I directly monitored endogenous ROS contents in seedlings that were similarly treated with light and ascorbate. ROS facilitate the conversion of nonfluorescent 2',7'-dichlorodihydrofluorescein diacetate (H_2DCFDA) to fluorescent 2',7'-dichlorofluorescein (DCF) and thus relative fluorescence intensities reflect relative contents of endogenous ROS (Zhong et al., 2009). H_2DCFDA-mediated fluorescent staining assays revealed that ROS accumulated to a higher level in dark-exposed seedlings than light-exposed seedlings at high temperatures (Fig. 5A, B). Notably, exogenous application of ascorbate reduced ROS contents in dark-exposed seedlings to a level comparable to that in light-exposed seedlings (Fig. 5A, B), which is consistent with the effects of ascorbate on the induction of thermotolerance (Fig. 4A, B).

I analyzed the effects of light priming on thermal-induction of APX enzyme activity. It was found that thermo-induced APX enzyme activity of light-preincubated seedlings was more prominent than that of dark-preincubated seedlings. These observations indicate that light priming activates APX enzyme (Fig. 6). Taken

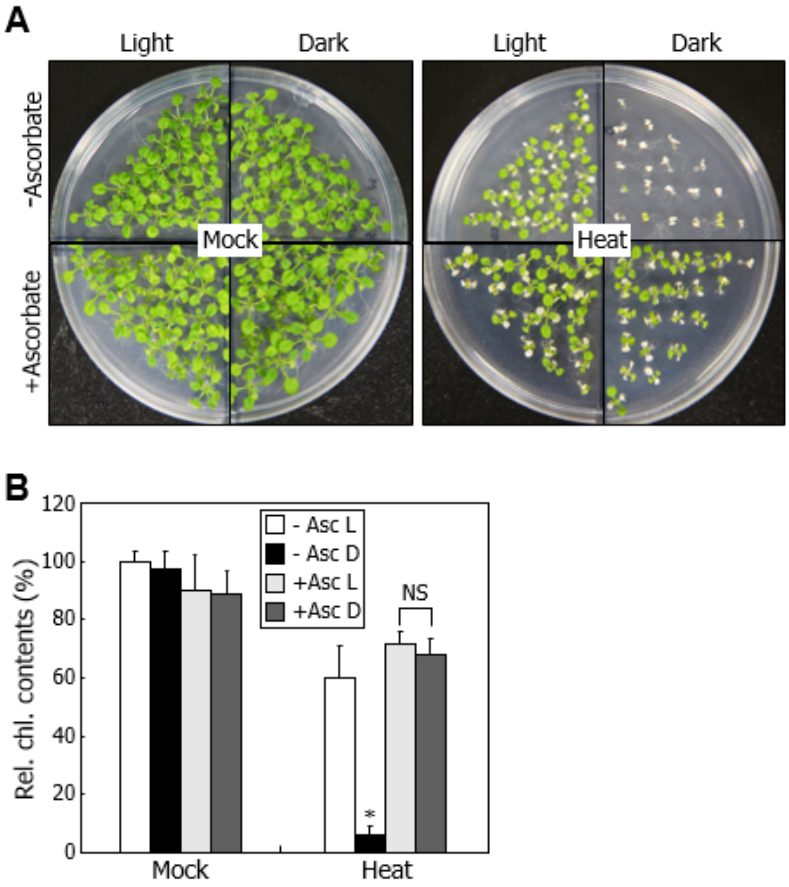

Figure 4. Light priming enhances ROS detoxification during thermotolerance development

Seven-day-old Col-0 seedlings grown under LDs at 23°C were further incubated in either light or darkness for 2 h. At ZT8, seedlings were subjected to heat treatment at 45°C for 45 min. Biological triplicates, each consisting of ~20 seedlings, were statistically analyzed (*t*-test, $*P < 0.01$). Bars indicate SE. **(A, B)** Effects of ascorbate (Asc) on thermotolerance development. Seedlings grown in either presence or absence of 0.5 mM Asc for 7 d were heat-treated. Thermotolerance phenotypes **(A)** and relative chlorophyll contents **(B)** were assayed. NS, no significance.

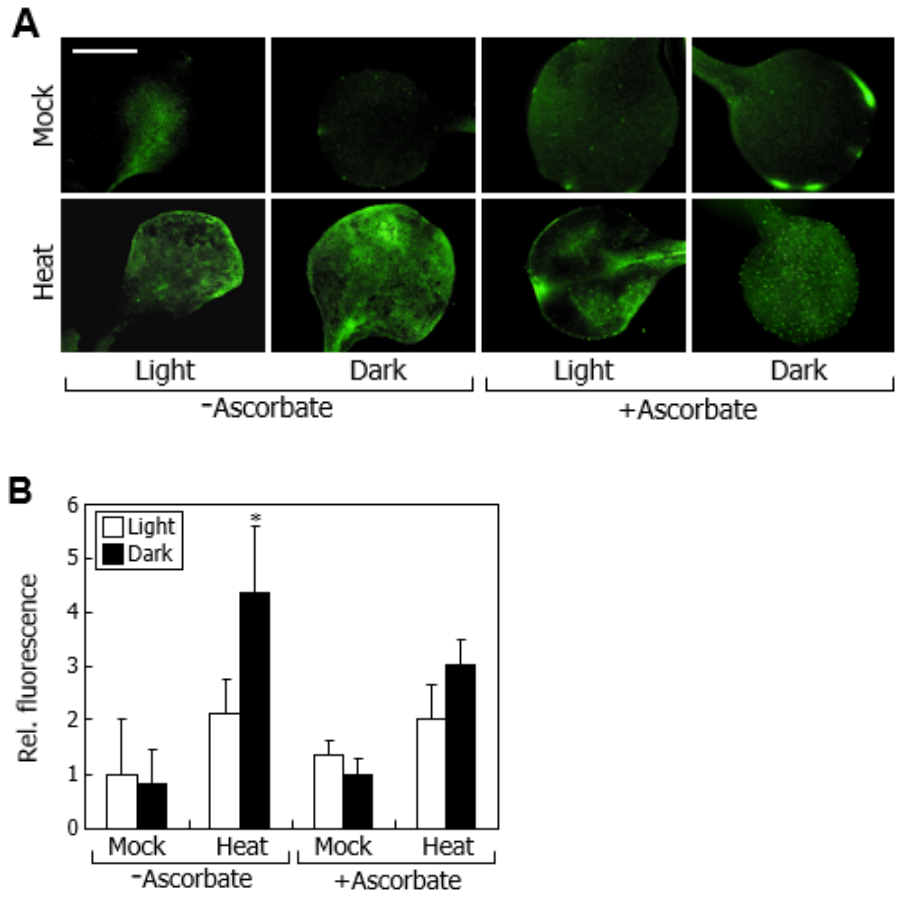

Figure 5. Effects of light priming on ROS accumulation

Seven-day-old Col-0 seedlings grown under LDs at 23°C were further incubated in either light or darkness for 2 h. At ZT8, seedlings were subjected to heat treatment at 45°C for 45 min. **(A, B)** Effects of light priming on ROS accumulation. Seedlings were treated with H_2DCFDA for fluorescent detection of ROS **(A)**. Relative fluorescence intensity was quantitated **(B)**. Scale bar, 600 μm.

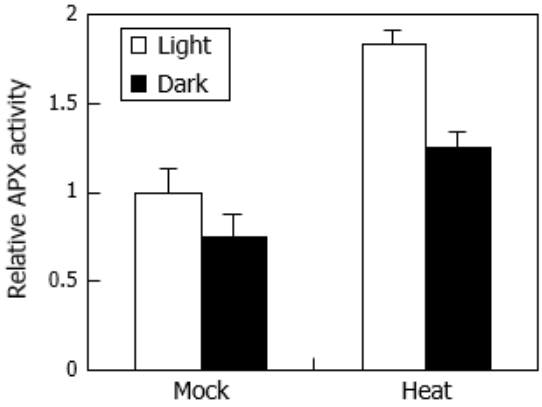

Figure 6. Measurement of APX enzyme activity

Seven-day-old seedlings grown under LDs were incubated under light or dark condition for 2 h. Temperature of LD was 23°C. Seedlings were then subjected to 45°C for 45 min and harvested for assaying APX enzyme activity. The relative APX activity of light-primed seedlings under the mock condition was set to 1. Bars indicate SE.

together, these observations verify that light priming of the APX2-mediated ROS detoxification is closely linked with thermotolerance development.

Light primes the HSF-mediated ROS detoxification

My data indicate that light priming is required for the thermal induction of *APX2* gene expression. Thus, a question was how the light priming event is related with upstream factors that regulate the thermal induction of *APX2* gene. It has been previously shown that HSF transcription factors directly bind to the specific *cis*-element in the promoters of heat-responsive genes, which is often termed heat shock element (HSE) (Guo et al., 2008). The *APX2* gene promoter contains a copy of HSE, and HSFA1b is shown to bind to the HSE sequence (Panchuk et al., 2002). There are four members of HSFA1 transcription factors, HSFA1-a, -b, -d, and -e, in the *Arabidopsis* genome, and they redundantly function during thermotolerance responses (Liu et al., 2011).

I therefore employed the quadruple *hsfa1-a, -b, -d,* and *-e* knockout mutant (*QK*) (Liu et al., 2011) in order to investigate the roles of HSFA1 transcription factors in light-gated ROS detoxification and thermotolerance development. Thermotolerance assays revealed that light priming of thermotolerance development was compromised in the light-exposed *QK* seedlings (Fig. 7A, B). Accordingly, light-gated induction of *APX2* gene expression was also impaired in the *QK* seedlings (Fig. 7C), supporting the critical roles of HSFA1 transcription factors in mediating the light-primed induction of thermotolerance development.

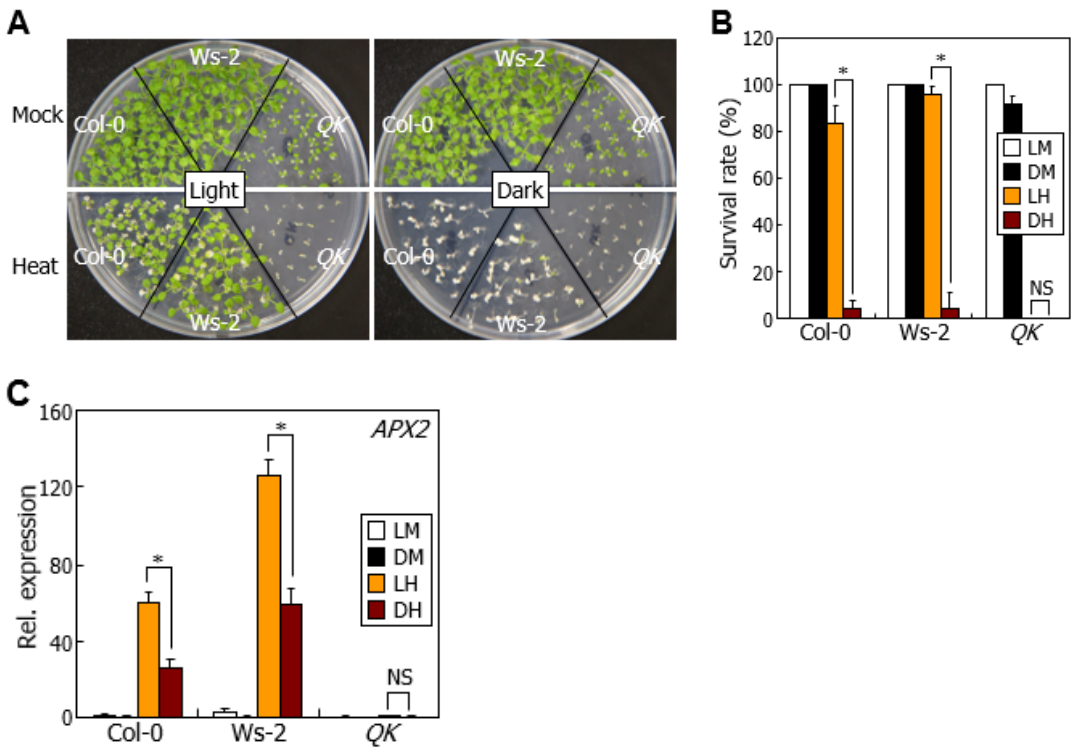

Figure 7. Light-gated ROS detoxification requires HSFs during thermotolerance development

Seven-day-old seedlings grown under LDs at 23°C were further incubated in either light or darkness for 2 h. At ZT8, seedlings were subjected to heat treatment. Biological triplicates, each consisting of ~50 seedlings, were statistically analyzed (*t*-test, **P* < 0.01, difference from light). Bars indicate SE. The quadruple *hsfa1* mutant (*QK*) was included in the assays. **(A)** Thermotolerance of Col-0, Ws-2, and *QK* seedlings under either light or dark conditions. **(B)** Survival rate. **(C)** Transcript levels of *APX2* gene. Whole seedlings were used for total RNA extraction.

I next asked whether the HSFA1-mediated regulation of *APX2* gene expression is involved in the light-enhanced ROS detoxification. H_2DCFDA staining assays revealed that ROS accumulated to similar levels in both light-exposed and dark-exposed *QK* seedlings unlike the efficient light priming of ROS detoxification in light-exposed wildtype seedlings (Fig. 8A, B). It is notable that ROS also accumulated to a relatively high level in *QK* seedlings even at 23°C, implying that HSFA1 transcription factors function in maintaining ROS homeostasis under normal growth conditions and their activity is rapidly elevated under heat stress conditions (Liu et al., 2011).

Photoreceptor-mediated light signaling primes thermotolerance development

Plant photoreceptors sense distinct ranges of light wavelengths (Lau and Deng, 2012). To explore specific light wavelengths and associated photoreceptors that mediate the light priming of thermotolerance induction, I performed thermotolerance assays under different light wavelengths. Seedlings were exposed to different light wavelengths for 2 h prior to heat treatment. It was found that red and blue lights efficiently enhanced thermotolerance development, as analyzed by measurements of survival rate and chlorophyll contents in heat-treated seedlings (Fig. 9A, B). Far-red light preincubation also enhanced thermotolerance, but the extent of enhancement was much weaker than those by red and blue lights. These observations suggest that various photoreceptors would be involved in the light priming event of thermotolerance development.

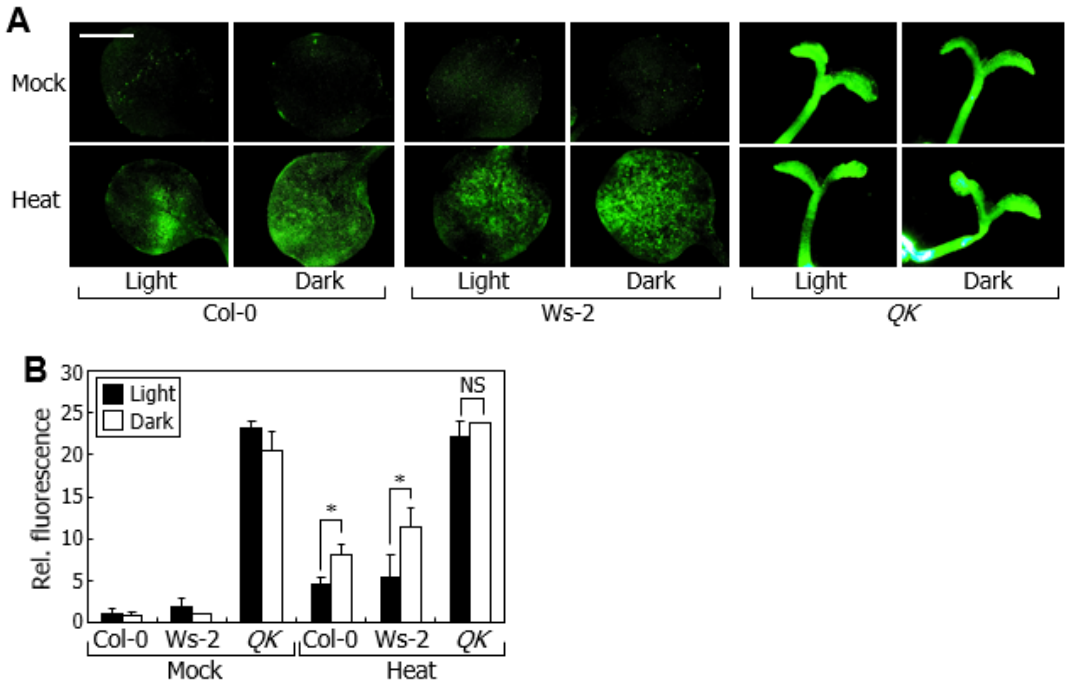

Figure 8. Effects of light priming on ROS accumulation in *hsfa1 QK* mutant Seven-day-old seedlings grown under LDs at 23°C were further incubated in either light or darkness for 2 h. At ZT8, seedlings were subjected to heat treatment. **(A)** H_2DCFDA staining. Scale bar, 600 μm. **(B)** Relative fluorescence intensity. NS, no significance.

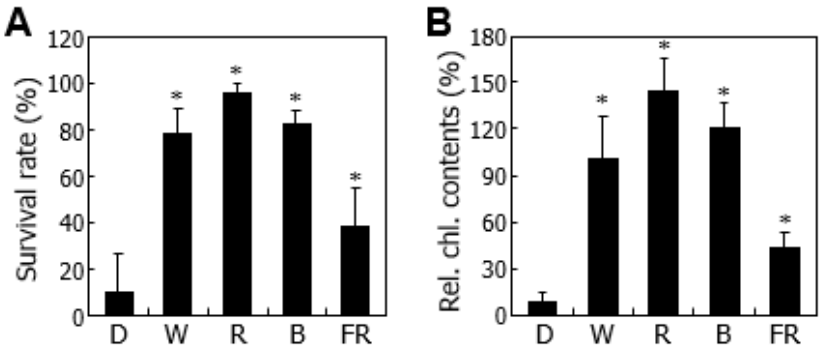

Figure 9. Thermotolerance of Col-0 seedlings under different light wavelengths
Seven-day-old seedlings grown under LDs at 23°C were further incubated in different light regimes at ZT6 for 2 h. Seedlings were then subjected to heat treatment. The heat-treated seedlings were allowed to recover under constant light at 23°C for 5 d. Biological triplicates, each consisting of ~15 seedlings, were averaged and statistically analyzed (*t*-test, $*P < 0.01$). Bars indicate SE. D, dark; W, white light; R, red; B, blue; FR, far-red.

I found that the effectiveness of far-red light was relatively weaker compared to those of red and blue lights in priming the onset of thermotolerance. The phyA photoreceptor is responsible for sensing far-red light, and the phyA-defective mutant exhibits skotomorphogenesis under far-red light conditions (Casal et al., 2014). To further examine the functional linkage between light-primed thermotolerance development and far-red light, the light priming of *APX2* gene expression was assayed in *phyA* mutant seedlings that were preincubated under far-red light conditions. The result showed that thermal induction of *APX2* gene expression did not occur in both Col-0 and mutant seedlings (Fig. 10A), indicating that far-red light and phyA do not play a primary role in the light-gated ROS detoxification. In contrast, blue light priming was able to induce *APX2* expression during thermotolerance development, while it still occurred in the *cry1cry2* double mutant at high temperatures (Fig. 10B). Together, these data support that phyA, CRY1, and CRY2 are not the primary photoreceptors that mediate the light priming of thermotolerance development.

My data on the priming of thermotolerance development by different light wavelengths showed that red light is the most effective among the light wavelengths tested. Notably, thermotolerance assays revealed that red light-primed thermotolerance development was largely compromised in phyB-defective mutant seedlings (Fig. 11C, D). Accordingly, the light-gating effects of red light on the thermal induction of *APX2* gene expression were significantly impaired in the mutant seedlings (Fig. 12), unlike *phyA* and *cry1 cry2* mutant seedlings.

There are eight members of APX homologues in *Arabidopsis* genome

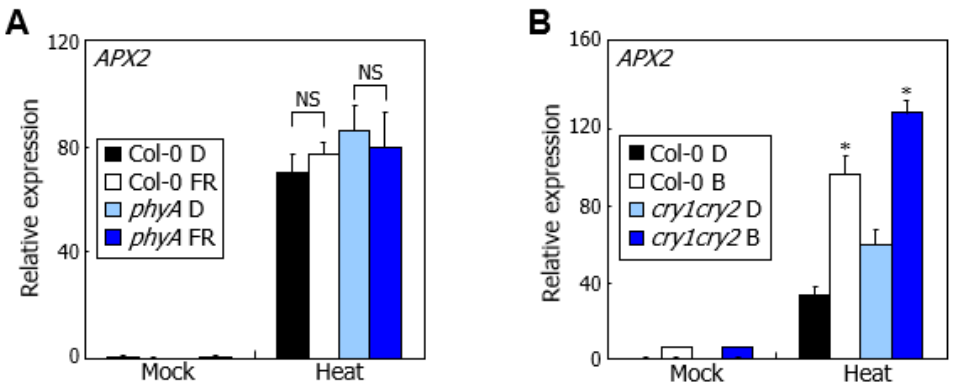

Figure 10. Expression of *APX2* gene in *Arabidopsis* mutants that are defective in photoreceptors

Seven-day-old seedlings grown under LDs at 23°C were further incubated under different light regimes at ZT6 for 2 h. D, dark; R, red; dark; FR, far-red; B, blue. Seedlings were then exposed to 45°C for 45 min. Whole seedlings were used for total RNA extraction for gene expression assays. Transcript levels were analyzed by reverse transcription-mediated quantitative real-time PCR (RT-qPCR). Biological triplicates were averaged and statistically analyzed (*t*-test, $*P < 0.01$, difference from dark). Bars indicate SE. **(A)** *APX2* transcription in *phyA* mutant. NS, no significance. **(B)** *APX2* transcription in *cry1 cry2* mutant.

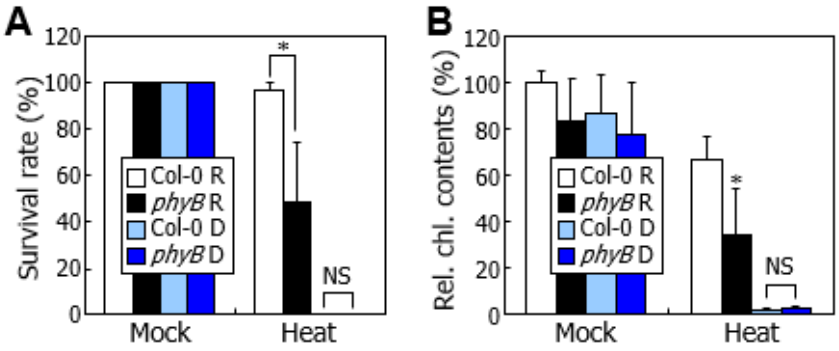

Figure 11. Thermotolerance of *phyB* mutant seedlings

Seven-day-old seedlings grown under LDs at 23°C were further incubated in different light regimes at ZT6 for 2 h. Seedlings were then subjected to heat treatment. The heat-treated seedlings were allowed to recover under constant light at 23°C for 5 d. Biological triplicates, each consisting of ~15 seedlings, were averaged and statistically analyzed (*t*-test, $*P < 0.01$). Bars indicate SE. Survival rates **(A)** and relative chlorophyll contents **(B)** were analyzed. NS, no significance.

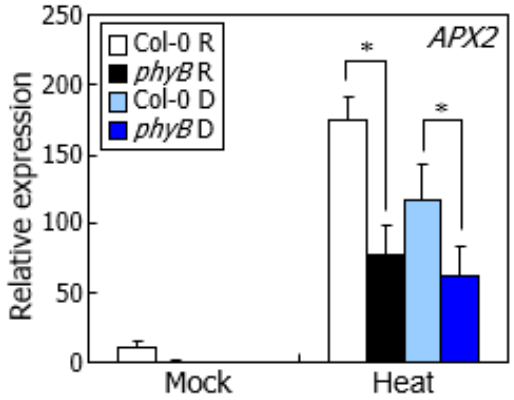

Figure 12. Levels of *APX2* transcripts in heat-treated seedlings

Seven-day-old seedlings grown under LDs at 23°C were further incubated in different light regimes at ZT6 for 2 h. Seedlings were then subjected to heat treatment. The heat-treated seedlings were allowed to recover under constant light at 23°C for 5 d. Transcript levels were analyzed by RT-qPCR. Biological triplicates, each consisting of ~15 seedlings, were averaged and statistically analyzed (*t*-test, **P* < 0.01). Bars indicate SE.

(Panchuk et al., 2005). Therefore, I also examined expression of *APX* family genes in *phyB* mutant seedlings. Gene expression analysis showed that transcript levels of *APX1*, *APX3*, *APX4*, and *APX6* genes were slightly induced at high temperatures but with ~2 fold (Fig. 13). Especially, thermal-induction of *APX1* gene expression was more prominent in red light-pretreated seedlings than that in dark-pretreated seedlings. It is notable that thermal-induction pattern of *APX2* gene was more than 50 fold. Therefore, it is likely that APXs collectively contribute to light-priming of thermotolerance and APX2 is particularly important among the APX family. It has been reported that various ROS scavenging enzymes function in *Arabidopsis* (Mittler et al. 2004). Gene expression analysis revealed that *GPX* and *CAT* genes were not significantly induced by both heat treatment and light pretreatment (Fig. 14). These observations suggest that GPX and CAT pathways would not be related to light-priming of thermotolerance.

I next examined ROS accumulation in red light-preincubated *phyB* mutant seedlings at high temperatures. H_2DCFDA-mediated fluorescent staining revealed that ROS levels were higher in the red light-primed *phyB* mutant seedlings than in Col-0 seedlings at high temperatures (Fig. 15). Collectively, these observations indicate that the light priming of APX2-mediated ROS detoxification and thermotolerance development is mediated primarily by phyB, although roles of other photoreceptors, such as phyD and phyE, would not be excluded.

The phyB photoreceptor exerts its role in governing the red light-responsive gene transcription through interactions with PIF transcription factors (Xu et al., 2015), raising a question as to whether PIFs are involved in the light priming

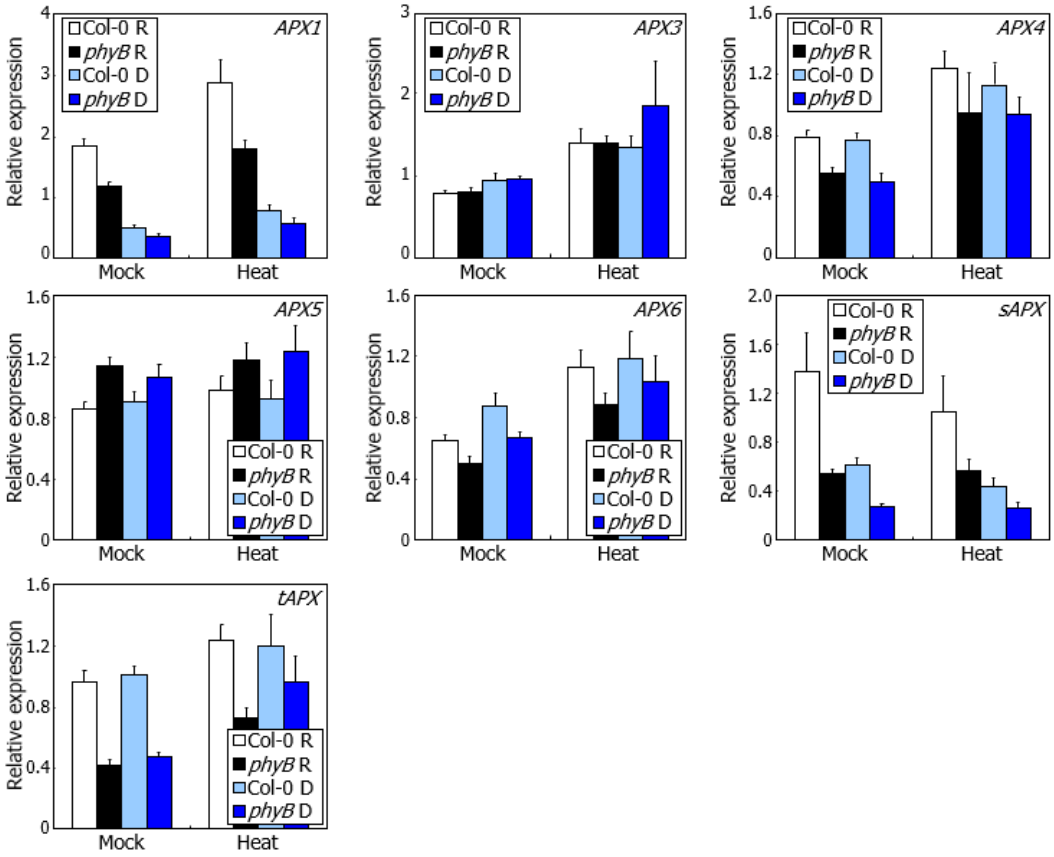

Figure 13. Expression of *APX* family genes in Col-0 and *phyB* mutant

Seedlings grown under LDs for seven days were further incubated under red light or darkness at ZT6 for 2 h. Temperature of LD was 23°C. Seedlings were then subjected to 45°C for 45 min. Heat-treated whole seedlings were used for total RNA extraction. Biological triplicates were averaged and statistically analyzed. Bars indicate SE. D and R denote dark and red light, respectively.

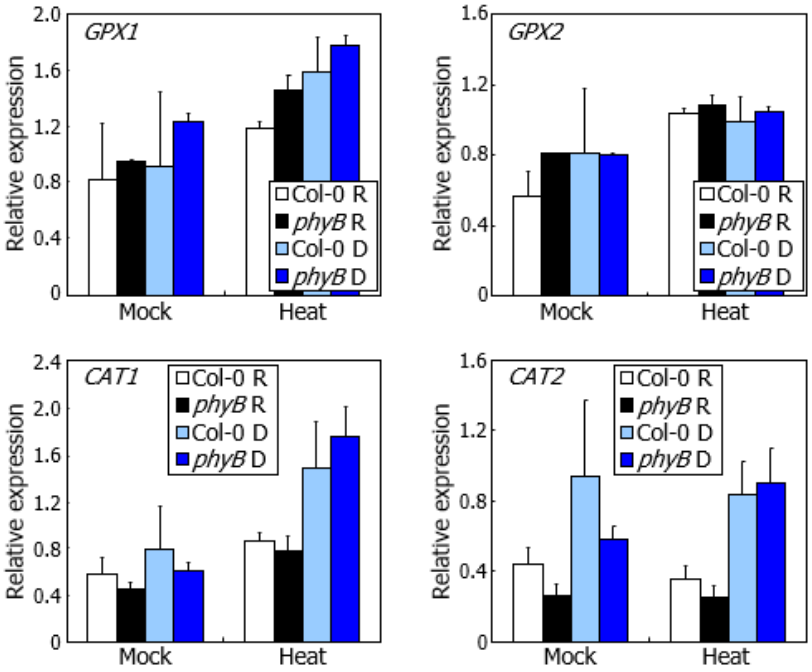

Figure 14. Expression of genes related to ROS detoxification

Seven-day-old seedlings grown under LDs transferred different light regimes at ZT6 for 2 h. Temperature of LD was 23°C. Seedlings were then subjected to 45°C for 45 min. Heat-treated whole seedlings were used for total RNA extraction. Biological triplicates were averaged and statistically analyzed. Bars indicate SE. D and R denote dark and red light, respectively.

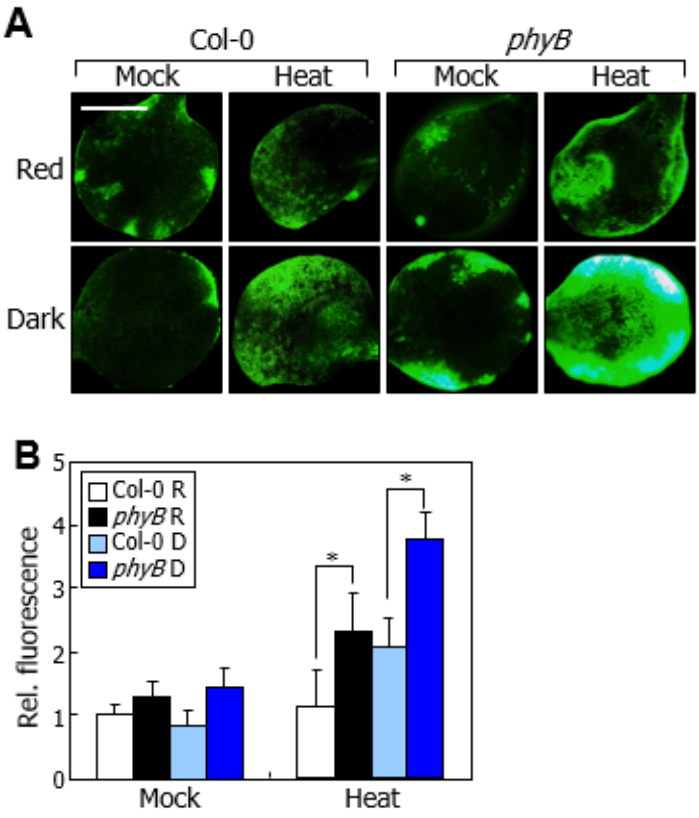

Figure 15. ROS accumulation in heat-treated seedlings

Seven-day-old seedlings grown under LDs at 23°C were further incubated in different light regimes at ZT6 for 2 h. Seedlings were then subjected to heat treatment. After heat treatment, seedlings were subjected to H_2DCFDA staining **(A)**. Relative fluorescence intensity was measured **(B)**. Scale bar, 600 μm. Biological triplicates, each consisting of ~15 seedlings, were averaged and statistically analyzed (*t*-test, $*P < 0.01$). Bars indicate SE.

event of thermotolerance development. It was found that red light-gated thermotolerance was still observed in the quadruple *pifq* mutant (Fig. 16A, B), which harbors quadruple mutations in *PIF1*, *PIF3*, *PIF4*, and *PIF5* genes (Zhang et al. 2013). In addition, thermal induction patterns of *APX2* gene expression were not discernibly different between Col-0 and the *pifq* mutant seedlings at high temperatures (Fig. 16C). Thus, it is evident that PIF-mediated light signaling is not directly involved in the light priming of thermotolerance.

It has been recently reported that retrograde chloroplast signals gate the thermal induction of *HSP* gene expression (Dickinson et al., 2018). I observed that light primes the thermal induction of at least *HSP70* and *HSP101* genes during thermotolerance development (Fig. 3). I therefore asked whether phyB-mediated light priming of thermotolerance development is linked with chloroplast-mediated gating of thermotolerance. Gene expression studies revealed that light-gated induction of *HSP* gene expression at high temperatures still occurred in *phyB* mutant seedlings (Fig. 17A), suggesting that the signaling pathway governing the phyB-mediated light priming of thermotolerance is functionally separated from that directing the chloroplast-mediated gating of thermotolerance.

I next asked whether chloroplast signals are involved in the light priming of *APX2* gene expression at high temperatures. It is known that 3-(3,4-dichlorophenyl)-1,1-dimethylurea (DCMU) triggers the photosynthetic electron flow from photosystem II to plastoquinone, leading to accumulation of oxidized plastoquinone pool, whereas 2,5-dibromo-3-methyl-6-isopropyl -p-benzoquinone (DBMIB) triggers the electron flow from plastoquinone to

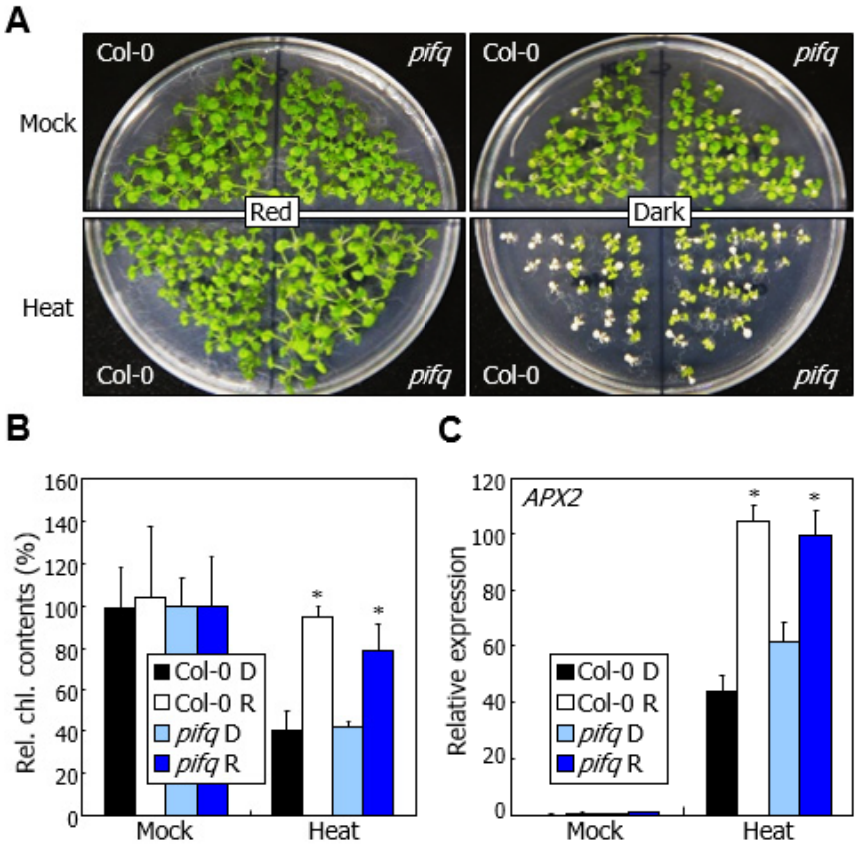

Figure 16. Thermotolerance responses in *Arabidopsis* mutants that are defective in PIF transcription factors

Seven-day-old seedlings grown under LDs at 23°C were further incubated under different light regimes at ZT6 for 2 h. D, dark; R, red. Seedlings were then exposed to 45°C for 45 min. Whole seedlings were used for total RNA extraction for gene expression assays. Biological triplicates were averaged and statistically analyzed (*t*-test, $*P < 0.01$, difference from dark). Biological triplicates, each consisting of ~15 seedlings, were averaged and statistically analyzed (*t*-test, $*P < 0.01$, difference from dark). Bars indicate SE. **(A)** Thermotolerance of the quadruple *pif1 pif3 pif4 pif5* mutant (*pifq*). **(B)** Relative chlorophyll contents in *pifq* mutant. **(C)** *APX2* transcription in *pifq* mutant.

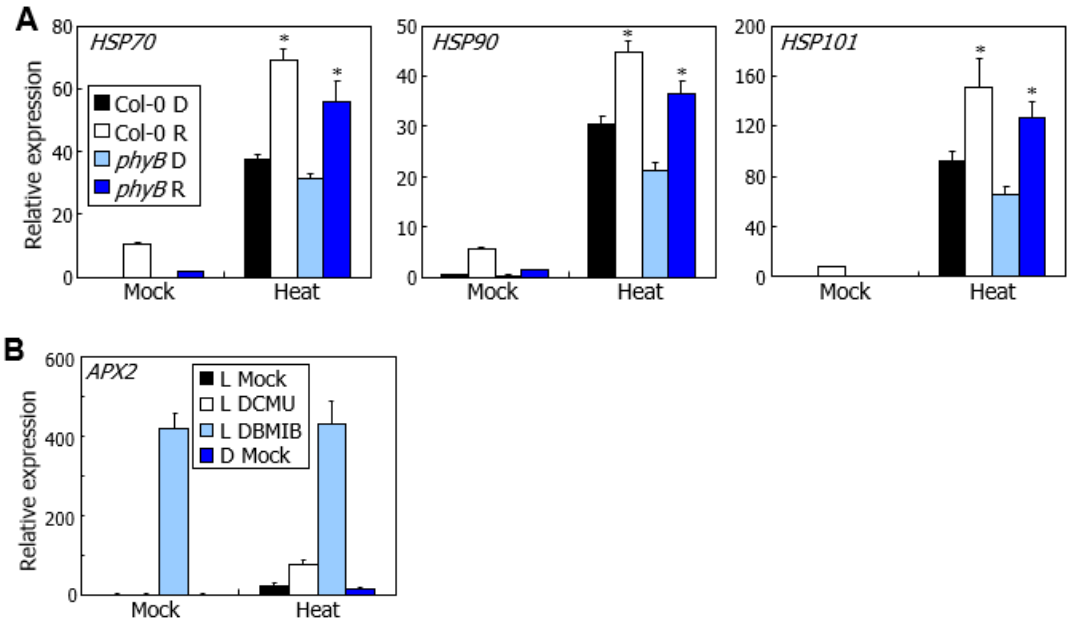

Figure 17. PhyB-primed thermotolerance is functionally distinct from chloroplast-gated thermotolerance

(A) *HSP* transcription in *phyB* mutant. Seven-day-old seedlings grown under LDs at 23°C were further incubated under different light regimes at ZT6 for 2 h. Seedlings were then subjected to 45°C for 45 min. Heat-treated whole seedlings were used for total RNA extraction. Biological triplicates were averaged and statistically analyzed (*t*-test, **P* < 0.01, difference from dark). Bars indicate SE. D and R denote dark and red light, respectively. **(B)** Effects of 3-(3,4-dichlorophenyl)-1,1-dimethylurea (DCMU) and 2,5-dibromo-3-methyl-6-isopropyl-p-benzoquinone (DBMIB) on *APX2* transcription at high temperatures. Seven-day-old Col-0 seedlings grown under LDs at 23°C were treated with either 30 μM DCMU or 50 μM DBMIB for 2 h before heat treatment.

cytochrome b6f complex, resulting in accumulation of reduced plastoquinone pool (Sherameti et al., 2002). It has been previously shown that while the thermal induction of *HSP70* expression is increased by DBMIB treatment, it is suppressed by DCMU treatment (Dickinson et al., 2018). My chemical treatment assays revealed that the thermal induction of *APX2* gene expression is increased by both DCMU and DBMIB (Fig. 17B). It has been previously reported that H_2O_2 activates HSFA1 transcription factors in *Arabidopsis* (Dickinson et al., 2018). Since *APX2* is the target of HSFA1 transcription factors, it is likely that DBMIB-induced ROS trigger HSFA1-mediated induction of *APX2* expression. These observations indicate that the phyB-gated thermal acceleration of ROS detoxification is distinct from the retrograde chloroplast-mediated gating of *HSP* gene induction.

PhyB-mediated priming of ROS detoxification leads to induction of thermotolerance

My data depict that the red light photoreceptor phyB mediates the light priming of ROS detoxification and thus thermotolerance development at high temperatures (Fig. 15). Thus, I finally asked whether the thermo-sensitive phenotype of *phyB* mutant is associated with disruption of ROS scavenging capability in the mutant. To answer the question, I examined thermotolerance phenotypes of the mutant in the presence of the ascorbate which is the substrate of APX enzymes. The thermo-susceptible phenotype of the *phyB* mutant was efficiently recovered in the presence of ascorbate, as verified by measurements of survival rates (Fig. 18A, B). This observation confirms that phyB-gated APX activity is functionally

linked with light priming of thermotolerance development. I also examined whether light priming of thermotolerance depends on GPX activity. Thermotolerance assay revealed that the effects of light-priming was still observed even in the presence of glutathione (GSH) (Fig. 19A, B) which is the substrate of GPX enzymes (Ramírez et al., 2013) suggesting that GPX pathway is not involved in light priming of thermotolerance. Taken together, phyB-mediated priming of APX activity leads to ROS detoxification thereby enhancing plant thermotolerance.

Altogether, my data illustrate that phyB-mediated light signaling, and perhaps that mediated by other photoreceptors as well, primes the development of thermotolerance via the APX2-mediated ROS detoxification (Fig. 20). The phyB-mediated light priming depends on the HSFA1 transcription factors that directly regulate the expression of the *APX2* gene, showing that the phyB-mediated light signals and the HSFA1-mediated temperature signals converge through the APX2-mediated ROS detoxification process. In nature, plants often experience high temperature conditions during the light period (Park et al., 2017). Therefore, the phyB-mediated light priming of thermotolerance development would provide an adaptation strategy that ensures plant survival under heat stress conditions.

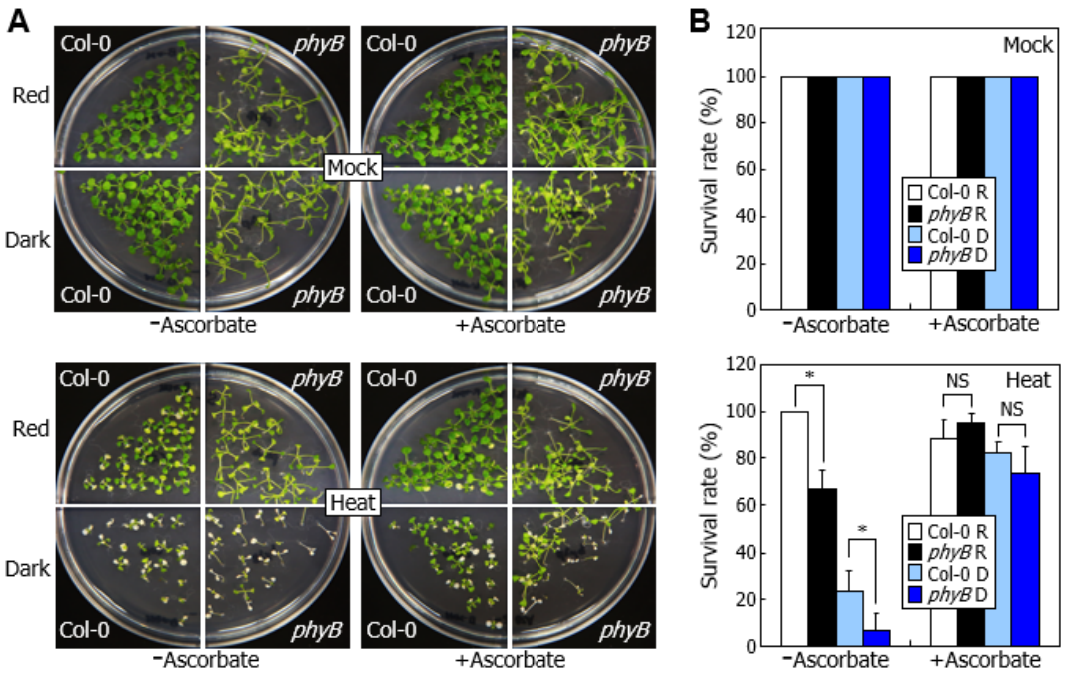

Figure 18. PhyB-mediated light signals prime ROS detoxification during thermotolerance development

Seven-day-old seedlings grown under LDs at 23°C in the presence or absence of 0.5 mM Asc for 7 d were exposed to either red light or darkness for 2 h. At ZT8, the seedlings were subjected to heat treatment. Biological triplicates, each consisting of 42 seedlings, were analyzed statistically (*t*-test, $*P < 0.01$, difference from Col-0). **(A, B)** Effects of Asc on the induction of thermotolerance in *phyB* mutant seedlings. Heat-treated seedlings were allowed to recover at 23°C under constant light for 5 d **(A)**. Survival rates were analyzed **(B)**. Bars indicate SE.

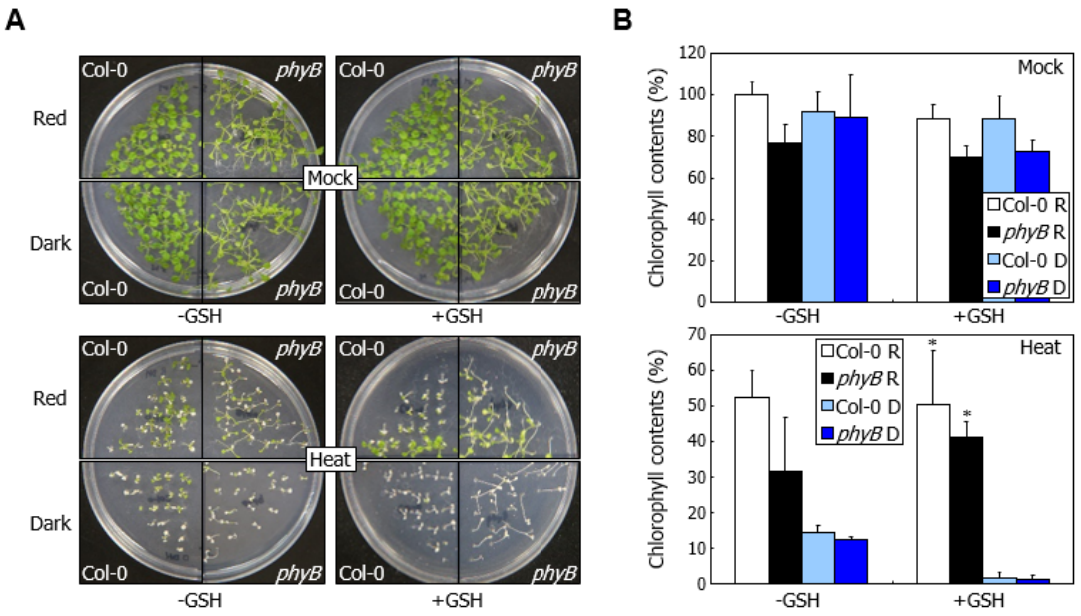

Figure 19. The effects of GSH on red light-primed thermotolerance

Seedlings grown under LDs in the presence of 1 mM Glutathione (GSH) for seven days were exposed to either red light or darkness for 2 h. Temperature of LD was 23°C. At ZT8, the seedlings were subjected to heat treatment. Biological triplicates, each consisting of 42 seedlings, were analyzed statistically (*t*-test, **P* < 0.01, difference from dark). **(A, B)** Effects of GSH on the induction of thermotolerance in *phyB* mutant seedlings. Heat-treated seedlings were allowed to recover at 23°C under constant light for 5 d **(A)**. Chlorophyll contents were analyzed **(B)**. Bars indicate SE.

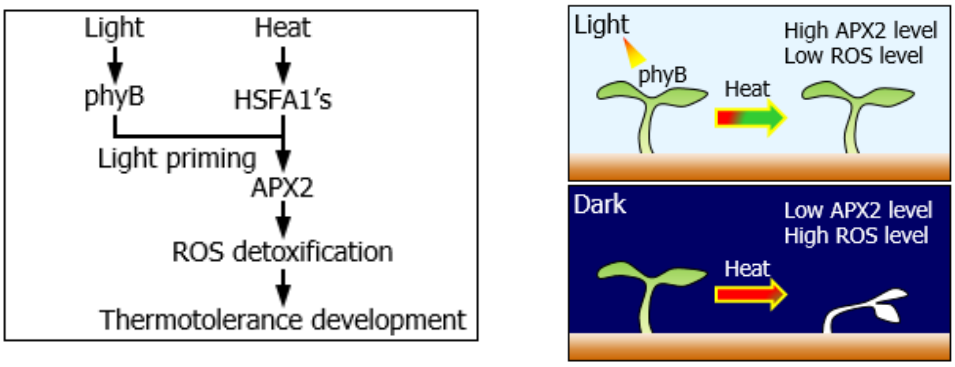

Figure 20. Working scheme for the light priming of thermotolerance development

Red light-activated phyB primes the thermo-induced *APX2* expression, resulting in a reduction of ROS accumulation in light-grown seedlings.

DISCUSSION

Signaling crosstalks between light and temperature cues during thermotolerance

Complicated functional relationships between light and temperature signaling events have been described extensively in plant environmental adaptation responses (Lee et al., 2012; Dickinson et al., 2018; Park and Park, 2018). One typical example is cold acclimation, in which cold activation of C-repeat binding factors (CBFs) plays central roles (Lee et al., 2012). It has been reported that plants grown under SDs exhibit enhanced freezing tolerance than those grown under LDs and *CBF* gene expression is markedly elevated under SDs (Lee et al., 2012). This acclimation mechanism enables plants to prepare for forthcoming cold temperatures under SDs, which are prevailing in the fall. Warm temperature responses are also linked to light signaling. Phytochromes, which are otherwise well-characterized red/far-red light photoreceptors, have been recently reported to function as thermosensors (Jung et al., 2016; Legris et al., 2016). Furthermore, circadian rhythms help thermomorphogenic responses to occur at specific time periods during the day (Zhu et al., 2016; Park et al., 2017). It is believed that these molecular and physiological mechanisms as a whole enable plants to enhance plant adaptation capability to high temperatures.

In this work, I showed that light primes the ROS detoxification reaction during the acquisition of thermotolerant capacity at high temperatures, providing

an additional example of light-temperature signaling crosstalks. My data are also supported by the recent report that describes the gating of thermotolerance development by chloroplast-derived signals (Dickinson et al., 2018). Sun light is the ultimate source of energy on the earth, and temperature is considered as a typical type of energy. In this sense, it is easily predictable that average temperature is relatively higher when photoperiod is longer (Park et al., 2017). It is therefore natural that plants have evolved a light priming system, with which they are able to prepare for possible heat stress in near future. This interpretation is also consistent with the previous view that light conditions enable plants to anticipate upcoming temperature fluctuations to prepare for appropriate temperature responses that would be required for optimal plant growth and performance (Griebel and Zeier, 2008; Lee et al., 2012). I believe that the light-temperature signaling crosstalk uncovered in this work would provide an excellent example for understanding the evolutionary relationship between light and temperature responses in plants.

Photoreceptor-mediated light signaling primes thermotolerance development

I found that the red light photoreceptor phyB mediates the light-gated thermotolerance response. The APX2 enzyme catalyzes the conversion of hydrogen peroxide to water, thus reducing ROS accumulation at high temperatures (Panchuk et al., 2002). The thermal induction of *APX2* gene expression was impaired in the *phyB* mutant. It has been recently reported that chloroplast signals also gate thermotolerance (Dickinson et al., 2018). Thus, a question was whether the phyB-mediated priming

of thermotolerance is related with the chloroplast-mediated gating of thermomorphogenesis.

HSPs act as molecular chaperones during thermotolerance development (Queitsch et al., 2000). Light activates photoreceptors and enhances chloroplast signaling (Lee et al., 2017). In addition, common signaling mechanisms have been identified between photoreceptors and chloroplast retrograde signaling (Martín et al., 2016). Furthermore, treatment with chemicals that affect the redox status of plastoquinone pool modulated the *APX2* expression in a pattern that is distinct from the mode of *HSP* gene expression in response to the chemicals during chloroplast-derived signaling. Therefore, it is postulated that light primes thermotolerance development by at least two distinct signaling pathways: the phyB-gated ROS detoxification and the chloroplast-gated protein quality control.

Various priming mechanisms have been described widely in various environmental adaptation processes, and their fundamental scheme has been considered as a plant memory process (Mauch-Mani et al., 2017). Epigenetic regulation is tightly linked with diverse memory processes in plants (Iwasaki and Paszkowski, 2014). Especially, hypermethylation events, such as H3K4me2 and H3K4me3, are known to be associated with transcriptional memory during thermotolerance development (Lämke et al., 2016). In addition, the distribution patterns of H3K9me2 and H3K27me3 in the promoter of *FLOWERING LOCUS C* (*FLC*) gene are responsive to long-term exposure to low temperatures, simply termed vernalization (Kim and Sung, 2013). It is possible that epigenetic regulation might also underlie the phyB-mediated priming of ROS detoxification and

thermotolerance development.

There are several reports supporting that phyB-mediated signaling is involved in epigenetic regulation. Red light illumination promotes seed germination by suppressing the expression of gene encoding the zinc-finger transcription factor *SOMNUS* (*SOM*) via the phyB-PIF1 module (Kim et al., 2008). Notably, the Jumonji C-containing histone arginine demethylases have been identified as the epigenetic regulators working downstream of SOM to promote gibberellic acid biosynthesis (Cho et al., 2012). Studies on natural genetic variations in *Arabidopsis* have also shown that phyB and histone deacetylase 6 are involved in light-controlled chromatin compaction events (Tessadori et al., 2009). It will be interesting to examine whether these epigenetic regulators also mediate the phyB-gated *APX2* gene expression at high temperatures.

Light-gated ROS detoxification and thermotolerance development

ROS function as critical signaling mediators in various cellular pathways and in adjusting redox status in plant cells (Mubarakshina et al., 2010; Noctor and Foyer, 2016). However, over-accumulation of ROS often causes oxidative damages on biological molecules and cellular structures and chlorophyll bleaching (Zhong et al., 2009), entailing that endogenous levels of ROS should be tightly regulated. It is known that high temperatures trigger ROS production (Panchuk et al., 2002). Accordingly, thermal adaptation mechanisms in plants possess efficient ROS scavenging systems to cope with the harmful chemicals (Lee et al., 2015). Several

ROS scavenging pathways have been described in plants (Mittler et al., 2004). Among them, APX, GPX and catalase are crucial enzymes that convert H_2O_2 to H_2O. I found that APX enzymes act as significant enzymes during red light-primed thermotolerance. On the other hand, I found that GPX and catalase would not be involved in light priming of thermotolerance. Therefore, it is likely that although they share similar chemical events, ROS scavenging pathways have distinct functions during plant growth and development. It is also not able that thermal-induction of APX2 gene was more prominent than that of other APX genes suggesting that APX2 is the major ROS scavenging factor during light-gated thermotolerance.

My findings describe that light primes thermotolerance development by activating the APX2-mediated ROS detoxification reaction. Conversely, exogenous application of the ROS scavenger ascorbate mimics the light gating effects on the induction of thermotolerance. Genes encoding ascorbate peroxidase enzymes are widely conserved in virtually all higher plant species (Caverzan et al., 2012). Considering the critical role of APX2 enzymes in triggering thermotolerance response, it would be possible to apply the light-gated ROS detoxification mechanism to enhance sustainable growth in crop plants under heat stress conditions. It will also be interesting to examine whether the phyB-mediated light priming mechanism would also mediate plant adaptation to global warming, which is emerging as a worldwide ecological issue in recent decades.

ACKNOWLEDGEMENT

I thank Dr. Yee-Yung Charng for providing *QK* mutant seeds and the *Arabidopsis* Biological Resource Center for *Arabidopsis* plant materials.

CHAPTER 2

HOS1 activates DNA repair systems to enhance plant thermotolerance

INTRODUCTION

Plants possess an astonishing capability of effectively adapting to a wide range of temperatures, ranging from freezing to near-boiling temperatures (Wanner et al., 1999; Wahid et al., 2007). Yet, heat is a critical obstacle to plant survival. The deleterious effects of heat shock on cell function include misfolding of cellular proteins, disruption of cytoskeletons and membranes, and disordering of RNA metabolism and genome integrity (Toivola et al., 2010; Welch et al., 1986; Boulon et al., 2010). Plants stimulate diverse heat shock response pathways in response to abrupt temperature increases.

Stressful biotic and abiotic factors, such as high temperatures or heat shock, trigger reactive oxygen species (ROS) burst in eukaryotes, which impair biological molecules and structures, including protein denaturation and DNA modifications and strand breakage (You et al., 2015). In addition, heat stress triggers genetic disturbance that is caused by the induction of DNA damages and the inhibition of DNA repair activity (Kantidze., 2016; Larkindale., 2005). While plant responses to heat stress extensively studied in terms of physiological and morphological alterations and signaling mediators in recent decades, such as HEAT SHOCK PROTEINs (HSPs) and the HEAT SHOCK FACTORs (HSFs) (Kantidze et al., 2016), how plants deal with heat stress to sustain DNA integrity has not been explored at the molecular level.

There have been great progress in the field in recent years, which is

further facilitated by technological advances. The comet assay is essentially a type of single cell gel electrophoresis, which enables the efficient access of DNA integrity at the single cell level regardless of cell division status. In particular, the comet assay analysis has been fruitfully applied to verify the genetic integrity with an additional advantage of potential application to different species without prior knowledge on DNA sequence (Menke et al., 2001). It has long been recognized that heat exposed cells are more sensitive to chemical and physical agents that trigger double-stranded DNA break (Manova et al., 2015), suggesting that heat shock inhibits the functioning of the DNA repair componets. Indeed, accumulating evidence strong support that heat shock inhibit a wide variety of components constituting diverse DNA repair mechanisms (Kantidze et al., 2016).

HIGH EXPRESSION OF OSMOTICALLY RESPONSIVE GENES 1 (HOS1) is RING-finger E3 ubiquitin ligase protein that functions as a cold signaling attenuator by degrading target proteins (Lee et al., 2001; Lazaro., 2012). Recent papers demonstrate that HOS1 acts as chromatin remodeling factor in regulation of flowering time (Cheng et al., 2020). In addition, HOS1 binds with the nuclear pore complex and promotes nuclear cytoplasmic mRNA export, maintaining circadian periodicity under various light and temperature conditions (MacGregor and Penfield, 2015). Therefore, HOS1 plays in various regulatory mechanisms in plants.

In this work, I demonstrated that the chromatin modifier HOS1 stimulates the transcription of genes encoding the components of DNA repair systems, which contributes to the acquisition of thermotolerance. HOS1 proteins are stabilized through direct interactions with the molecular chaperone HSP90 under high

temperature conditions. HOS1 directly binds to the chromatin of genes encoding the constituents of DNA repair systems in *Arabidopsis*, directly linking DNA repair with thermotolerance. Consequently, DNA damages were more prevailing in HOS1-deficient mutants under stressful high temperature conditions. Furthermore, in conjunction with the well-established roles of HOS1 in the induction of cold-tolerant responses, it is proposed that HOS1 plays a central role in plant adaptation to a wide range of environmental temperatures in nature.

MATERIALS AND METHODS

1. Plant materials and growth

All *Arabidopsis thaliana* lines used were in Columbia (Col-0) background, unless specified otherwise. Sterilized seeds were cold-imbibed (4°C) in darkness for 3 d and allowed to germinate on ½x Murashige and Skoog-agar (MS-agar) plates under long days (LDs, 16-h light and 8-h dark). White light illumination was provided at light intensity of 120 μmol photons $m^{-2}s^{-1}$ using fluorescent FLR40D/A tubes (Osram). Plants were grown in a controlled culture room set at 23°C with relative humidity of 60%.

The T-DNA insertional knockout mutants, *hos1-3, hos1-5, pif4-101, hos1-3 pif4-101, hda6,* and *hda15-1,* have been described previously (Jung et al., 2013; Kim et al., 2017). The *hsfa1a hsfa1b hsfa1d hsfa1e* quadruple knockout (*hsfa1* QK) mutants in Col-0 and Ws-2 background have been described previously (Swindell et al., 2007). The 35S:*MYC-HOS1* transgenic plants have been described previously (Jung et al., 2013). The RECQ2-deficient *recq2* mutant (SALK-087178.32.55.) was isolated from a pool of T-DNA insertional lines deposited in the *Arabidopsis* Biological Resource Center (ABRC, Ohio State University). The *atwhy2* (SAIL-694-A11), *atr* (SALK-032841.54.00.), *tdp1* (WiscDsLox361D04), *top3a-2* (GABI-476A12), *uvh6* (SALK-006580), and *wrnexo* (SALK-003278) mutants were also isolated from the mutant pool deposited in the ABRC. The *hos1-3 recq2* double mutant was generated by crossing *hos1-3* and *recq2* mutants. A gene encoding

a modified HOS1 protein (mHOS1) harboring H75Y and C89S substitutions was expressed driven by the cauliflower mosaic virus (CaMV) 35S promoter using the myc-pBA vector in the *hos1-3* mutant (Seo et al., 2010). A RECQ2-coding cDNA was overexpressed driven by the CaMV 35S promoter in the *hos1-3* mutant using the pEarleyGate 203 vector (Earley et al., 2006).

2. Thermotolerance assay

Seven-day-old *Arabidopsis* seedlings grown on MS-agar plates at 23°C under LDs were exposed to 37°C for appropriate durations. The heat-treated seedlings were allowed to recover at 23°C for 5 d under constant light conditions. For pharmacological treatments, geldanamycin (GDA), an antibiotic that inhibits HSP90 function (Ochel et al., 2001), was included at a final concentration of 10 μM in MS liquid, in which seedlings were floated during heat treatments. Radicicol, a macrolactone antibiotic that inhibits HSP90 function (Sharma et al., 1998), was used at a final concentration of 10 μM. Cisplatin, a crosslinking agent, was used at a final concentration of 10 μM. Mitomycin C (MMC) was used at a final concentration of 10 μg/ml (Rohrig et al., 2018). MG132, a 26S proteasome inhibitor (Lee and Goldberg, 1998), was used at a final concentration of 10 μM. The pharmacological reagents were purchased from Signal-Aldrich.

For analysis of electrolyte leakage, aerial parts of heat-treated seedlings were floated on 0.4 M sorbitol solution in darkness for 12 h, after which sample conductivity of the solution was measured. Then, the seedling sample solutions were boiled in the same solution for 5 min, and total conductivity of the solution

was measured. Electrolyte leakage is represented by relative conductivity, which is calculated by dividing sample conductivity by total conductivity. Conductivity was measured using the Orion 5-star conductivity meter (Thermo Fisher Scientific).

For measurements of chlorophyll contents, heat-treated seedlings were allowed to recover at 23°C for 5 d under constant light conditions. Chlorophylls were extracted from the seedlings by soaking in 100% methanol at 4°C for 2 h in complete darkness. Chlorophyll contents were analyzed using the Mithras LB940 multimode microplate reader (Berthold Technologies). The absorbance data were collected using the MikroWin 2010 software (Berthold Technologies). The contents of chlorophyll a and chlorophyll b were calculated from the absorbance values at 650 and 660 nm (Lee et al., 2015). Total chlorophyll contents were calculated by summing up those of chlorophyll a and chlorophyll b. Relative chlorophyll contents were calculated by dividing total chlorophyll contents of heat-treated seedlings by those of seedlings treated under mock conditions.

To examine the effects of heat acclimation on the HOS1-mediated induction of thermotolerance, seven-day-old seedlings were exposed to 37°C for 2 h and incubated at 23°C for 2 h before exposure to 45°C for 7 h. The heat-treated seedlings were allowed to recover at 23°C for 5 d under constant light conditions.

3. Gene expression analysis

Total RNA samples were extracted from seven-day-old seedlings grown on MS-agar plates and pretreated extensively with RNase-free DNase to get rid of genomic DNA contamination before use. RNA concentration was measured using the

NanoDrop 2000 spectrophotometer (Thermo Fisher Scientific). Analysis of transcript levels was performed by reverse transcription-mediated quantitative PCR (RT-qPCR) along with the rules proposed to assure reproducible and accurate measurements (Udvardi et al., 2008). RT-qPCR reactions were conducted in 384-well blocks with the Applied Biosystems QuantStudio 6 Flex Real-Time PCR System (Life Technologies) using the SYBR Green I master mix in a volume of 10 μl. A two-step thermal cycling profile employed was 15 s at 95°C for denaturation and 50 s at 60-65°C, depending on the calculated melting temperatures of PCR primer pairs used, for concomitant annealing and polymerization. PCR primers were designed using the Primer Express Software installed in the system and listed in Supplementary Table 1. An additional round of 10 min at 65°C was provided at the end of individual thermal cycles for the completion of PCR reactions. An *eIF4A* gene (At3g13920) was included in the RT-qPCR reactions as internal control to standardize the differences in the amounts of cDNA samples used. Gene expression data collection and analysis were conducted using the QuantStudio Real-Time PCR V1.1 software (Life Technologies).

4. Protein stability

Seven-day-old seedlings grown on MS-agar plates at 23°C under LDs were exposed to 37°C for varying durations. Whole seedlings were harvested for the extraction of total proteins. The MYC-HOS1 proteins were immunologically detected using an anti-MYC antibody (Millipore). The HOS1 proteins and HSP90 proteins were immunodetected using an anti-HOS1 antibody (AbClon) and an anti-HSP90 antibody

(Millipore), respectively. TUBULIN (TUB) proteins were similarly immunodetected using an anti-TUB antibody for protein quality control. The horseradish peroxidase (HRP)-conjugated secondary antibodies, goat anti-mouse IgG-HRP and goat anti-rabbit IgG-HRP (Millipore), were used for chemiluminescent western blot detection. Gel images were collected using the Fusion Molecular Imaging V15.18 software (Vilber Lourmat). Three independent biological samples were analyzed per each assay.

5. RNA sequencing

Seven-day-old seedlings grown on MS-agar plates at 23°C under LDs were exposed to 37°C for 1.5 d. Total RNA samples were extracted from whole seedlings. The RNA samples were then subjected to RNA sequencing in Chunlab, Inc. (Seoul, Korea). Biological triplicates were statistically analyzed. Genes with P values < 0.15 and thermal induction by more than 4-fold in Col-0 seedlings but no discernible thermal induction in *hos1-3* seedlings were regarded as differentially expressed genes. Gene ontology (GO) analysis was performed using the Biological Networks Gene Ontology tool (BiNGO) with Benjamini-Hochberg corrected $P < 0.01$. The network diagram shows significantly overrepresented GO terms. The raw RNA-seq data were deposited in the NCBI's SRA database with accession number of PRJNA658831.

6. Comet assay

Comet assays were conducted, essentially as described previously (Menke et al., 2001). Briefly, approximately 150 mg of plant materials were used for individual assays, which were performed in darkness. Microscopic slide glasses were coated with a layer of 1% normal melting point agarose and dried at room temperatures. Seedlings were sliced with a razor blade in 400 μl PBS buffer (160 mM NaCl, 4 mM NaH_2PO_4, 8 mM Na_2HPO_4, pH 7.2) containing 50 mM EDTA. Two drops of nuclei suspension (approximately 40 μl each) were put separately on each slide, mixed with the same volume of 1% low melting point agarose at 42°C, and covered with cover glasses. Nuclei were then extracted using high salt buffer (2.5 M NaCl, 100 mM EDTA, 10 mM Tris-HCl, pH 7.3) for 20 min at room temperatures. Following equilibration for 5 min in 1x TBE buffer 90 mM Tris-borate, 2 mM EDTA, pH 8.5) on ice, electrophoresis was performed at room temperatures using 1 X TBE running buffer at 30V (1V/cm, 15 mA) for 6min. The gels were visualized by staining with SYBR Green I and photographed using the Carl Zeiss LSM510 confocal microscope. Comet images were processed using the Zen 2 software (blue edition, Carl Zeiss). Three independent biological samples, in which at least 10 nuclei were photographed for each sample, were examined, and the data were analyzed using the Casp-1.2.3b2 software (http://casplab.com/).

7. Chromatin immunoprecipitation (ChIP)

The ChIP assays were conducted, essentially as described previously (Lee et al., 2014). Briefly, ten-day-old seedlings grown on MS-agar plates under LDs were vacuum-infiltrated with 1% (v/v) formaldehyde for cross-linking. The plant materials

were thoroughly ground in liquid nitrogen after quenching the cross-linking process and resuspended in 30 ml of nuclear extraction buffer (1.7 M sucrose, 10 mM Tris-Cl, pH 7.5, 2 mM $MgCl_2$, 0.15% Triton-X-100, 5 mM β-mercaptoethanol, 0.1 mM PMSF) containing a mixture of protease inhibitors (Sigma-Aldrich). The resuspended sample was filtered through miracloth filters (Millipore) and centrifuged at 4,300 X g for 20 min at 4°C. Nuclear fractions were isolated by the sucrose cushion method, lysed in lysis buffer (50 mM Tris-Cl, pH 8.0, 0.5 M EDTA, 1% SDS) containing a mixture of protease inhibitors, and sonicated to obtain chromatin fragments of 400-700base pairs.

Five μg of anti-MYC antibody (Millipore) was added to the chromatin preparation and incubated at 4°C for 16 h. The protein G-agarose beads (Millipore) were then added to the solution for 1 h. The mixture was then centrifuged at 4,000X g for 2 min at 4°C. Following reverse cross-linking of the precipitates, residual proteins were removed using proteinase K. DNA fragments were purified using a silica membrane spin column (Promega). Quantitative PCR was performed to determine the amounts of DNA enriched in chromatin preparations, and the values were normalized to the amount of input in each sample. For ChIP assays using an anti-H3Ac antibody (Millipore), the values were normalized to the amount of *eIF4A* DNA fragments in each sample.

8. Analysis of endogenous ROS contents

The 2',7'-dichlorodihydrofluorescein diacetate (H_2DCFDA, Sigma-Aldrich) fluorescent dye was used at a final concentration of 10 μM for the detection

of hydrogen peroxide. For H_2DCFDA staining, cotyledons of seven-day-old seedlings were incubated in the H_2DCFDA staining solution for 20 min at room temperatures. The plant samples were then destained by washing thoroughly with deionized water and visualized by optical microscopy (Olympus). Microscopic images were collected using the cellSens Standard software (Olympus). The ImageJ program was used for the quantification of stain intensity (http://rsb.info.nih.gov/ij/).

The DAB staining solution (1 mg/ml) and the NBT staining solution (1 tablet/50 ml) were used for analyzing the endogenous contents of hydrogen peroxide and superoxide radicals, respectively. Seven-day-old seedlings grown on MS-agar plates at 23°C were subjected to histochemical stainingat 23°C or 37°C for 1 h in complete darkness. The plant samples were then destained with deionized water and visualized by the EOS 5D Mark III camera (Canon). The stain intensity was quantitated using the ImageJ program.

9. Infrared thermography

Thermal images of seven-day-old seedlings incubated at different temperatures were recorded using the thermal imaging camera T420 (FLIR Systems) and analyzed using the FLIR tools (http://www.flirkorea.com/home/).

10. Transcriptional activation activity assay

A set of reporter and effector plasmids was constructed. The reporter plasmid contains 4 copies of the GAL4 upstream activation sequence and the β-glucuronidase

(GUS) reporter gene. To construct the 35S:*HOS1* effector plasmids, HOS1-coding sequences were fused in-frame to the GAL4 DNA-binding domain-coding sequence, and the fusions were subcloned into an expression vector containing the CaMV 35S promoter. The *HOS1* gene sequences tested include a full-size, an N-terminally truncated, and a C-terminally truncated sequences encoding amino acid residues 1-927, 457-927, and 1-457, respectively. *Arabidopsis* mesophyll protoplasts were isolated from three-week-old Col-0 plants. The reporter and effector plasmids were cotransformed into *Arabidopsis* protoplasts by a polyethylene glycol-calcium transfection method. GUS activities were measured by the fluorometric method, as described previously (Seo et al., 2011). A CaMV 35S promoter-luciferase construct was also cotransformed for internal control. The luciferase assay was performed using the luciferase assay system kit (Promega).

11. Yeast two-hybrid

To examine the physical interactions between HOS1 and HSP90, I employed yeast two-hybrid screening using the BD Matchmaker system (Takara). The pGADT7 vector was used for GAL4 activation domain, and the pGBKT7 vector was used for GAL4 DNA-binding domain. The HOS1-coding sequences were subcloned into the pGBKT7 vector. The HSP90-coding sequence was subcloned into the pGADT7 vector. The yeast strain used for transformation was AH109 (Leu-, Trp-, Ade-, His-), which harbors chromosomally integrated reporter genes encoding β-galactosidase (lacZ) and HIS3 enzyme under the control of the GAL1 promoter.

Transformation of yeast cells was performed according to the manufacturer's instruction. Colonies obtained were restreaked on a selective medium lacking Leu, Trp, Ade, and His. To prevent nonspecific growth of yeast cells, 3-amino-1,2,4-triazole was included in the media at a final concentration of 15 mM.

12. Bimolecular fluorescence complementation (BiFC)

Bimolecular fluorescence complementation (BiFC) was also employed to examine the potential interactions between HOS1 and HSP90. The YFP^{N}-HOS1 and HSP90-YFP^{C} constructs were coexpressed transiently in *Arabidopsis* protoplasts by a polyethylene glycol-calcium transfection method. Sixteen hours following cotransfection, the subcellular distribution of HOS1 and HSP90 proteins was visualized by differential interference contrast microscopy and fluorescence microscopy. Reconstitution of YFP fluorescence was observed using the Zeiss LSM510 confocal microscope (CarlZeiss) with the following YFP filter setup: excitation 513 nm, 458/514 dichroic, and emission 560-615 nm bandpass filter.

13. Trypan blue staining

Dead cells in plant tissues were selectively visualized by trypan blue staining, as described previously (Menke et al., 2001). Whole seedlings were soaked in a lactophenol-trypan blue staining solution (10 ml of lactic acid, 10 ml of glycerol, 10 g of phenol, 10 mg of trypan blue, 10 ml of deionized water). The staining solution containing plant samples was boiled for 1 min and incubated overnight

at room temperatures. They were then distained by incubating in the destaining solution (lactophenol:ethanol=1:2) for 30 min at room temperatures.

14. Statistical analysis

The statistical significance between two means of measurements was determined using the one-sided Student *t*-test with *P* values of < 0.01 or < 0.05. To analyze statistical significance for more than two populations, one-way analysis of variance (ANOVA) with *post hoc* Tukey test ($P < 0.01$) or two-way ANOVA with *post hoc* Fisher's multiple comparison test ($P < 0.05$) was employed. Statistical analyses were performed using the IBM SPSS Statistics 25 software (https://www.ibm.com/).

Primers	Sequences	Usage
eIF4A-F	5′-TGACCACACAGTCTCTGCAA	RT-qPCR
eIF4A-R	5′-ACCAGGGAGACTTGTTGGAC	"
HSP60-F	5′-CAGAATGAGCTGGAGCAGGA	"
HSP60-R	5′-TGGGACCCATGGTGACTTTA	"
HSP70-F	5′-TGAGGCAGATGAGTTCGAGG	"
HSP70-R	5′-CTCCTGCACCACCCATATCA	"
HSP90.1-F	5′-TGCGAGGTCTGGAACAAAAG	"
HSP90.1-R	5′-ACCACCAGCTTGAGACTCCC	"
HSFA1a-F	5′-TGCATTGTCTGGTGGACACA	"
HSFA1a-R	5′-GAAGAGCCTTGTCGGTTGGT	"
HSFA1b-F	5′-GTGTCGAGGTGGGGAAGTTT	"
HSFA1b-R	5′-TTTGTTGTTGCCTTTGCTCC	"
HSFA2-F	5′-GGGGAGGTTGAGAGGTTGAA	"
HSFA2-R	5′-TTGGCAAGGAACGTCATCAT	"
AtMSH5-F	5′-AGAGCTGCTTGCCTGTTTCT	"
AtMSH5-R	5′-GTGAAGGCCATAGCTCAGCA	"
AtWHY2-F	5′-TGGTCGATTGTTCGCACCTT	"
AtWHY2-R	5′-TACGCTCACCAATAGCAGGC	"
TOP3A-F	5′-ACAAGACATCCTGCATGGGG	"
TOP3A-R	5′-GCTCCAGTTAGACTCTCCGC	"
RECQ2-F	5′-GTCGAAGCGCATTTTTCCGT	"
RECQ2-R	5′-GCTTGCGTTTCTTGCACCAT	"
RAD50-F	5′-CACGGTGAGCTGGAGAAACT	"
RAD50-R	5′-GGCTAAACGCTCCAGGTCTT	"
TDP1-F	5′-CGAGAAGTGGTTGGCTGAGT	"
TDP1-R	5′-ATTGCCAGCAGCATAACCCT	"
HOS1-F	5′-GCACAAGGATGCAACCAGAC	"
HOS1-R	5′-TTGTTTCATCTGACCGCCAT	"
UVH6-F	5′-AGCTTCCATTATCACCTGTA	"
UVH6-R	5′-TTAGCGTCTAGGGCTCGCTT	"
RECQ2-P1-F	5′-ATATATATATTTTTTTCCAAAAGTTAACGGT	ChIP-PCR
RECQ2-P1-R	5′-CATGACTAGTTTAACTCAATTTTTCAG	"
RECQ2-P2-F	5′-TTTATAAAACTTACTCGGTTTTTTTGATAAA	"
RECQ2-P2-R	5′-ACTGTAGCTCCAAATAATTGTAGTG	"
RECQ2-P3-F	5′-CTTGGGAAACACTTGCCCT	"
RECQ2-P3-R	5′-CTTTGAAGCACCAGACAGA	"
RECQ2-P4-F	5′-ACACTTTTCAAATAGGTCATTTGGA	"
RECQ2-P4-R	5′-AATATATATGTTTAAAAGAAGAAGAAAAGTTAT	"
RECQ2-P5-F	5′-TTTTTTATAATAATTTCTATAGAATTCTTTTAATAT	"
RECQ2-P5-R	5′-TGCTGCATCACAACGACAAGTA	"
YUC8-F	5′-CAACTCCCAATAAAAGACCATCA	"
YUC8-R	5′-TGGTTTCCTCAATCAATTTTCAA	"
HOS1-MYC-F	5′-AAACCCGGGAGATGGATACGAGAGAAATCAACGG	Subcloning
HOS1-MYC-R	5′-CCTTAATTAATCATCTTGCTGCGAATCTACG	"
HOS1-H75Y-F	5′-CATGTGGTTATGCCTCCTTG	"
HOS1-H75Y-R	5′-CAAGGAGGCATAACCACATG	"
HOS1-C89S-F	5′-GGTGTGATGTTTCTCCTATCTG	"
HOS1-C89S-R	5′-CAGATAGGAGAAACATCACACC	"
GAL4DB-HOS1-F	5′-ACCCGGGAATGGATACGAGAGAAATCAA	"
GAL4DB-HOS1-R	5′-AAAGTCGACTCATCTTGCTGCGAAT	"
GAL4DB-HOS1-C-F	5′-ACCCGGGACTCCAGGAAGCTTGTAG	"
GAL4DB-HOS1-N-R	5′-AAAGTCGACTCAGAGTGCCTCCTC	"

Table 2. Primers used in Chapter 2

The primers were designed using the NCBI Primer-BLAST software

(https://www.ncbi.nlm.nih.gov/tools/primer-blast/) in a way that their calculated melting temperatures are in a temperature range of 50 - 60°C. F, forward primer. R, reverse primer.

RESULTS

HOS1 is required for the acquisition of thermotolerance

During the course of analyzing the pleiotropic phenotypes of HOS1-deficient mutants (Lee et al., 2001; Lazaro et al., 2012; Jung et al., 2013), I found that the *hos1-3* and *hos1-5* mutants exhibited a significantly reduced thermotolerance compared to that observed in wild-type Col-0 seedlings (Fig. 21A-C). Electrolyte leakage assays showed that cellular integrity was disturbed more severely in the mutants following heat shock (Fig. 21D). In contrast, transgenic overexpression of *HOS1* gene enhanced thermotolerance (Fig. 22). On the other hand, the *hos1-3* mutant still exhibited acquired thermotolerance, comparable to that observed in Col-0 seedlings (Fig. 23). These observations indicate that HOS1 is functionally associated with basal thermotolerance but not linked with acquired thermotolerance.

Thermomorphogenic traits, such as elongated hypocotyls and leaf hyponasty, enhance leaf cooling under warm environments (Crawford et al., 2012; Park et al., 2017). HOS1 attenuates hypocotyl thermomorphogenesis by suppressing the activity of PHYTOCHROME INTERACTING FACTOR 4 (PIF4) (Kime et al., 2017). Infrared thermal imaging of heat-treated seedlings revealed that leaf temperatures were not discernibly different in Col-0 and *hos1-3* seedlings (Fig. 24). In addition, the *hos1-3 pif4-101* double mutant still exhibited a reduced thermotolerance, like the *hos1-3* mutant (Fig. 25). Conversely, it has been reported

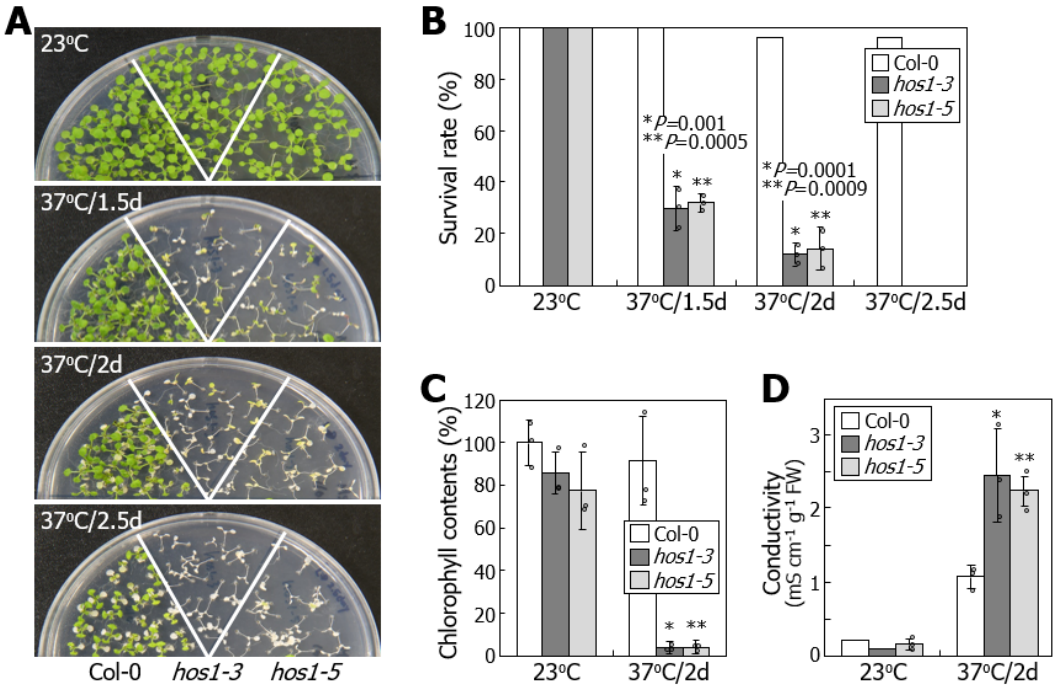

Figure 21. HOS1 is required for the acquisition of thermotolerance

Seven-day-old seedlings grown on MS-agar plates at 23°C were exposed to 37°C for the indicated durations. Three measurements, each consisting of 15-20 seedlings, were statistically analyzed using one-sided Student *t*-test (**C**; **P* = 0.01917, ***P* = 0.01722, **D**; **P* = 0.034, ***P* = 0.013, difference from Col-0). Error bars indicate standard error of the mean (SE). The circles indicate individual data points. d, day. **(A-C)** Thermotolerance phenotypes of *hos1* mutants. Heat-treated seedlings were allowed to recover at 23°C for 5 d under constant light conditions before taking photographs **(A)**. Survival rates and relative chlorophyll contents were measured (**B** and **C**, respectively). **(D)** Electrolyte leakage assays. Conductivity was measured using seedlings that were allowed to recover at 23°C for 2 d following heat treatments.

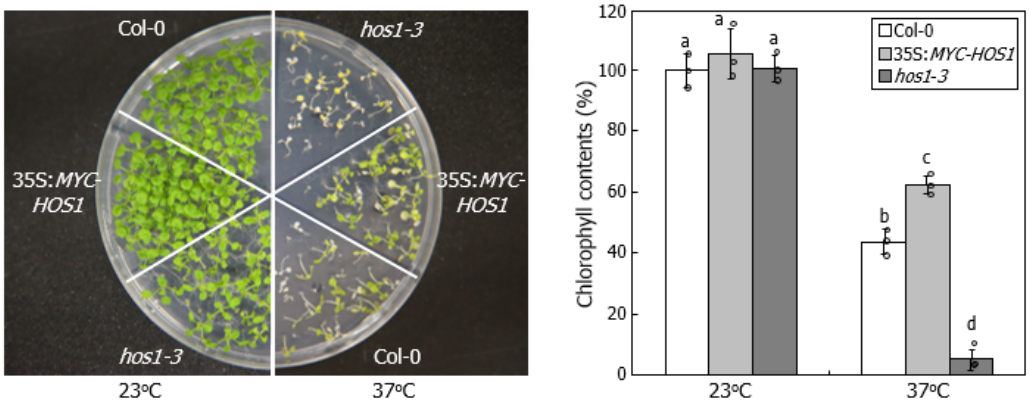

Figure 22. Thermotolerance phenotypes of 35S:*MYC-HOS1* transgenic plants

Seven-day-old seedlings grown on Murashige and Skoog-agar (MS-agar) plates at 23°C were exposed to 37°C for 4 d. Heat-treated seedlings were allowed to recover at 23°C for 5 d under constant light conditions before taking photograph. Chlorophyll contents were measured. Three measurements, each consisting of 15-20 seedlings, were statistically analyzed. Error bars indicate SE. Different letters represent significant differences ($P < 0.01$) determined by one-way analysis of variance (ANOVA) with *post hoc* Tukey test. The circles indicate individual data points.

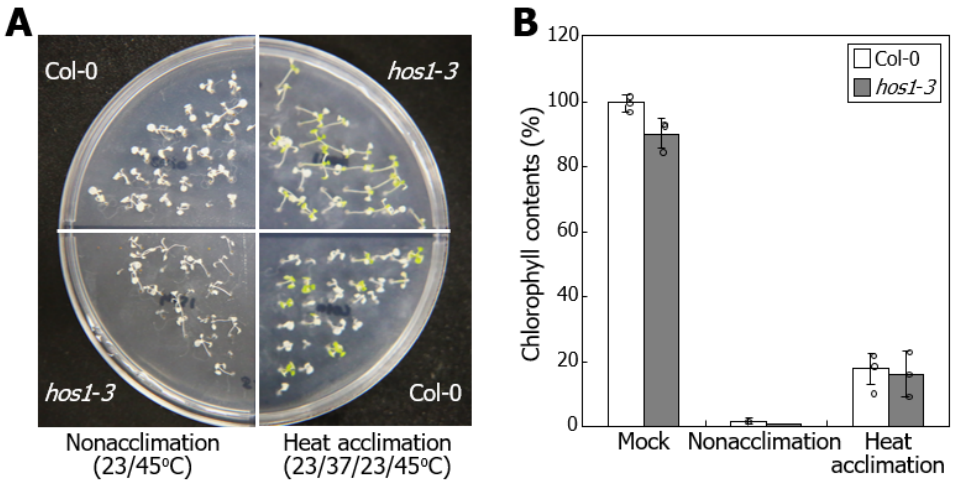

Figure 23. Acquired thermotolerance phenotypes of *hos1-3* mutant

Seven-day-old seedlings grown on MS-agar plates at 23°C were heat-acclimated by incubating at 37°C for 2 h and further incubated at 23°C for 2 h prior to heat treatments. The heat-acclimated seedlings were exposed to 45°C for 7 h and then allowed to recover at 23°C for 5 d under constant light conditions before taking photographs **(A)**. Chlorophyll contents were measured **(B)**. Biological triplicates, each consisting of 15-20 seedlings, were statistically analyzed using one-sided Student *t*-test (*$P < 0.01$, difference from Col-0). Error bars indicate SE. The circles indicate individual data points.

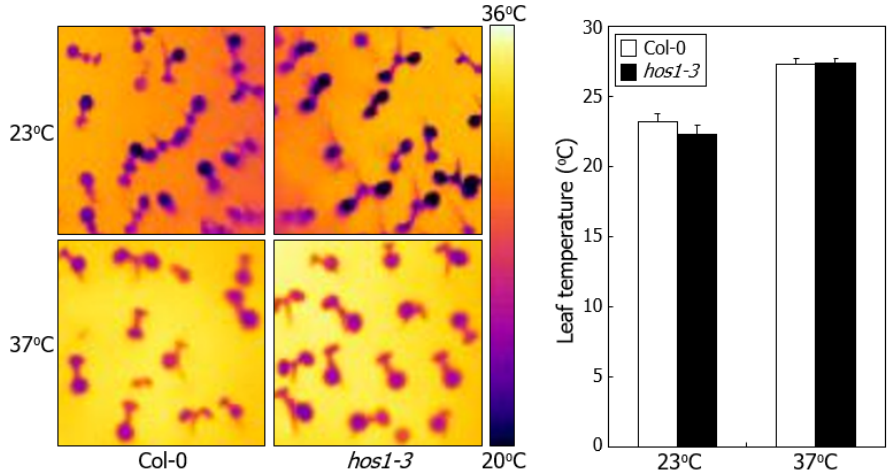

Figure 24. Thermal images of heat-treated seedlings

Seven-day-old seedlings grown on MS-agar plates at 23°C were exposed to 37°C for 1.5 d, and leaf temperatures were monitored using a thermal imaging infrared camera. The vertical colored node represents a range of temperatures. Two independent measurements, each consisting of 15 seedlings, were performed in parallel to ensure the reproducibility of thermal imaging and quantitation. The upper side of each box plot indicates median. Error bars indicate SE (one-sided *t*-test, $*P < 0.01$, difference from Col-0).

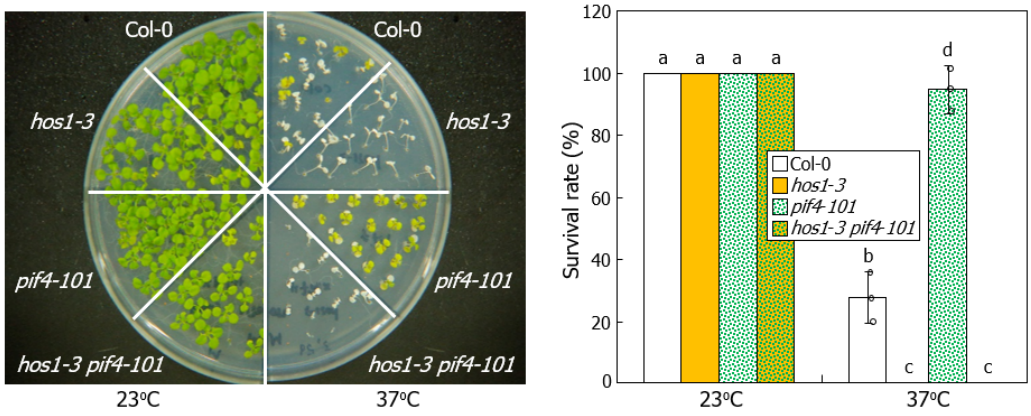

Figure 25. Thermotolerance phenotypes of *hos1-3 pif4-101* double mutant

The *hos1-3* mutant was genetically crossed with the PIF4-deficient *pif4-101* mutant, resulting in the *hos1-3 pif4-101* double mutant. Seven-day-old seedlings grown on MS-agar plates at 23°C were exposed to 37°C for 1.5 d. The heat-treated seedlings were allowed to recover at 23°C for 5 d under constant light conditions. Measurements of survival rate (right pannel). Biological triplicates, each consisting of 35-40 seedlings, were statistically analyzed. Error bars indicate SE. Different letters represent significant differences ($P < 0.01$) determined by one-way ANOVA with *post hoc* Tukey test. The circles indicate individual data points.

that the thermomorphogenic hypocotyl growth of the *hos1-3* mutant were compromised in the double mutant (Kim et al., 2017). The previous and my own observations indicate that the HOS1-mediated thermotolerance is independent of PIF4.

HOS1 possesses a RING-finger domain, which is essential for its ubiquitin ligase activity (Lee et al., 2001). It is known that the enzyme activity of HOS1 is disrupted by H75Y and C89S substitutions (Dong et al., 2006). Transgenic production of a modified protein (mHOS1) harboring the residue substitutions in the *hos1-3* mutant efficiently rescued the disturbed thermotolerance (Fig. 26, 27), showing that the enzyme activity is not necessary for the HOS1 function during thermotolerance.

Plant responses to heat stress are often mediated by reactive oxygen species (ROS) (Mittler et al, 2004). I observed that ROS accumulated to similar levels in Col-0 and *hos1*-3 seedlings at high temperatures (Fig. 28). Histochemical detection of hydrogen peroxide and superoxide radicals further supported that ROS accumulation is not functionally linked with the HOS1-mediated thermotolerance (Fig. 29).

DNA damage response is reduced in *hos1-3* mutant at high temperatures

To obtain molecular insights into how HOS1 regulates thermotolerance, I employed RNA sequencing analysis. The transcription of numerous genes was altered at

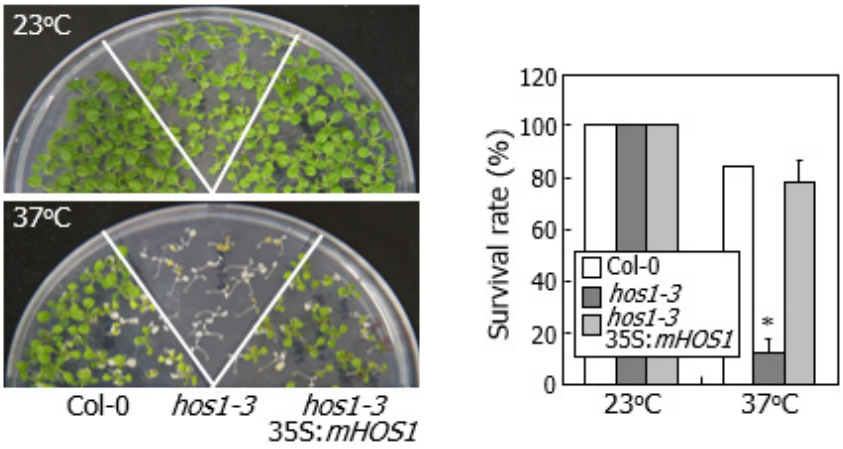

Figure 26. Complementation of *hos1-3* mutant

A gene sequence encoding the modified HOS1 protein (mHOS1) harboring H75Y and C89S substitutions was overexpressed driven by the cauliflower mosaic virus (CaMV) 35S promoter in the *hos1-3* mutant. Three measurements, each consisting of 15-20 seedlings, were statistically analyzed using one-sided Student *t*-test (**P* = 0.0005, difference from Col-0). Error bars indicate SE.

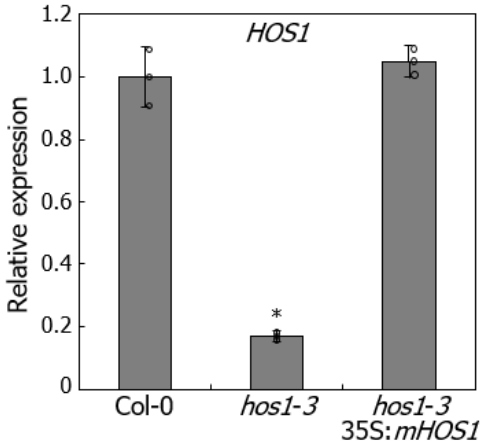

Figure 27. Transcription of *HOS1* gene in 35S:*mHOS1* *hos1-3* plants

The mHOS1-coding sequence was expressed driven by the cauliflower mosaic virus (CaMV) 35S promoter in the *hos1-3* mutant. Among multiple transgenic lines, one line exhibiting a transcript level similar to that observed in Col-0 plants was chosen for further analysis. Seedlings grown on MS-agar plates at 23°C for 7 d were exposed to 37°C for 1.5 d. Whole seedlings were used for total RNA preparation. Transcript levels were analyzed by reverse transcription-mediated quantitative PCR (RT-qPCR). Biological triplicates, each consisting of 15 seedlings, were statistically analyzed using one-sided Student *t*-test (*P = 0.0015, difference from Col-0). The upper side of each box plot indicates median. Error bars indicate SE. The circles indicate individual data points.

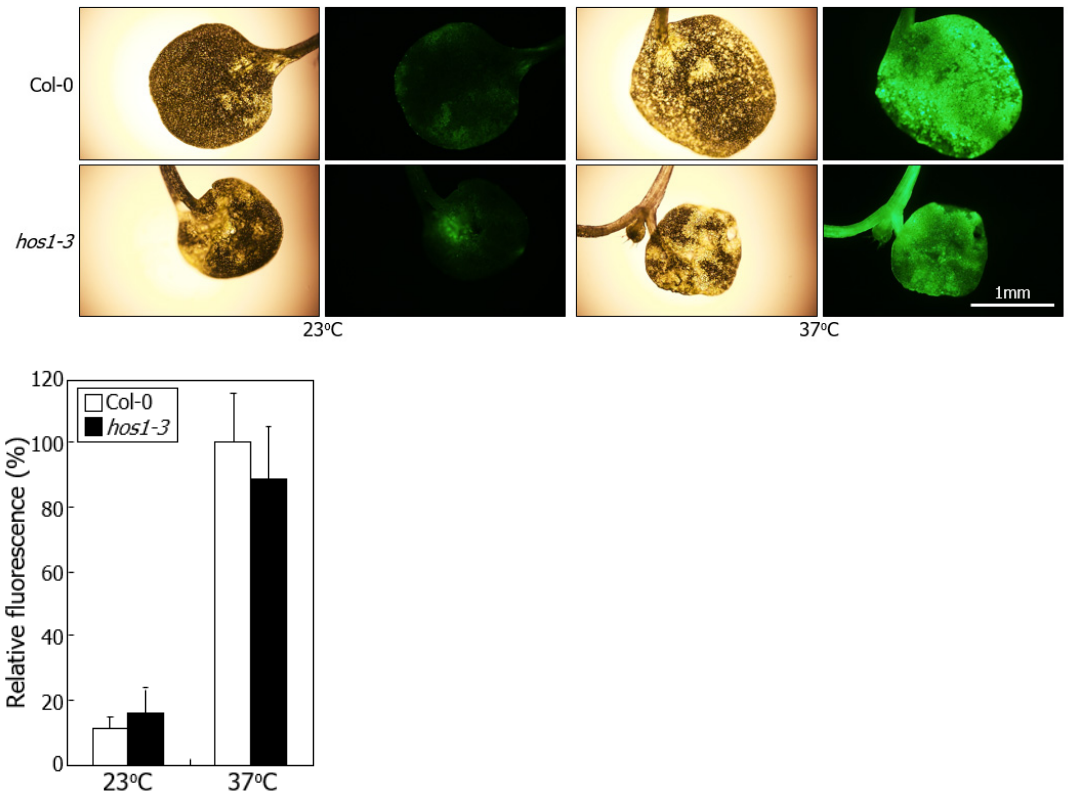

Figure 28. Thermal accumulation of reactive oxygen species (ROS)

Seven-day-old seedlings grown on MS-agar plates at 23°C were exposed to 37°C for 2 h. The cotyledons of heat-treated seedlings were treated with 2',7'-dichlorodihydrofluorescein diacetate (H_2DCFDA) for the fluorescent detection of endogenous ROS. Ten seedlings were statistically analyzed (one-sided *t*-test, $*P < 0.01$, difference from Col-0). The upper side of each box plot indicates median. Error bars indicate SE.

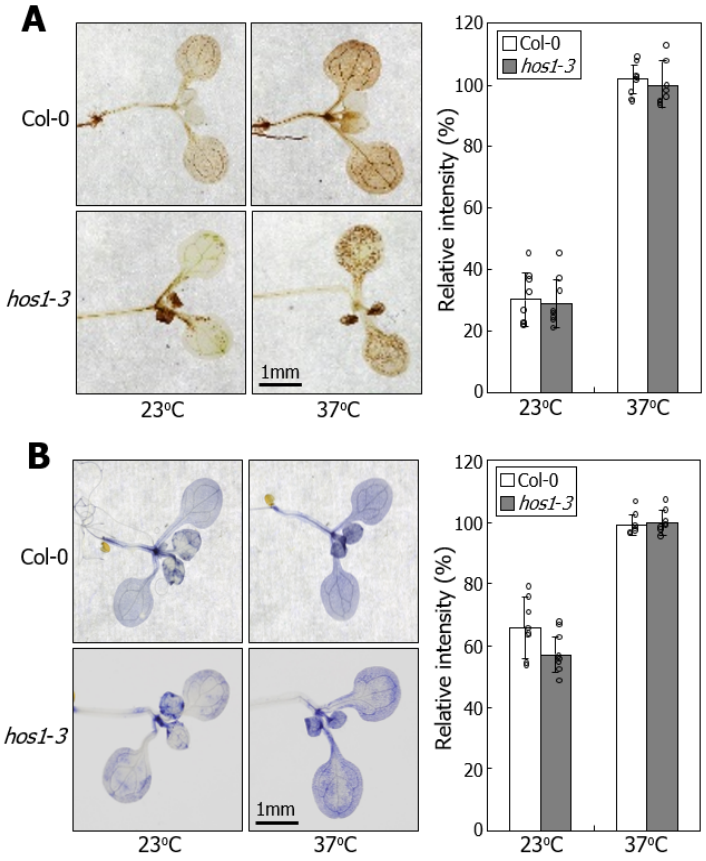

Figure 29. Histochemical detection of hydrogen peroxide

Seven-day-old whole seedlings were heat-treated and whole seedlings were subjected to 3,3′-diaminobenzidine (DAB) staining and nitro blue tetrazolium (NBT) staining. In **A** and **B**, staining intensities were quantitated using the ImageJ software. Eight seedlings were statistically analyzed (one-sided *t*-test, $*P < 0.01$, difference from Col-0). Error bars indicate SE. The circles indicate individual data points.

high temperatures, and the discrepancy of global gene expression profiles between Col-0 and *hos1-3* seedlings was more prominent at high temperatures (Fig. 30), suggesting that HOS1 mediates the transcriptional control of thermal responses. Analysis of gene ontology (GO) enrichment revealed that many genes belonging to diverse cellular, metabolic, and adaptive processes were differentially expressed in the mutant (Fig. 31). In particular, genes related to DNA repair responses were thermally upregulated in Col-0 seedlings, but their thermal regulation was largely compromised in the *hos1-3* seedlings (Fig. 32, 33). Accordingly, comparative analysis of DNA integrity by comet assay, which is widely employed to visualize DNA damages (Menke et al., 2001), revealed that DNA damages were more prominent in the *hos1-3* seedlings, especially at high temperatures, than in Col-0 seedlings (Fig. 34). Together, these observations indicate that HOS1 is involved in the maintenance of genomic integrity under heat stress.

HOS1 mediates the thermal induction of *RECQ2* gene during thermotolerance response

I next examined the thermotolerance phenotypes of DNA damage response-related mutants. Among the mutants tested, the RECQ2-deficient *recq2* mutant exhibited the most prominent reduction of thermotolerance (Fig. 35, 36). In addition, DNA damages were more severe in the mutant at high temperatures (Fig. 37), suggesting that RECQ2 is involved in the HOS1-mediated maintenance of genomic integrity at high temperatures. The RECQ2 DNA helicase unwinds the displacement loop

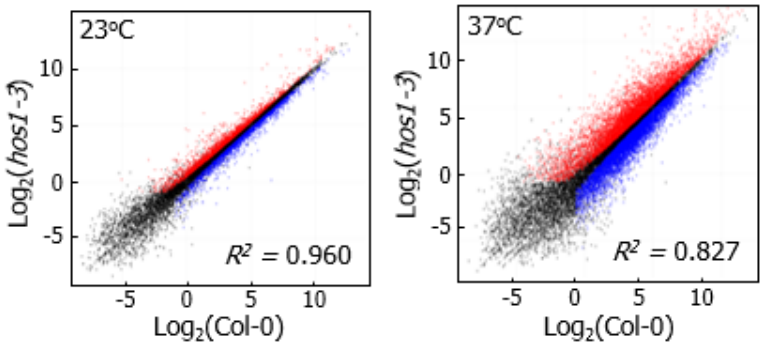

Figure 30. Scatter plots of related gene expression values obtained by RNA sequencing analysis

Seven-day-old seedlings grown on MS-agar plates at 23°C were exposed to 37°C for 1.5 d. Total RNA samples were extracted from whole seedlings. Biological triplicates, each consisting of 10 seedlings, were statistically analyzed. Expression values were plotted between Col-0 wild-type and *hos1-3* mutant seedlings. Blue spots indicate genes down-regulated in the *hos1-3* seedlings. Red spots indicate those up-regulated in the mutant seedlings. Black spots indicate those unaltered in the mutant seedlings.

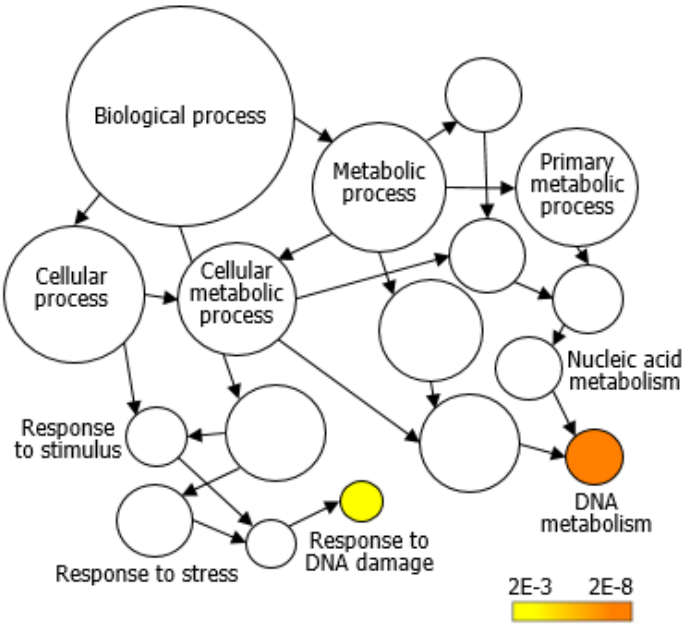

Figure 31. Gene ontology analysis of HOS1-regulated genes at high temperatures

Seven-day-old seedlings grown on MS-agar plates at 23°C were exposed to 37°C for 1.5 d. Total RNA samples were extracted from whole seedlings. Biological triplicates, each consisting of 10 seedlings, were statistically analyzed. Gene ontology analysis of HOS1-regulated genes at high temperatures. The network diagram visualizes the results of analysis using the Biological Networks Gene Ontology tool.

Locus	Gene	Up/down
At1G04020	At5BARD1	Up
At1G13635	Unknown	Up
At1G31360	RECQ2	Up
At1G71260	AtWHY2	Up
At2G21800	AtEME1A	Up
At2G28560	AtRAD51B	Up
At2G31970	RAD50	Up
At2G45280	AtRAD51C	Up
At3G10010	DML2	Up
At3G12710	Unknown	Up
At3G20475	AtMSH5	Up
At3G23100	XRCC4	Up
At3G48190	ATM	Up
At3G52905	Unknown	Up
At5G07400	Unknown	Up
At5G07660	SMC6A	Up
At5G15170	TDP1	Up
At5G26680	FEN1	Up
At5G44680	Unknown	Up
At5G44750	REV1	Up
At5G63920	TOP3A	Up
At5G64630	FAS2	Up

Figure 32. Thermal induction of DNA damage response genes

Seven-day-old seedlings grown on MS-agar plates at 23°C were exposed to 37°C for 1.5 d. Total RNA samples were extracted from whole seedlings. Biological triplicates, each consisting of 10 seedlings, were statistically analyzed. The selected genes were thermo-induced by more than 4-fold in Col-0 seedlings, but the thermal induction largely disappeared in the *hos1-3* seedlings. Among 292 genes thermally induced by more than 4-fold, 22 genes were predicted to be involved in DNA repair response.

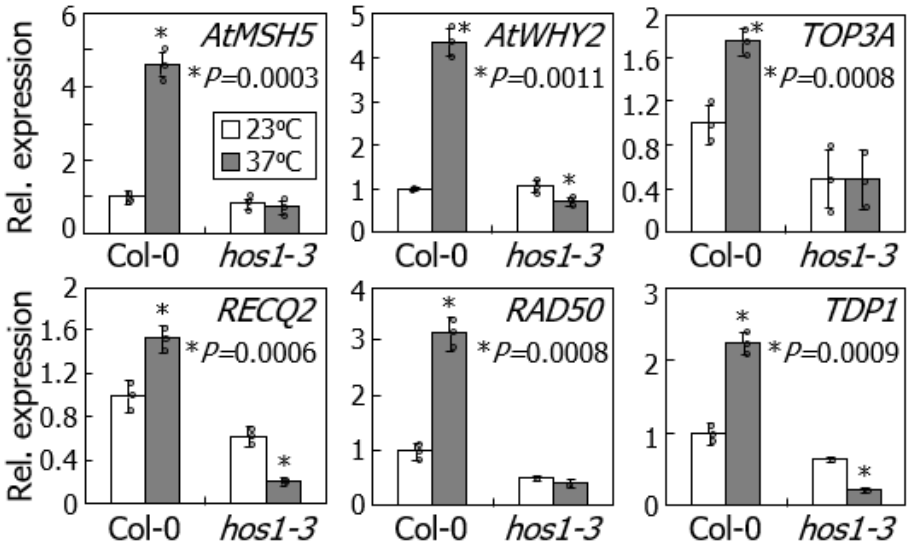

Figure 33. RT-qPCR analysis of selected DNA damage response genes

Seven-day-old seedlings grown on MS-agar plates at 23°C were exposed to 37°C for 1.5 d. Total RNA samples were extracted from whole seedlings. Biological triplicates, each consisting of 15 seedlings, were statistically analyzed using one-sided Student *t*-test (*$P < 0.01$, difference from 23°C). The upper side of each box plot indicates median. Error bars indicate SE. The circles indicate individual data points.

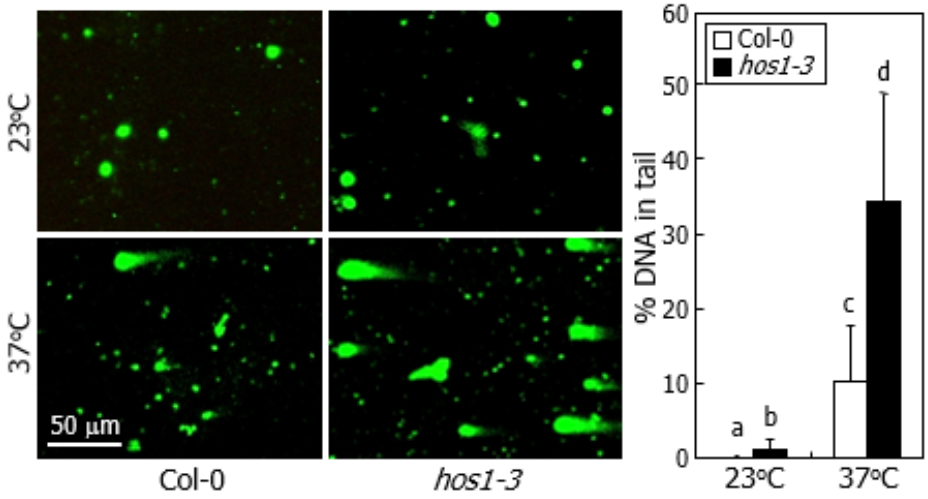

Figure 34. Comet assays on heat-treated *hos1-3* seedlings

Seven-day-old seedlings grown on MS-agar plates at 23°C were exposed to 37°C for 1.5 d. DNA breaks were quantitated by measuring the tail ratio of total fluorescence intensity in comet-shaped DNA spots using the caslab program (http://casplab.com/). DNA spots in a range of 8-12 were statistically analyzed. Error bars indicate standard deviation from the mean (SD). Different letters represent significant differences ($P < 0.01$) determined by one-way analysis of variance (ANOVA) with *post hoc* Tukey test.

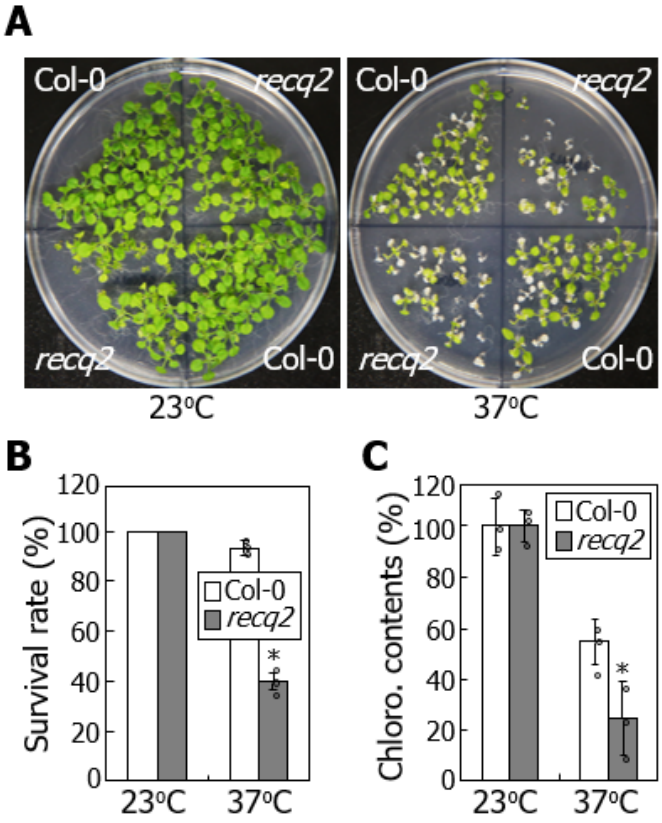

Figure 35. Thermotolerance phenotypes of *recq2* mutant

Seven-day-old seedlings grown on MS-agar plates at 23°C were exposed to 37°C for 1.5 d and allowed to recover at 23°C for 5 d under constant light conditions **(A)**. Survival rates and chlorophyll contents were measured (**B** and **C**, respectively). Biological triplicates, each consisting of 50 or 10 seedlings (**B** or **C**, respectively), were statistically analyzed (one-sided *t*-test, **P* = 0.003 **(B)** or 0.008 **(C)**, difference from Col-0). The upper side of each box plot indicates median. Error bars indicate SE. The circles indicate individual data points.

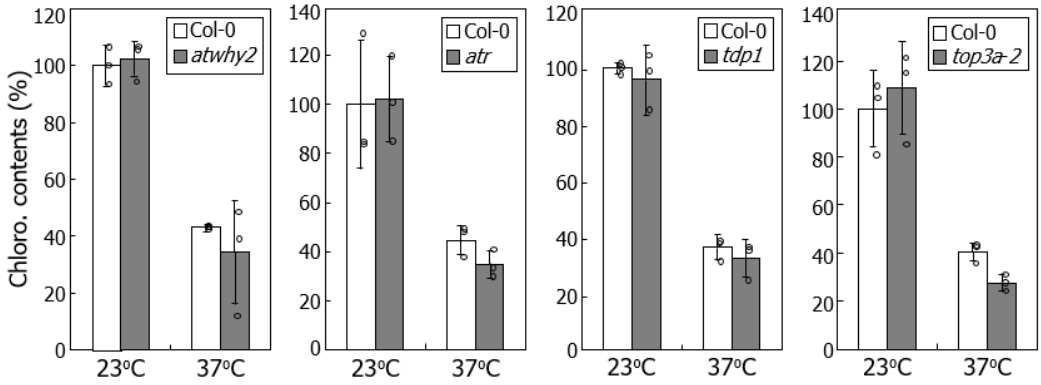

Figure 36. Chlorophyll contents in DNA damage response-related mutants

Seven-day-old seedlings grown on MS-agar plates at 23°C were exposed to 37°C for 1.5 d. The heat-treated seedlings were allowed to recover at 23°C for 5 d under constant light conditions before measuring chlorophyll contents. Biological triplicates, each consisting of 15-20 seedlings, were statistically analyzed. The selected mutants are defective in genes that were predicted to be involved in the HOS1-mediated induction of thermotolerance from RNA sequencing analysis. The upper side of each box plot indicates median. Error bars indicate SE (one-sided *t*-test, $*P < 0.01$, difference from Col-0). The circles indicate individual data points.

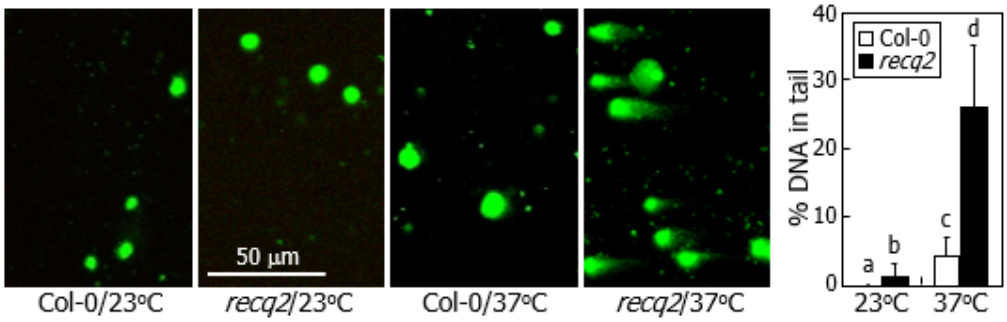

Figure 37. Comet assays on *recq2* mutant

Seven-day-old seedlings grown on MS-agar plates at 23°C were exposed to 37°C for 1.5 d. DNA breaks were quantitated by measuring the tail ratio of total fluorescence intensity in comet-shaped DNA spots using the caslab program (http://casplab.com/). DNA spots of 8-12 were statically analyzed. Different letters represent significant differences ($P < 0.01$) determined by one-way ANOVA with *post hoc* Tukey test. Error bars indicate SD.

of homologous recombination intermediates *in vitro*, and it has been predicted to act as a component of DNA repair pathways (Kobbe et al., 2008). It physically interacts with the WERNER SYNDROME-LIKE EXONUCLEASE exonuclease (AtWRNexo) (Hartung et al., 2000). I observed that the AtWRNexo-deficient mutant did not exhibit altered thermotolerance (Fig. 38), unlike the *recq2* mutant, suggesting that AtWRNexo is not functionally associated with the HOS1-mediated thermotolerance.

My data indicate that HOS1 is related with the thermal induction of *RECQ2* gene. To investigate how HOS1 mediates the *RECQ2* transcription, I first employed chromatin immunoprecipitation (ChIP)-qPCR assays using a set of conserved sequence regions containing G-box and GATA-box in the *RECQ2* promoter (Fig. 39, 40). I found that HOS1 highly enriched *RECQ2* chromatin domains harboring P3 and P5 sequences at high temperatures (Fig. 39, 41).

While HOS1 lacks any distinct DNA-binding motifs and its direct binding to DNA is not proven (MacGrefor and Penfield, 2015; Wang et al., 2015), it acts as a chromatin modifier through physical interactions with HISTONEDE ACETYLASE6 (HDA6) and HDA15 in modulating the epigenetic control of *FLOWERING LOCUS C* transcription during thermosensory flowering (Jung et al., 2013). I found that *Arabidopsis* mutants lacking HDA6 or HDA15 exhibited a thermotolerance phenotype indistinguishable from that of Col-0 seedlings (Fig. 42), indicating that the HOS1-HDA6/15 mediated epigenetic control is not involved in the development of thermotolerance. Consistently, the histone modifications were unaltered in the *RECQ2* chromatin at high temperatures (Fig. 43, 44).

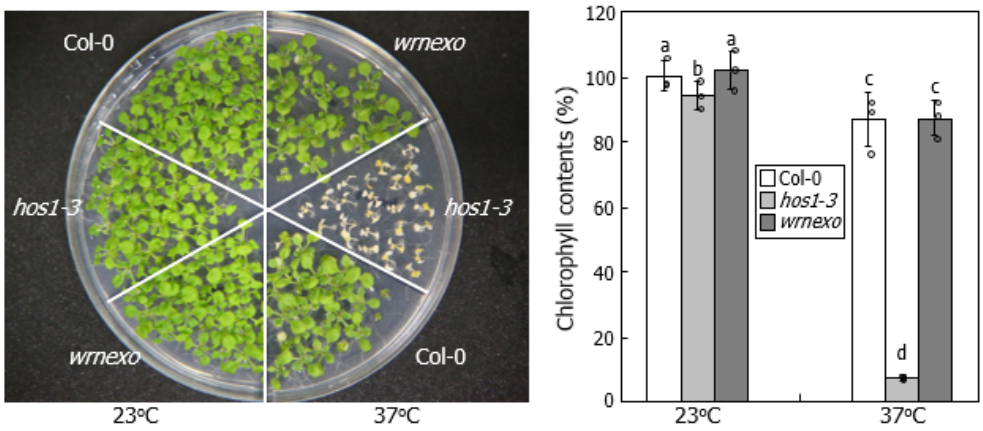

Figure 38. Thermotolerance phenotypes of *wrnexo* mutant

The RECQ2 protein physically interacts with WERNER SYNDROME-LIKE EXONUCLEASE (WRNexo), a 3'-5' exonuclease that participates in sustaining DNA integrity. Seven-day-old seedlings grown on MS-agar plates at 23°C were exposed to 37°C for 1.5 d and then allowed to recover at 23°C for 10 d under constant light conditions. Biological triplicates, each consisting of 10 seedlings, were statistically analyzed. Error bars indicate SE. Different letters represent significant differences ($P < 0.01$) determined by one-way ANOVA with *post hoc* Tukey test. The circles indicate individual data points.

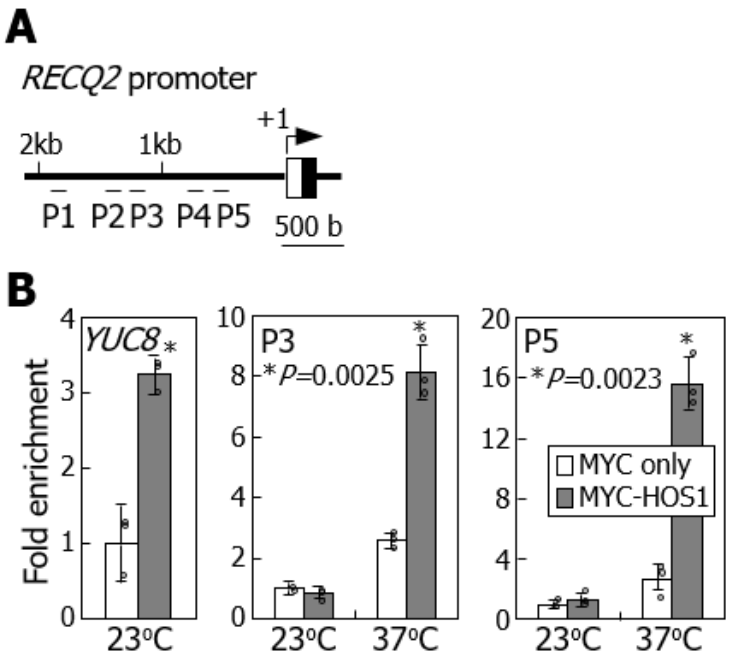

Figure 39. Binding of HOS1 to *RECQ2* chromatin

(A) Sequence elements in *RECQ2* promoter. The P1-P5 sequence regions were chosen for ChIP-qPCR assays. **(B)** Binding of HOS1 to *RECQ2* chromatin. ChIP-qPCR assays were performed using the 35S:*MYC-HOS1* transgenic plants. Five measurements were statistically analyzed (one-sided *t*-test, difference from MYC only). Error bars indicate SD. The *YUC8* promoter sequence was included as positive control in the assays. The circles indicate individual data points.

Figure 40. *RECQ2* promoter sequences examined in chromatin immunoprecipitation (ChIP)-qPCR

The conserved G-box and GATA-box sequences were underlined in green and blue, respectively.

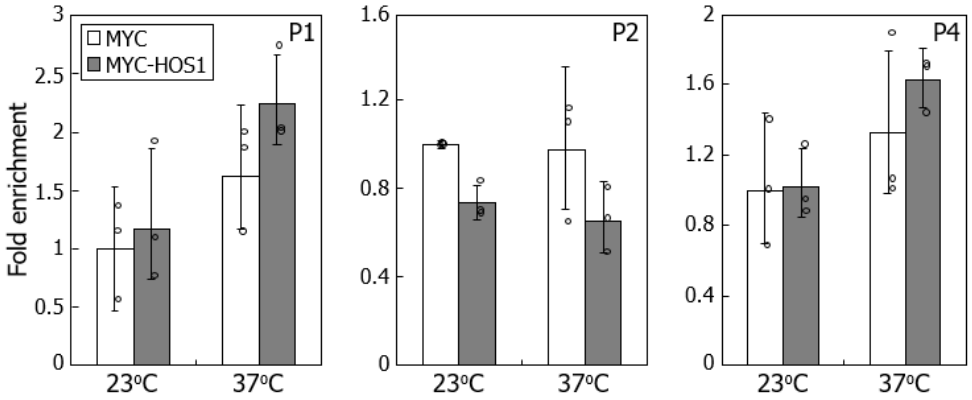

Figure 41. Control data for ChIP-qPCR assays

ChIP-qPCR assays were performed using the 35S:*MYC-HOS1* transgenic plants. Five measurements were statistically analyzed (one-sided *t*-test, difference from MYC only). Error bars indicate SD. The data with P1, P2, and P4 sequence elements were displayed. The circles indicate individual data points.

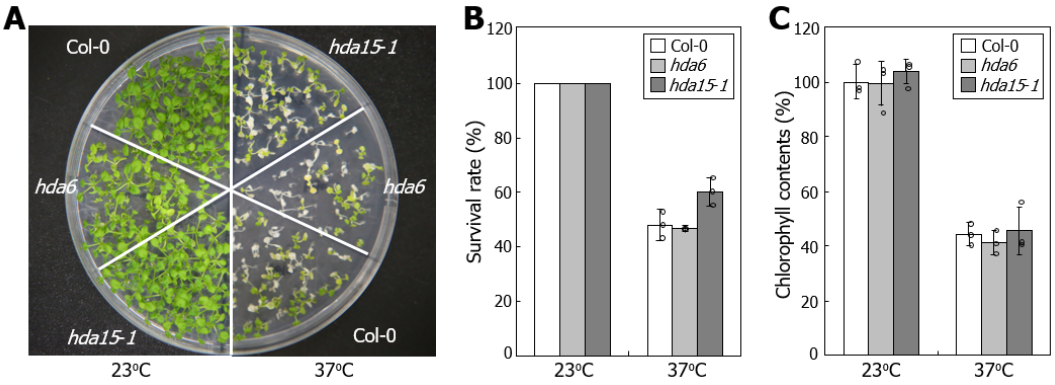

Figure 42. Two histone deacetylase (HDAC)-deficient mutants, *hda6* and *hda15-1*, were included in the thermotolerance assays

(A) Seven-day-old seedlings grown on MS-agar plates at 23°C were exposed to 37°C for 4 d and then allowed to recover at 23°C for 5 d under constant light conditions. Survival rates and chlorophyll contents were measured (**B** and **C**, respectively). Biological triplicates, each consisting of 50 or 10 seedlings (**B** or **C**, respectively), were statistically analyzed (one-sided *t*-test, $*P < 0.01$, difference from Col-0). The upper side of each box plot indicates median. Error bars indicate SE. The circles indicate individual data points.

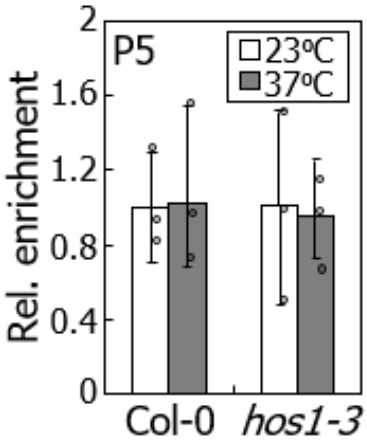

Figure 43. Histone modifications at *RECQ2* chromatin

Seven-day-old seedlings were used. An anti-H3Ac antibody was used for immunoprecipitation. Histone modifications in the P5 sequence were analyzed by ChIP-qPCR. Three measurements were statistically analyzed (one-sided *t*-test, **P* < 0.05, difference from 23°C). The upper side of each box plot indicates median. Error bars indicate SD. The circles indicate individual data points.

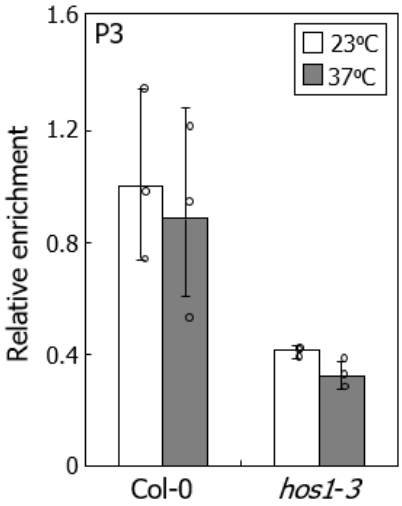

Figure 44. Histone modifications in the P3 sequence region of *RECQ2* chromatin

Seven-day-old seedlings were used. An anti-H3Ac antibody was used for immunoprecipitation. Histone modifications in the P3 sequence were analyzed by ChIP-qPCR. Three measurements were statistically analyzed (one-sided *t*-test, **P* < 0.05, difference from 23°C). The upper side of each box plot indicates median. Error bars indicate SD. The circles indicate individual data points.

HOS1 acts as a transcriptional coregulator through interactions with transcription factors, such as PIF4 (Kim et al., 2017). Transcriptional activation activity assays in *Arabidopsis* protoplasts showed that expression of a full-size *HOS1* gene, but not the N-terminally and C-terminally truncated forms, led to the induction of the β-glucuronidase reporter gene (Fig. 45). Together with the association of HOS1 with *RECQ2* chromatin, these observations indicate that HOS1 acts as a transcriptional coregulator of *RECQ2* gene and both the N-terminal and C-terminal domains are required for its transactivation activity.

To verify the functional relationship between HOS1 and RECQ2, I produced *hos1-3 recq2* double mutant by cross. I observed that the thermotolerance of the double mutant was comparable to that of the *hos1*-3 mutant (Fig. 46, 47), demonstrating that the *HOS1* and *RECQ2* genes constitute a single genetic pathway in regulating thermotolerance. In addition, overexpression of *RECQ2* gene in the *hos1-3* mutant restored the reduced thermotolerance (Fig. 48), further supporting the HOS1-RECQ2 linkage. The incomplete complementation of the *hos1-3* thermotolerance phenotypes by *RECQ2* overexpression would be because HOS1 also regulates other targets in addition to *RECQ2*.

I next examined the functional significance of HOS1 and RECQ2 in triggering DNA repair response by employing genotoxins, such as *cis*-diamminedichloroplatinum (II) and mitomycin C, which damage DNA molecules by triggering cross-linking of nucleotides (Rohrig et al., 2018). Both the *hos1-3* and *recq2* seedlings were more sensitive to these genotoxins than Col-0 seedlings at high temperatures (Fig. 49-51), signifying the regulatory roles of HOS1 and

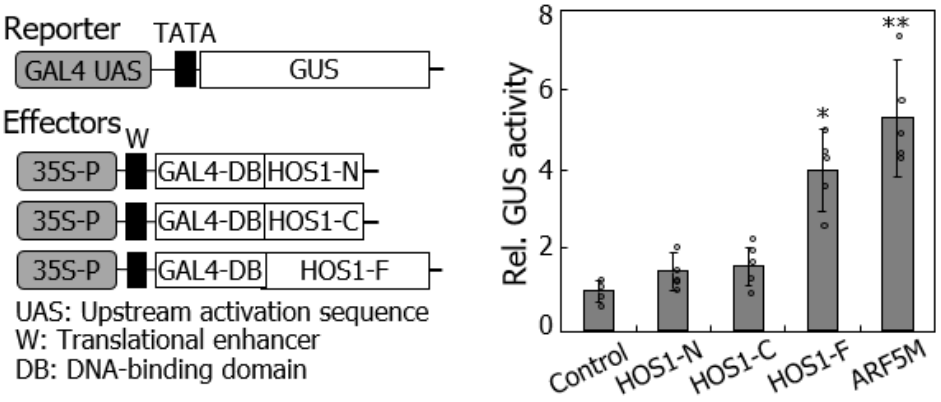

Figure 45. Transcriptional activation activity assays in *Arabidopsis* protoplasts

A set of reporter and effector constructs was generated (left diagram). The vectors were cotransformed into *Arabidopsis* protoplasts. The 35S promoter-luciferase construct was included as internal control in the assays. Relative GUS activities were determined fluorimetrically (right graph). ARF5M was positive control. A full-size (HOS1-F, residues 1-927), a C-terminally truncated (HOS1-N, residues 1-457), and a N-terminally truncated (HOS1-C, residues 457-927) HOS1 forms were assayed. Five measurements were statistically analyzed (one-sided *t*-test, **P* = 0.00821, ***P* = 0.00367, difference from control). The upper side of each box plot indicates median. Error bars indicate SD. The circles indicate individual data points.

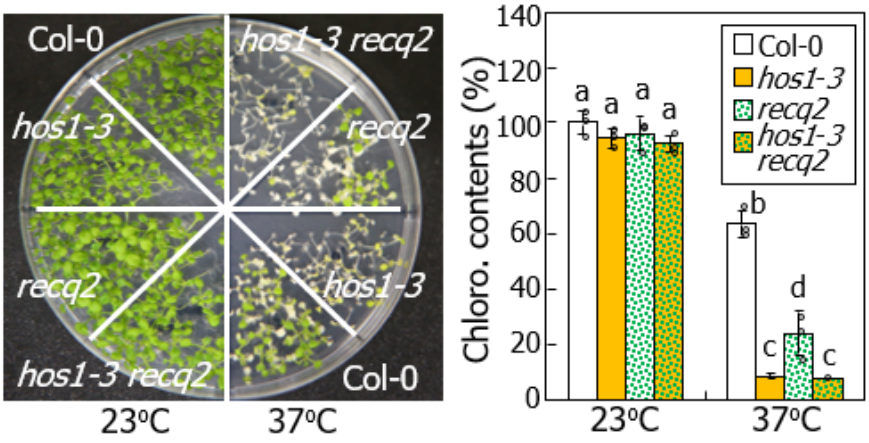

Figure 46. Thermotolerance phenotypes of *hos1-3 recq2* mutant

Seven-day-old seedlings grown on MS-agar plates at 23°C were exposed to 37°C for 1.25 d. Three measurements, each consisting of 20 seedlings, were statically analyzed. Error bars indicate SE. Different letters represent significant differences ($P < 0.01$) determined by one-way ANOVA with *post hoc* Tukey test. The circles indicate individual data points. Chloro. contents: Chlorophyll contents

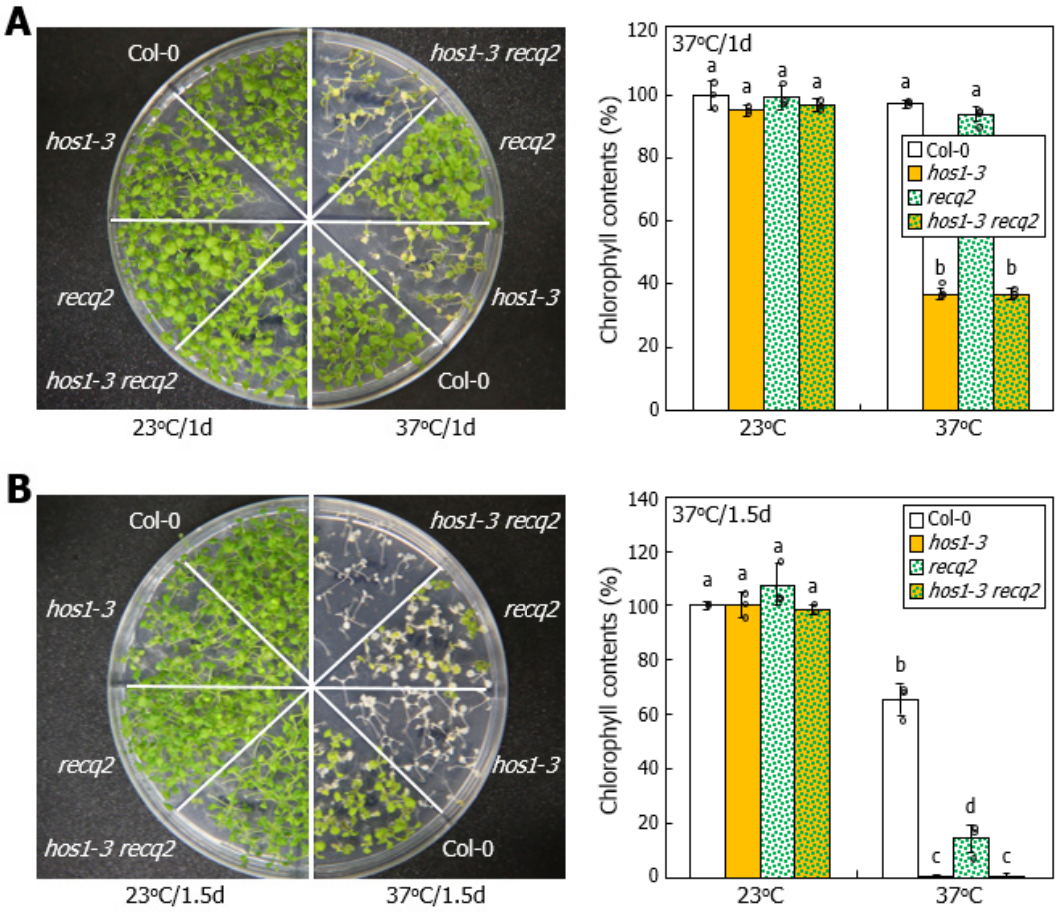

Figure 47. Thermotolerance phenotypes of *hos1-3 recq2* double mutant

Seven-day-old seedlings grown on MS-agar plates at 23°C were exposed to 37°C for either 1 d **(A)** or 1.5 d **(B)** and then allowed to recover at 23°C for 5 d under constant light conditions (left photographs). Chlorophyll contents were measured (right graphs). Biological triplicates, each consisting of 10 seedlings, were statistically analyzed. Error bars indicate SE. Different letters represent significant differences ($P < 0.01$) determined by one-way ANOVA with *post hoc* Tukey test. The circles indicate individual data points.

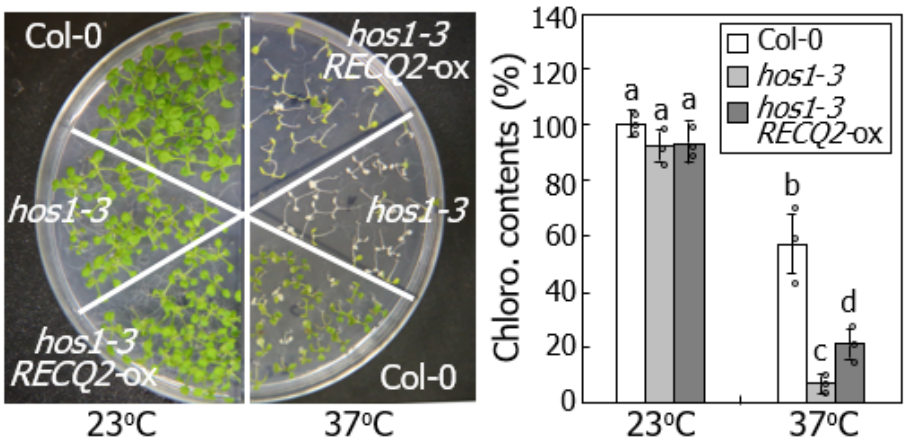

Figure 48. Thermotolerance phenotypes of *hos1-3 RECQ2*-ox plants

A RECQ2-coding sequence was overexpressed driven by the CaMV 35S promoter in the *hos1-3* mutant. Seedlings were exposed to 37°C for 2 d and allowed to recover at 23°C for 3 d under constant light conditions. three measurements, each consisting of 20 seedlings, were statically analyzed. Error bars indicate SE. Different letters represent significant differences ($P < 0.01$) determined by one-way ANOVA with *post hoc* Tukey test. The circles indicate individual data points. Chloro. contents: Chlorophyll contents

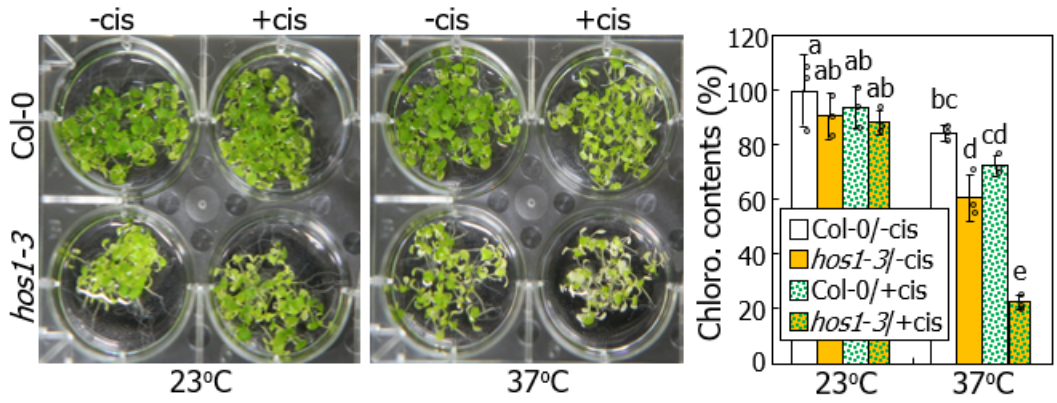

Figure 49. Thermotolerance phenotypes of *hos1-3* mutant in the presence of cisplatin

Seven-day-old seedlings grown on MS-agar plates at 23°C were transferred to liquid MS cultures containing 10 μM cisplatin (cis) and exposed to 37°C for 20 h. Heat-treated seedlings were allowed to recover at 23°C for 10 d under constant light conditions. Three measurements, each consisting of 20 seedlings, were statically analyzed. Error bars indicate SE. Different letters represent significant differences ($P < 0.05$) determined by two-way ANOVA with *post hoc* Fisher's multiple comparison test. The circles indicate individual data points. Chloro. contents: Chlorophyll contents

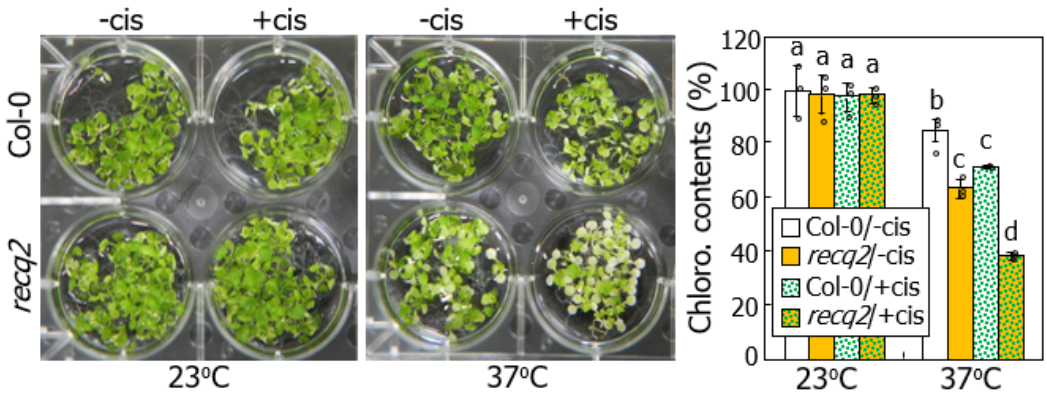

Figure 50. Thermotolerance phenotypes of *recq2* mutant in the presence of cisplatin

Seven-day-old seedlings grown on MS-agar plates at 23°C were transferred to liquid MS cultures containing 10 μM cisplatin (cis) and exposed to 37°C for 20 h. Heat-treated seedlings were allowed to recover at 23°C for 10 d under constant light conditions. Three measurements, each consisting of 20 seedlings, were statically analyzed. Error bars indicate SE. Different letters represent significant differences ($P < 0.05$) determined by two-way ANOVA with *post hoc* Fisher's multiple comparison test. The circles indicate individual data points. Chloro. contents: Chlorophyll contents

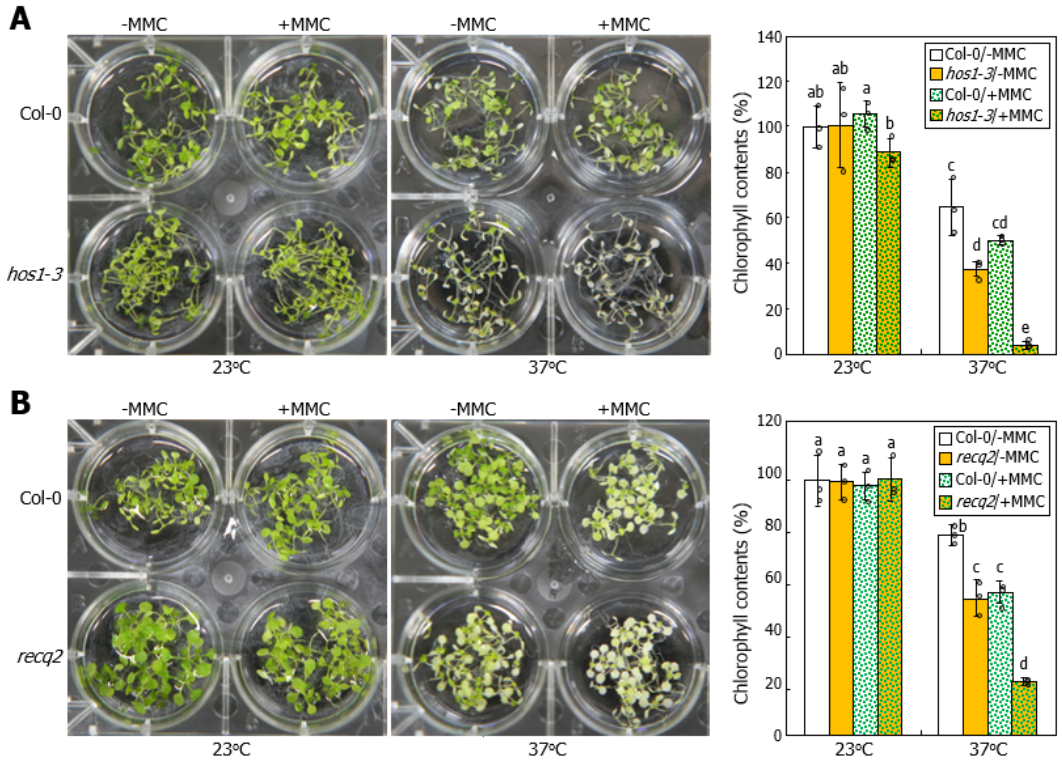

Figure 51. Effects of mitomycin on thermotolerance

(A, B) Seven-day-old seedlings grown on MS-agar plates at 23°C were transferred to liquid MS cultures containing 10 μg/ml MMC, which is known to damage DNA molecules by inducing cross-linking of nucleotides, and exposed to 37°C for 1 d. Heat-treated seedlings were allowed to recover at 23°C for 5 d **(A)** and 10 d **(B)** under constant light conditions (left photographs). Three measurements of chlorophyll contents, each consisting of 15-20 seedlings, were statistically analyzed (right graph). Error bars indicate SE. Different letters represent significant differences ($P < 0.05$) determined by two-way ANOVA with *post hoc* Fisher's multiple comparison test.

RECQ2 in triggering DNA repair response under heat stress. Consistent with a previous report that DNA damages induce cell death (Borges et al., 2008), trypan blue exclusion test, which selectively stains dead cells (Koch et al., 1990), showed that cell death was more wide spread in the mutant leaves than in Col-0 leaves (Fig. 52).

A key question was how HOS1 incorporates thermal signals into the transcriptional control of DNA repair genes. HSPs and their upstream transcriptional regulators, heat shock factors (HSFs), play critical roles in the development of thermotolerance (Swindell et al., 2007). I found that the levels of *HSP* and *HSF* transcripts were not discernibly altered in the *hos1-3* seedlings (Fig. 53). The protein abundance of HSP90 was also unaffected in the mutants at high temperatures (Fig. 54), indicating that HOS1 does not affect the expression of *HSP* and *HSF* genes and the accumulation of their encoded proteins under heat stress.

The HSFA1-HSP90-HOS1 module activates DNA repair response at high temperatures

Notably, protein accumulation assays revealed that the levels of HOS1 were rapidly elevated by more than 5-fold following heat exposure (Fig. 55). Moreover, the HOS1 levels were elevated by approximately 3-fold in the presence of MG132 at normal temperatures (Fig. 56). These observations point out that HOS1 abundance is maintained at a relatively low level through the 26S proteasome-mediated degradation at normal temperatures but the degradation pathways are suppressed

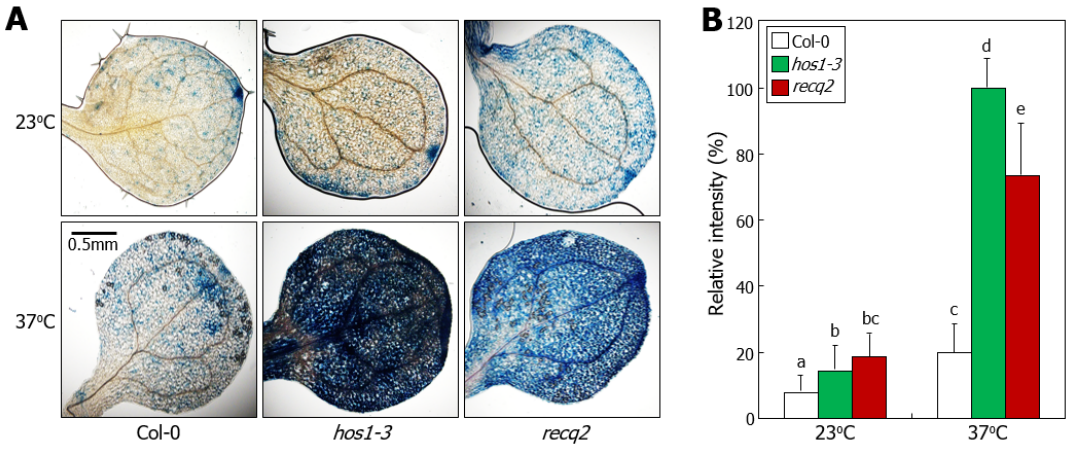

Figure 52. Cell death increases in *hos1-3* and *recq2* mutants at high temperatures

Seven-day-old seedlings grown on MS-agar plates at 23°C were exposed to 37°C for 1.5 d and then allowed to recover at 23°C for 5 d under constant light conditions. The second rosette leaves of heat-treated seedlings were subjected to trypan blue staining **(A)**, a common way of analyzing cell viability by selectively staining dead cells. Staining intensities were quantitated using the imageJ program **(B)**. Ten representative rosette leaves were statistically analyzed. Error bars indicate SE. Different letters represent significant differences ($P < 0.01$) determined by one-way ANOVA with *post hoc* Tukey test.

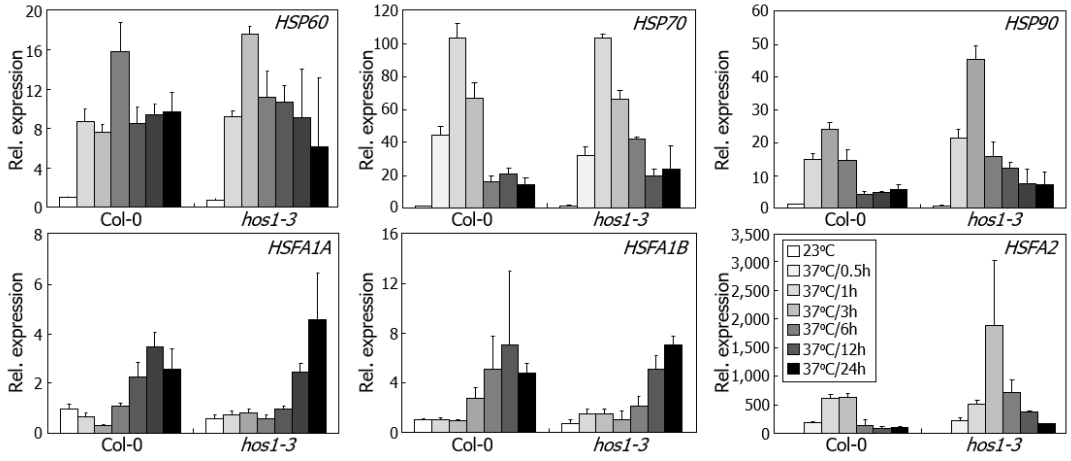

Figure 53. Transcription of heat response genes in the *hos1-3* mutant at high temperatures

Seven-day-old seedlings grown on MS-agar plates at 23°C were exposed to 37°C for the indicated durations. Whole seedlings were used for total RNA preparation. Transcript levels were analyzed by RT-qPCR. Biological triplicates, each consisting of 15 seedlings, were statistically analyzed. The upper side of each box plot indicates median. Error bars indicate SE. h, hour.

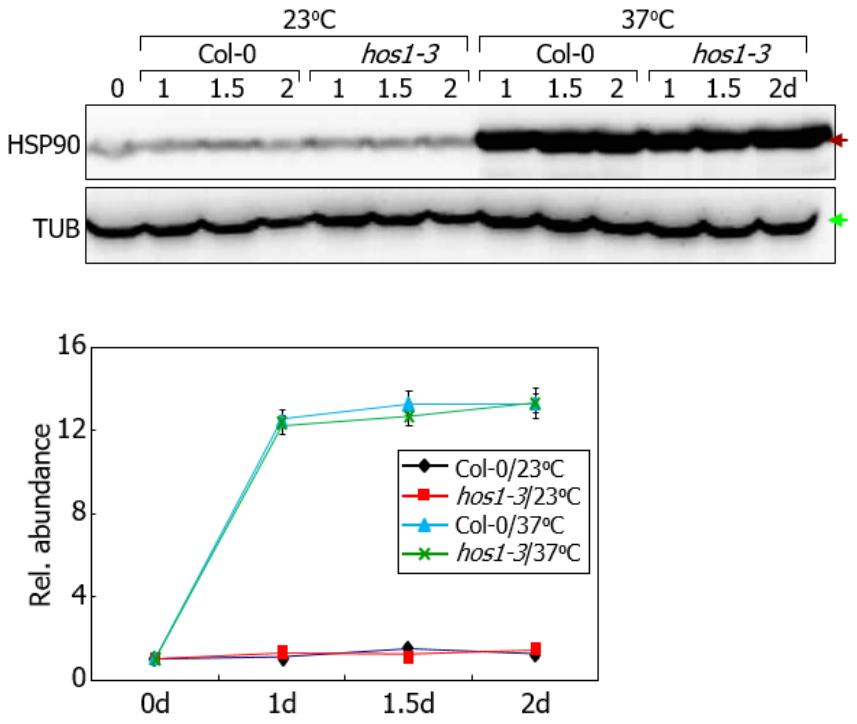

Figure 54. HSP90 protein abundance in the *hos1-3* mutant

Seven-day-old seedlings grown on MS-agar plates at 23°C were exposed to 37°C for varying durations. Whole seedlings were used for the extraction of total proteins. d, day. Endogenous HSP90 proteins were immunologically detected using an anti-HSP90 antibody. Tubulin (TUB) proteins were similarly immunodetected for protein quality control. Brown arrows mark 90 kDa, and green arrows mark 50 kDa. Three immunoblots were statistically analyzed. Error bars indicate SD.

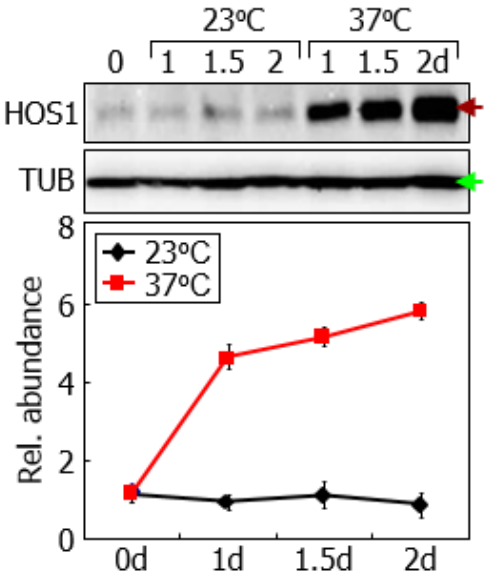

Figure 55. Thermal stabilization of HOS1

Seven-day-old 35S:*MYC-HOS1* transgenic seedlings grown at 23°C were exposed to 37°C for varying durations. Whole seedlings were used for the extraction of total proteins. d, day. h, hour. Immunoblots were statistically analyzed (n=3 biologically independent samples). The dot plots indicate median. Error bars indicate SD. Brown arrows mark 112 kDa, and green arrows mark 50 kDa. The MYC-HOS1 proteins were immunologically detected using an anti-MYC antibody. Tubulin (TUB) proteins were similarly analyzed using an anti-TUB antibody for protein quality control.

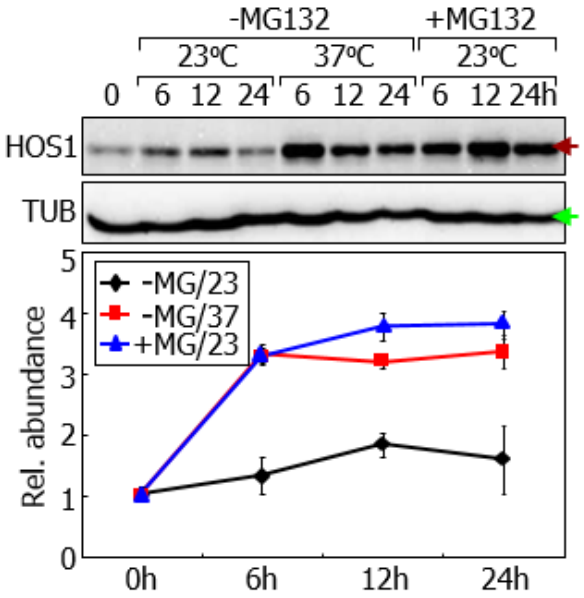

Figure 56. Effects of MG132 on HOS1 protein stability

Seven-day-old 35S:*MYC-HOS1* transgenic seedlings grown at 23°C were exposed to 37°C for varying durations in the presence of chemicals. Seedlings were incubated in liquid MS cultures containing 10 μM MG132. Whole seedlings were used for the extraction of total proteins. d, day. h, hour. Immunoblots were statistically analyzed (*n*=3 biologically independent samples). The dot plots indicate median. Error bars indicate SD. Brown arrows mark 112 kDa, and green arrows mark 50 kDa.

at high temperatures. In the meantime, the transcription of *HOS1* gene was elevated by less than 2-fold at high temperatures (Fig. 57). It is thus likely that the thermal activation of HOS1 function is exerted mainly at the protein level.

HSPs act as molecular chaperones that stabilize cellular proteins, including DNA-modifying enzymes (Jantschitsch and Trautinger, 2003), during plant thermal responses (Finka and Goloubinoff, 2013). It was notable that the thermal accumulation of HOS1 was largely attenuated in the presence of HSP90 inhibitors, geldanamycin (GDA) and radicicol (Fig. 58, 59). Inaddition, DNA breaks were more prominent when seedlings were treated with HSP90 inhibitors (Fig. 60, 61). Furthermore, the HOS1 thermostabilization was largely eliminated in the *HSP90*-RNAi plants (Fig. 62), which exhibited a significant reduction in thermotolerance and thermal induction of *RECQ2* transcription (Fig. 63). These observations indicate that HSP90 mediates the thermostabilization of HOS1. Consistent with the role of HSP90 in the HOS1-mediated thermotolerance, radicicol treatments reduced thermotolerance by approximately 80% in Col-0 seedlings (Fig. 64). Thermotolerance was also reduced, but to a lesser degree, in the *hos1-3* mutant when treated with radicicol, suggesting that HOS1 is not the sole target of HSP90 in inducing thermotolerance.

It has been reported that the thermal accumulation of HSP90 proteins is markedly reduced in the *hsfa1a/hsfa1b/hsfa1d/hsfa1e* quadruple knockout (*hsfa1* QK) mutant, which lacks HSF master regulators (Liu et al., 2011). I found that the thermal accumulation of HOS1 was reduced in the *hsfa1* QK mutant (Fig. 65). In addition, the *hsfa1* QK mutant seedlings exhibited reduction in thermotolerance and thermal induction of *RECQ2* transcription (Fig. 66), similar

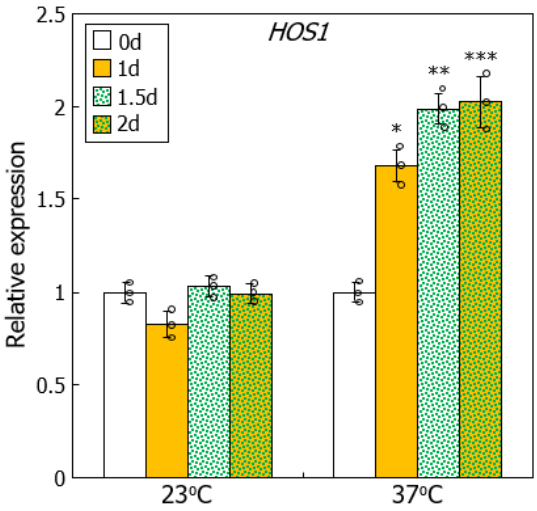

Figure 57. Effects of high temperatures on *HOS1* transcription

Seven-day-old Col-0 seedlings grown on MS-agar plates at 23°C were exposed to 37°C for the indicated durations before harvesting whole seedlings for total RNA extraction. d, day. Transcript levels were examined by RT-qPCR. Biological triplicates, each consisting of 10 seedlings, were statistically analyzed (one-sided *t*-test, **P* = 0.0005, ***P* = 0.0001, ****P* = 0.0009, difference from 0 d). Error bars indicate SE. The circles indicate individual data points.

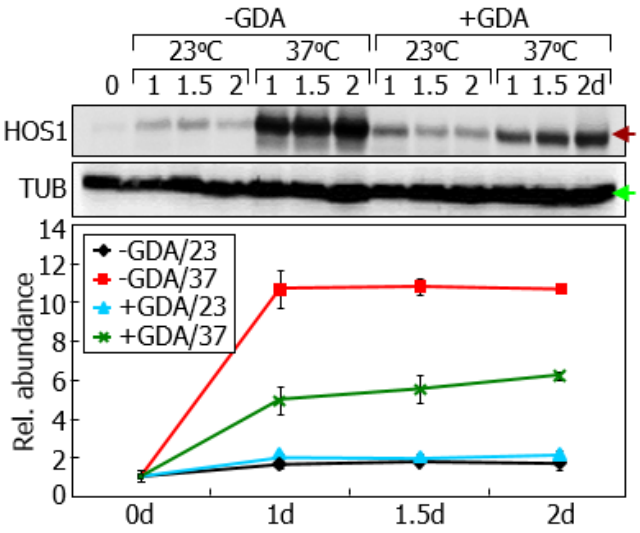

Figure 58. Effects of HSP90 inhibitor on thermal accumulation of HOS1

Seven-day-old 35S:*MYC-HOS1* transgenic seedlings grown at 23°C were exposed to 37°C for varying durations in the presence of chemicals. Geldanamycin (GDA) was included at the final concentration of 10 μM. Whole seedlings were used for the extraction of total proteins. d, day. h, hour. Immunoblots were statistically analyzed (*n*=3 biologically independent samples). The dot plots indicate median. Error bars indicate SD. Brown arrows mark 112 kDa, and green arrows mark 50 kDa.

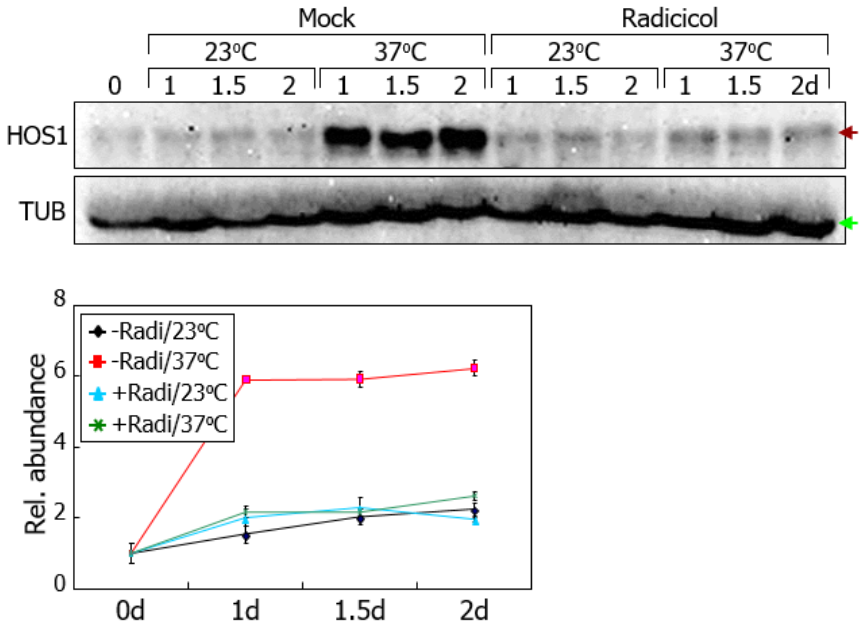

Figure 59. Effects of radicicol on the thermal accumulation of HOS1 proteins

Seven-day-old 35S:*MYC-HOS1* transgenic seedlings grown on MS-agar plates at 23°C were transferred to 37°C and subjected to treatments with 10 μM radicicol, an antibiotic inhibitor of HSP90. The MYC-HOS1 proteins were immunologically detected using an anti-MYC antibody. TUB proteins were assayed in parallel for loading control. Brown arrows mark 112 kDa, and green arrows mark 50 kDa. d, day. Immunoblots were quantitated using the ImageJ software, and three quantitations were statistically analyzed. The dot plots indicate median. Error bars indicate SD.

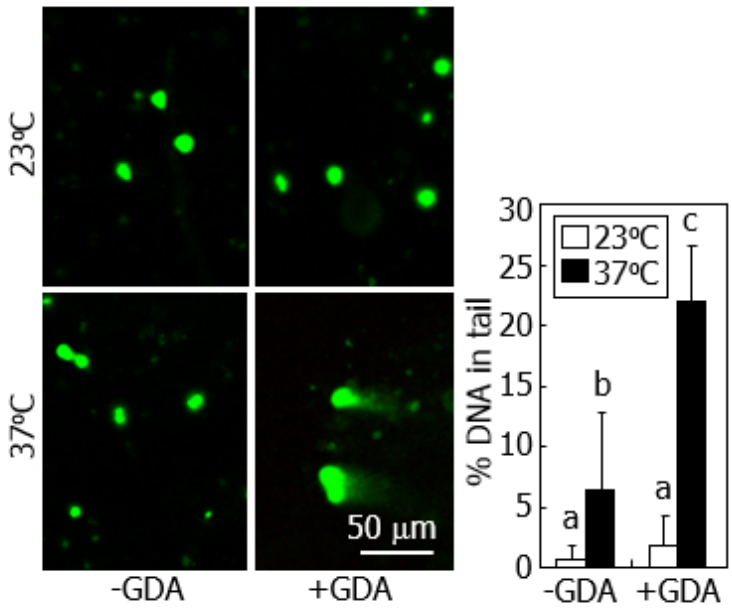

Figure 60. Comet assays in the presence of GDA

GDA was included at the final concentration of 10 µM in the assays. The tail ratio of total fluorescence intensity in comet-shaped DNA spots was quantitated using the caslab program. DNA spots of 8-12 were statistically analyzed. Error bars indicate SD. Different letters represent significant differences ($P < 0.01$) determined by one-way ANOVA with *post hoc* Tukey test.

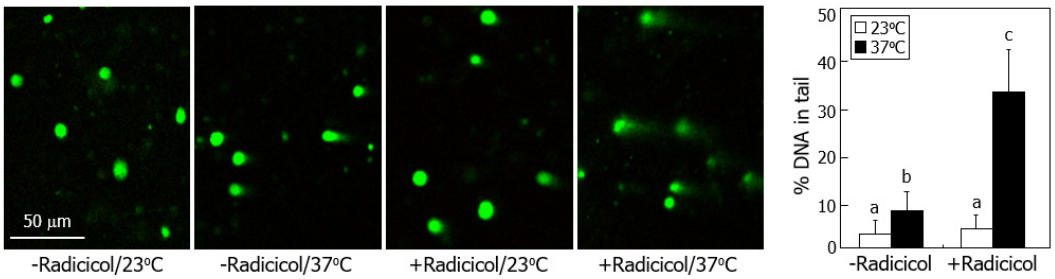

Figure 61. Comet assays in the presence of radicicol

Seven-day-old seedlings grown on MS-agar plates at 23°C were exposed to 37°C for 1.5 d. DNA breaks were quantitated by measuring the tail ratio of total fluorescence intensity in comet-shaped DNA spots. DNA spots of 8-12 were statistically analyzed. Error bars indicate SD. Different letters represent significant differences ($P < 0.01$) determined by one-way ANOVA with *post hoc* Tukey test.

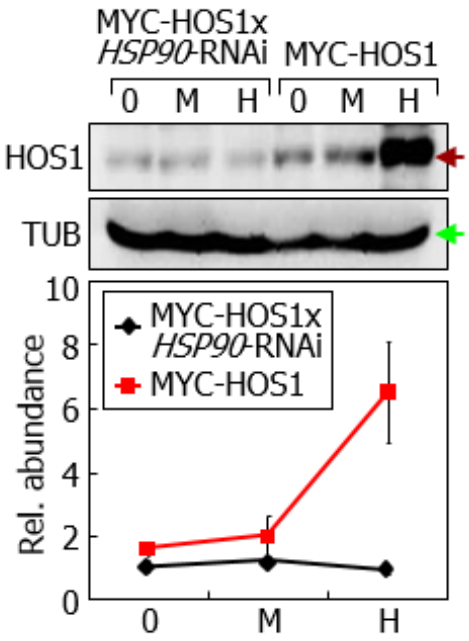

Figure 62. Thermal protein abundance of HOS1 in *HSP90*-RNAi plants

The *HSP90*-RNAi plant was crossed with the 35S:*MYC-HOS1* transgenic plant. Seedlings were incubated at either 23°C (M) or 37°C (H) for 1.5 d. An anti-MYC antibody was used for the immunodetection of MYC-HOS1. Immunoblots were statistically analyzed (n=3 biologically independent samples). The dot plots indicate median. Error bars indicate SD. Brown arrows mark 112 kDa, and green arrows mark 50 kDa.

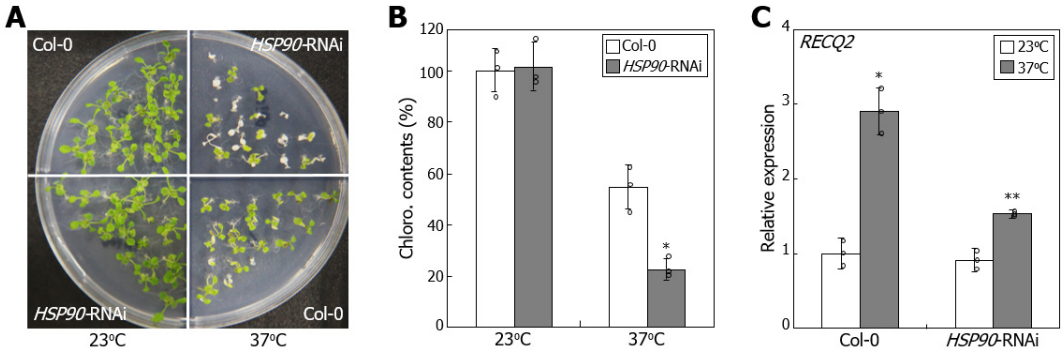

Figure 63. Thermotolerance phenotypes of *HSP90*-RNAi plants

(A, B) Thermotolerance phenotypes. Seven-day-old seedlings grown on MS-agar plates at 23°C were exposed to 37°C for 2 d. Heat-treated seedlings were allowed to recover at 23°C for 5 d under constant light conditions before taking photograph **(A)**. Chlorophyll contents were measured **(B)**. Three measurements, each consisting of 15-20 seedlings, were statistically analyzed using one-sided Student *t*-test (**P* = 0.008, difference from Col-0). **(C)** Transcription of *RECQ2* gene. Seven-day-old seedlings grown on MS-agar plates at 23°C were exposed to 37°C for 2 d. Whole seedlings were used for total RNA preparation. Transcript levels were analyzed by RT-qPCR. Biological triplicates, each consisting of 15 seedlings, were statistically analyzed (one-sided *t*-test, **P* = 0.0005, ***P* = 0.0007, difference from 23°C). In **B** and **C**, the upper side of each box plot indicates median. Error bars indicate SE. The circles indicate individual data points.

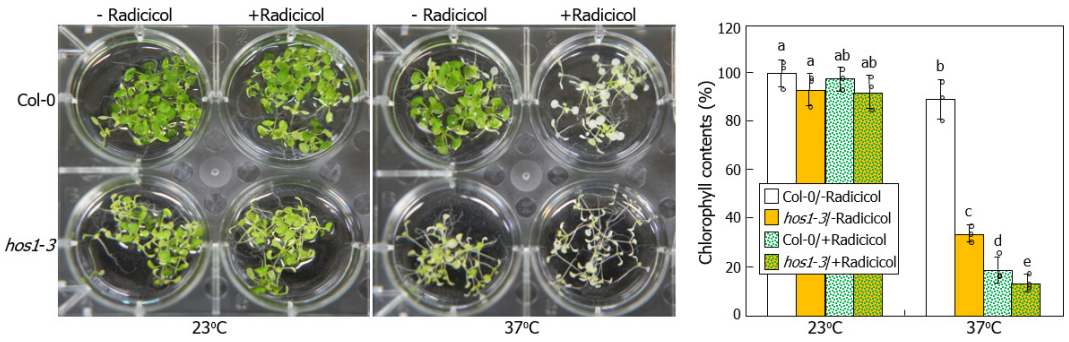

Figure 64. Thermotolerance phenotypes of *hos1-3* mutant in the presence of radicicol

Seven-day-old seedlings grown on MS-agar plates at 23°C were transferred to liquid MS cultures containing 10 μM radicicol and exposed to 37°C for 1 d. Heat-treated seedlings were allowed to recover at 23°C for 5 d under constant light conditions. Three measurements of chlorophyll contents, each consisting of 15-20 seedlings, were statistically analyzed. Error bars indicate SE. Different letters represent significant differences ($P < 0.05$) determined by two-way ANOVA with *post hoc* Fisher's multiple comparison test. The circles indicate individual data points.

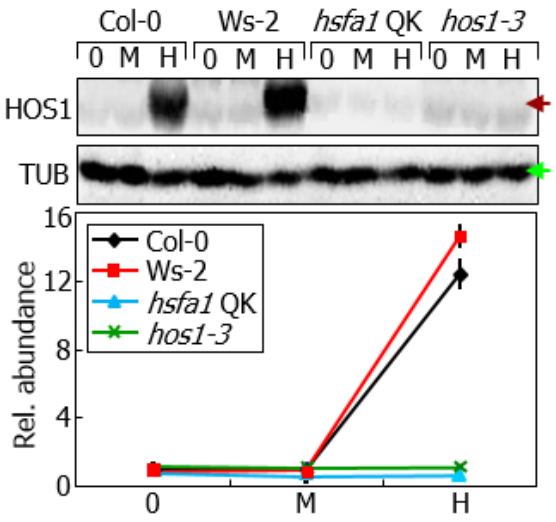

Figure 65. Thermal protein abundance of HOS1 in the *hsfa1* QK mutant

The *hsfa1* QK seedlings were heat-treated for 6 h, and an anti-HOS1 antibody was used for the immunodetection of HOS1. Immunoblots were statistically analyzed (*n*=3 biologically independent samples). The dot plots indicate median. Error bars indicate SD. Brown arrows mark 105 kDa, and green arrows mark 50 kDa.

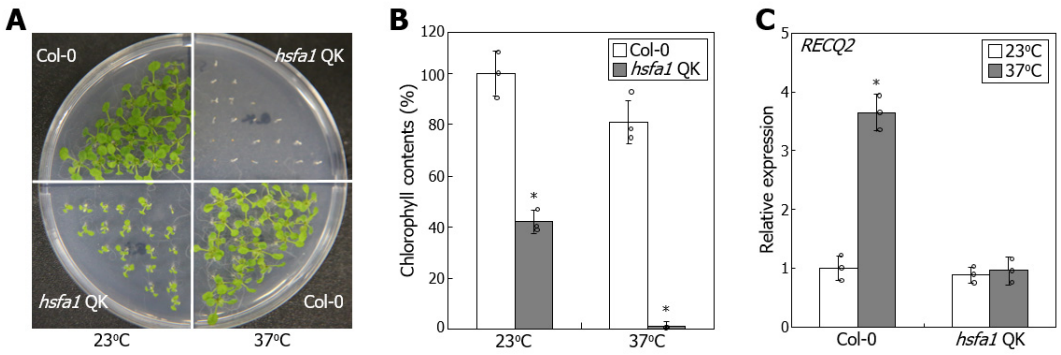

Figure 66. Thermotolerance phenotypes of *hsfa1a*/*hsfa1b*/*hsfa1d*/*hsfa1e* quadruple knockout (*hsfa1* QK) mutant

(A, B) Thermotolerance phenotypes. Seven-day-old *hsfa1* QK mutant seedlings grown on MS-agar plates at 23°C were exposed to 37°C for 1 d. Heat-treated seedlings were allowed to recover at 23°C for 5 d under constant light conditions before taking photograph **(A)**. Chlorophyll contents were measured **(B)**. Three measurements, each consisting of 15-20 seedlings, were statistically analyzed using one-sided Student *t*-test (**P* = 0.004, difference from Col-0). **(C)** Transcription of *RECQ2* gene. Seven-day-old seedlings grown on MS-agar plates at 23°C were exposed to 37°C for 1 d. Whole seedlings were used for total RNA preparation. Transcript levels were analyzed by RT-qPCR. Biological triplicates, each consisting of 15 seedlings, were statistically analyzed (one-sided *t*-test, **P* = 0.0002, difference from 23°C). In **B** and **C**, the upper side of each box plot indicates median. Error bars indicate SE. The circles indicate individual data points.

to what observed in the *HSP90*-RNAi plants (Fig. 63). Accordingly, DNA breaks were significantly elevated in the *hsfa1* QK mutant (Fig. 67), showing that the HSFA1-HSP90 module mediates the stabilization of HOS1 in the acquisition of thermotolerance. However, I did not detect any direct interactions between HSP90 and HOS1 in yeast cells and bimolecular fluorescence complementation assays (Fig. 68), raising a possibility that additional chaperone(s) or cochaperone(s) would be required for the HOS1 thermostabilization.

A critical issue regarding the thermoregulatory role of HOS1 is whether it regulates additional DNA repair genes other than *RECQ2* in maintaining genomic integrity. ULTRAVIOLET HYPERSENSITIVE 6 (UVH6) is a DNA repair helicase, and UVH6-deficient mutants are hypersensitive to UV and heat stress (Liu et al., 2003). While the *UVH6* gene was not identified as a differentially expressed gene in my RNA sequencing analysis, possibly because of technical limits in the identification process, I examined its potential involvement in the HOS1-mediated thermotolerance. The *UVH6* transcription was elevated by more than 4-fold at high temperatures, but its thermal induction largely disappeared in the *hos1-3* mutant. In addition, thermotolerance was significantly reduced in the UVH6-deficient mutant (Fig. 69). It is therefore envisaged that HOS1 mediates the thermal regulation of multiple DNA repair genes during thermotolerance.

DNA damages include various chemical alterations that disrupt genomic integrity in plants (Britt et al., 2004). Here, I demonstrate that HOS1 functions as a transcriptional coregulator of DNA repair genes during the establishment of thermotolerance, directly linking DNA repair to thermotolerance (Fig. 70).

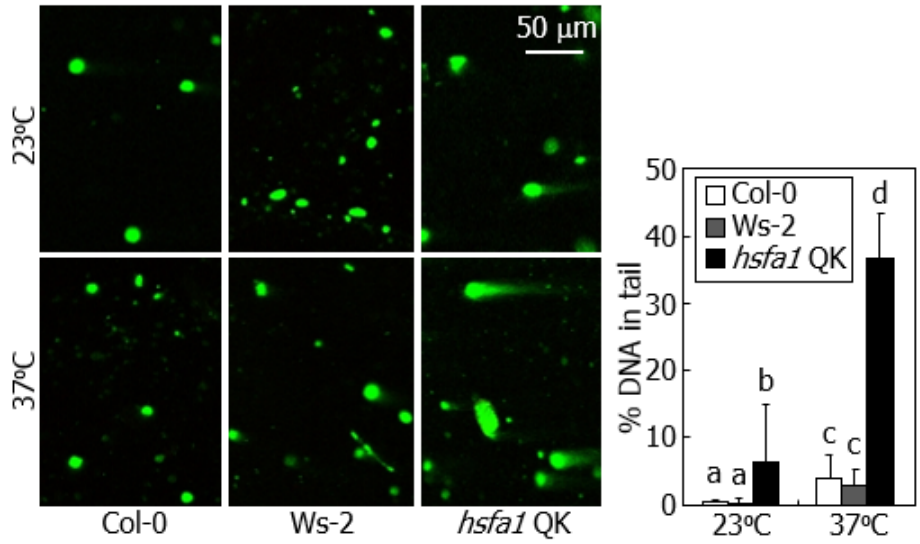

Figure 67. Comet assays on heat-treated *hsfa1* QK mutant

The *hsfa1* QK seedlings were heat-treated for 6 h. The tail ratio of total fluorescence intensity in comet-shaped DNA spots was quantitated using the caslab program. DNA spots of 8-12 were statistically analyzed. Error bars indicate SD. Different letters represent significant differences ($P < 0.01$) determined by one-way ANOVA with *post hoc* Tukey test.

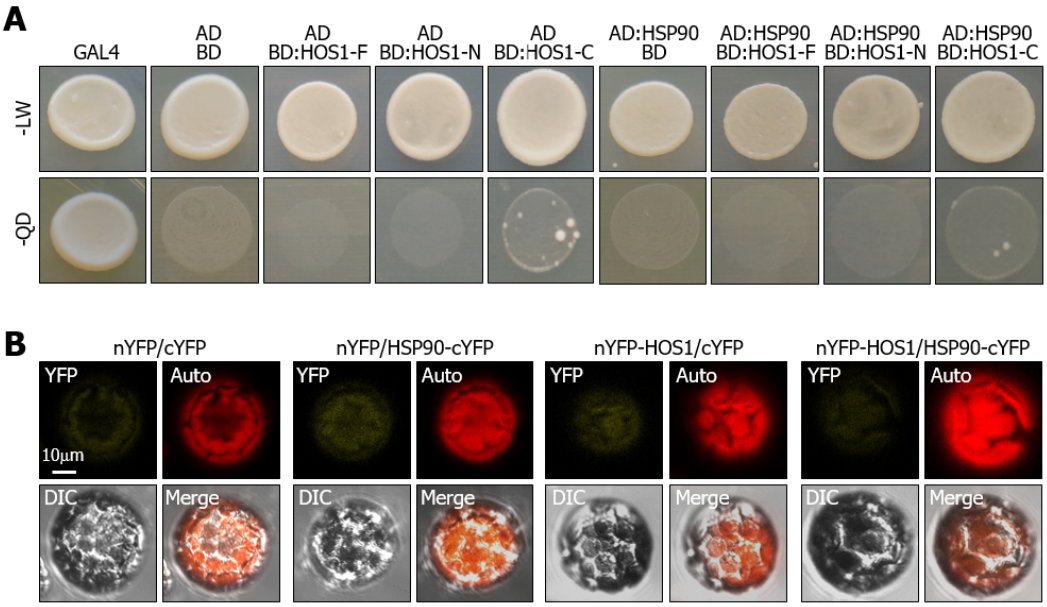

Figure 68. HOS1 does not interact physically with HSP90

(A) HOS1-HSP90 interactions in yeast cells. Potential interactions between HOS1 and HSP90 proteins were examined by yeast two-hybrid analysis. -LW denotes Leu and Trp dropout plates, and -QD denotes Leu, Trp, His, and Ade dropout plates. AD and BD, activation and DNA-binding domains, respectively. HOS1-F, -N, and -C constructs include residues 1-927, 1-457, and 457-927, respectively. **(B)** Bimolecular fluorescence complementation (BiFC). The HOS1-HSP90 interactions were examined in *Arabidopsis* protoplasts. The YFPN-HOS1 and HSP90-YFPC constructs were coexpressed transiently in *Arabidopsis* protoplasts and visualized by differential interference contrast (DIC) and fluorescence microscopy.

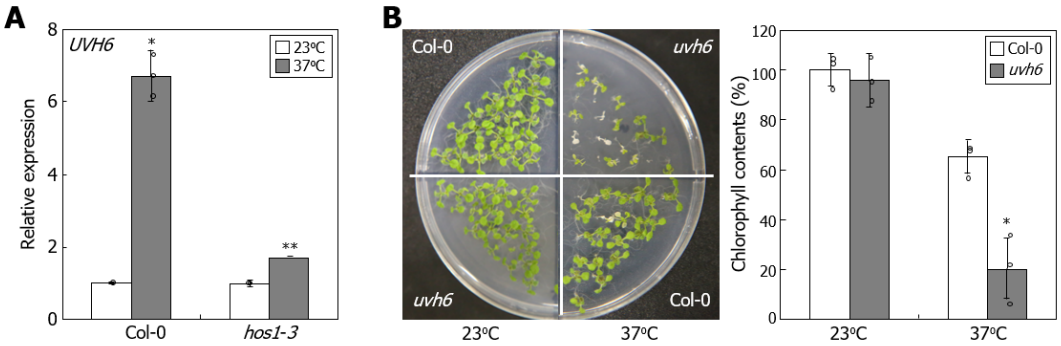

Figure 69. Thermotolerance phenotypes of *uvh6* mutant

(A) Transcription of *ULTRAVIOLET HYPERSENSITIVE 6* (*UVH6*) gene in *hos1-3* mutant at high temperatures. Seven-day-old seedlings grown on MS-agar plates at 23°C were exposed to 37°C for 1.5 d. Total RNA samples were extracted from whole seedlings. Transcript levels were analyzed by RT-qPCR. Biological triplicates, each consisting of 15 seedlings, were statistically analyzed using one-sided Student *t*-test (**P* = 0.0019, ***P* = 0.0017, difference from 23°C). The upper side of each box plot indicates median. Error bars indicate SE. The circles indicate individual data points. **(B)** Thermotolerance phenotypes of *uvh6* mutant. Seven-day-old UVH6-deficient *uvh6* mutant grown on MS-agar plates at 23°C were exposed to 37°C for 1.5 d and then allowed to recover at 23°C for 5 d under constant light conditions (left photographs). Chlorophyll contents were measured (right graph). Biological triplicates, each consisting of 10 seedlings, were statistically analyzed (one-sided *t*-test, **P* = 0.002, difference from Col-0). The upper side of each box plot indicates median. Error bars indicate SE. The circles indicate individual data points.

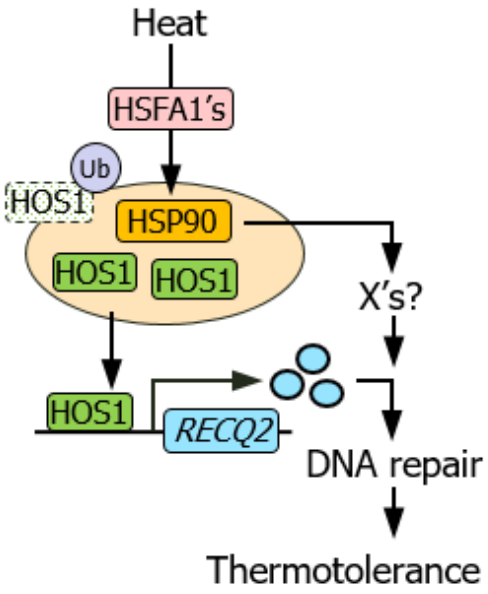

Figure 70. Acquisition of thermotolerance via the HOS1-mediated activation of DNA repair response

HOS1 is stabilized via the HSP90 chaperone cycle at high temperatures, and the thermostabilized HOS1 activates the RECQ2 DNA helicase, thus leading to the establishment of thermotolerance. It seems that additional regulators (X's) other than HOS1 are also involved in the RECQ2-mediated DNA repair response.

However, HOS1 is not related with acquired thermotolerance, which often depends on heat stress memory mostly through chromatin modifications (Yu et al., 2018). This view is supported by the lack of discernible histone modifications in *RECQ2* chromatin at high temperatures (Fig. 43, 44). My data also explain why RECQ2 have not been functionally defined by mutant analysis at normal temperatures (Rohrig et al., 2018).

DISCUSSION

DNA damage is common event to plants which were exposed to various stress conditions. Indeed, a number of abiotic stresses were caused to DNA damage of plants. The most well-known example is UV-B light which directly triggers DNA damage by including the formation of DNA strand break and disturbs transcription or DNA replications (Britt et al., 2004). In addition, heat is also abiotic stress and can affect DNA stability by inducing DNA break (Kantidze et al., 2016). Plants possess various DNA repair pathways to maintain DNA integrity (Manova and Gruszka, 2015; Hu et al., 2016). In this study, I demonstrated that HOS1-RECQ2 module contributes to unique DNA repair pathway, which induces thermotolerance of plants.

HOS1 is critical regulator in *Arabidopsis* as proteolytic and nonproteolytic regulator. The E3 ubiquitin ligase HOS1 acts as a cold signaling attenuator by degrading INDUCER OF CBF EXPRESSION 1 (ICE1) transcription factor and functions as regulator of photoperiodic flowering by degrading CONSTANTS (CO) transcription factor (Lee et al., 2001; Lazaro et al., 2012). Recent reports demonstrate that HOS1 can also act as nonproteolytic regulator, a chromatin remodeling factor, which modulates FLOWERING LOCUSC (FLC) chromatin in cold regulation of flowering time (Jung et al., 2013). Here, I present unique function of HOS1 as nonproteolytic regulator. HOS1 thermally up-regulates *RECQ2* transcript levels by using transcription activity of HOS1. It is supported that HOS1 is remarkable multi-functional regulator in plants.

HSPs are a family of proteins that are induced by heat. HSPs were known as molecular chaperones and possess various functions in organisms. It have been reported that HSPs work as components of the proteolytic systems by unwinding misfolded and irreversibly aggregated proteins (Ellis et al., 1989). Inaddition, other HSPs function as metabolic enzymes, regulatory proteins like transcription factors or kinases and component of sustaining cellular structure (Malmendal et al., 2006). My observations imply that HSP90 is required to stabilize the HOS1 protein under heat conditions. It is evident that HSPs are important regulator in heat-induced DNA repair pathway.

Recent studies show that HOS1 also acts as a chromatin modifier and a component of nuclear pore complexes (Jung et al., 2013; Cheng et al., 2020). It is possible that HOS1 mediates the epigenetic control of DNA repair genes and/or the nucleo-cytoplasmic transport of their mRNAs and proteins. It is notable that the widely conserved HSP90 thermostabilizes HOS1 during thermotolerance. It is known that the functions of HSPs are not confined to molecular chaperone activities; they also act as constituents of metabolic enzymes and regulatory proteins during various developmental and adaptive processes (Ellis et al., 1989). My findings would further broaden our understanding of HSP-mediated stress adaptation in plants.

ACKNOWLEDGEMENT

I thank Dr. Yee-Yung Charng for providing the *hsfa1 QK* mutant seeds and David Somers for providing the *HSP90*-RNAi plants and the ABRC for *Arabidopsis* plant materials. The *RECQ2* cDNA was kindly provided by Dr. Holger Puchta (Karlsruhe Institute of Technology, Germany). I thank Ju-Heon Kim for subcloning the *RECQ2* gene and Dr. Sangrea Shim for statistical analysis.

REFERENCES

Borges, H.L., Linden, R., and Wang, J.Y.J. (2008). DNA damage-induced cell death. Cell Res. 18:17–26.

Boulon, S., Westman, B.J., Hutten, S., Boisvert, F.M., and Lamond, A.I. (2010). The nucleolus under stress. Mol. Cell 40:216–227.

Britt, A. Repair of DNA damage induced by solar UV. (2004). Photosynth. Res. 81:105–112.

Casal, J.J., Candia, A.N., and Sellaro, R. (2014). Light perception and signalling by phytochrome A. J. Exp. Bot. 65:2835-2845.

Caverzan, A., Passaia, G., Rosa, S.B., Ribeiro, C.W., Lazzarotto, F., and Margis-Pinheiro, M. (2012). Plant responses to stresses: Role of ascorbate peroxidase in the antioxidant protection. Genet. Mol. Biol. 35:1011-1019.

Cheng, Z., Zhang, X., Huang, P., Huang, G., Zhu, J., Chen, F., Miao, Y., Liu, L., Fu, Y.F., and Wang, X. (2020). Nup96 and HOS1 are mutually stabilized and gate CONSTANS protein level, conferring long-day photoperiodic flowering regulation in *Arabidopsis*. Plant Cell 32:374–391.

Cho, J.N., Ryu, J.Y., Jeong, Y.M., Park, J., Song, J.J., Amasino, R.M., Noh, B.S., and Noh, Y.S. (2012). Control of seed germination by light-induced histone

arginine demethylation activity. Dev. Cell 22:736-748.

Crawford, A.J., McLachlan, D.H., Hetherington, A.M., and Franklin, K.A. (2012). High temperature exposure increases plant cooling capacity. Curr. Biol. 22:R396–R397.

Dickinson, P.J., Kumar, M., Martinho, C., Yoo, S.J., Lan, H., Artavanis, G., Charoensawan, V., Schottler, M.A., Bock, R., Jaeger, K.E. et al. (2018). Chloroplast signaling gates thermotolerance in *Arabidopsis*. Cell Rep. 22:1657-1665.

Dong, C.H., Agarwal, M., Zhang, Y., Xie, Q., and Zhu, J.K. (2006). The negative regulator of plant cold responses, HOS1, is a RING E3 ligase that mediates the ubiquitination and degradation of ICE1. Proc. Natl. Acad. Sci. U S A 103:8281–8286.

Earley, K.W., Haag, J.R., Pontes, O., Opper, K., Juehne, T., Song, K., and Pikaard, C.S. (2006). Gateway-compatible vectors for plant functional genomics and proteomics. Plant J. 45:616–629.

Ellis, R.J., van der Vies, S.M., and Hemmingsen, S.M. (1989). The molecular chaperone concept. Biochem. Soc. Symp. 55:145–153.

Finka, A., and Goloubinoff, P. (2013). Proteomic data from human cell cultures refine mechanisms of chaperone-mediated protein homeostasis. Cell Stress Chaperon. 18:591–605.

Fujii, Y., Tanaka, H., Konno, N., Ogasawara, Y., Hamashima, N., Tamura, S.,

Hasegawa, S., Hayasaki, Y., Okajima, K., and Kodama, Y. (2017). Phototropin perceives temperature based on the lifetime of its photoactivated state. Proc. Natl. Acad. Sci. U S A 114:9206-9211.

Griebel, T., and Zeier, J. (2008). Light regulation and daytime dependency of inducible plant defenses in *Arabidopsis*: phytochrome signaling controls systemic acquired resistance rather than local defense. Plant Physiol. 147:790-801.

Guo, L., Chen, S., Liu, K., Liu, Y., Ni, L., and Zhang, K. (2008). Isolation of heat shock factor HsfA1a-binding sites in vivo revealed variations of heat shock elements in *Arabidopsis thaliana*. Plant Cell Physiol. 49:1306-1315.

Hayes, S., Sharma, A., Fraser, D.P., Trevisan, M., Cragg-Barber, C.K., Tavridou, E., Fankhauser, C., Jenkins, G.I., and Franklin, K.A. (2017). UV-B perceived by the UVR8 photoreceptor inhibits plant thermomorphogenesis. Curr. Biol. 27:120-127.

Hartung, F., Plchová, H., and Puchta, H. (2000). Molecular characterisation of RecQ homologues in *Arabidopsis thaliana*. Nucleic Acids Res. 28:4275–4282.

Hu, Z., Cools, T., and De, V. L. (2016). Mechanisms used by plants to cope with DNA damage. Annu. Rev. Plant Biol. 29:439-462.

Iwasaki, M., and Paszkowski, J. (2014). Epigenetic memory in plants. EMBO J. 33:1987-1998.

Jantschitsch, C., and Trautinger, F. (2003). Heat shock and UV-B-induced DNA damage and mutagenesis in skin. Photochem. Photobiol. Sci. 2:899–903.

Jung, J.H., Park, J.H., Lee, S.M., To, T.K., Kim, J.M., Seki, M., and Park, C.M. (2013). The cold signaling attenuator HIGH EXPRESSION OF OSMOTICALLY RESPONSIVE GENE1 activates *FLOWERING LOCUS C* transcription via chromatin remodeling under short-term cold stress in *Arabidopsis*. Plant Cell 25:4378–4390.

Jung, J.H., Domijan, M., Klose, C., Biswas, S., Ezer, D., Gao, M., Khattak, A.K., Box, M., Charoensawan, V., Cortijo, S. et al. (2016). Phytochromes function as thermosensors in *Arabidopsis*. Science 354:886-889.

Kantidze, O.L., Velichko, A.K., Luzhin, A.V., and Razin, S.V. (2016). Heat stress-induced DNA damage. Acta Naturae 8:75–78.

Karyotou, K., and Donaldson, R.P. (2005). Ascorbate peroxidase, a scavenger of hydrogen peroxide in glyoxysomal membranes. Arch. Biochem. Biophys. 434:248-257.

Kim, D.H. and Sung, S. (2013). Coordination of the vernalization response through a VIN3 and FLC gene family regulatory network in *Arabidopsis*. Plant Cell 25:454-469.

Kim, D.H., Yamaguchi, S., Lim, S., Oh, E., Park, J., Hanada, A., Kamiya, Y., and Choi, G. (2008). SOMNUS, a CCCH-type zinc finger protein in *Arabidopsis*, negatively regulates light-dependent seed germination downstream of PIL5. Plant Cell 20:1260-1277.

Kim, J.H., Lee, H.J., Jung, J.H., Lee, S., and Park, C.M. (2017). HOS1 facilitates

the phytochrome B-mediated inhibition of PIF4 function during hypocotyl growth in *Arabidopsis*. Mol. Plant 13:274–284.

Kobbe, D., Blanck, S., Demand, K., Focke, M., and Puchta, H. (2008). AtRECQ2, a RecQ helicase homologue from *Arabidopsis thaliana*, is able to disrupt various recombinogenic DNA structures *in vitro*. Plant J. 55:397–405.

Koch, E., and Slusarenko, A. (1990). *Arabidopsis* is susceptible to infection by a downy mildew fungus. Plant Cell 2:437–445.

Lämke, J., Brzezinka, K., Altmann, S., and Bäurle, I. (2016). A hit-and-run heat shock factor governs sustained histone methylation and transcriptional stress memory. EMBO J. 35:162-175.

Larkindale, J., Hall, J.D., Knight, M.R. and Vierling, E. (2005). Heat stress phenotypes of *Arabidopsis* mutants implicate multiple signaling pathways in the acquisition of thermotolerance. Plant Physiol. 138:882-897.

Lau, O.S. and Deng, X.W. (2012). The photomorphogenic repressors COP1 and DET1: 20 years later. Trends Plant Sci. 17:584-593.

Lazaro, A., Valverde, F., Pineiro, M., and Jarillo, J.A. (2012). The *Arabidopsis* E3 ubiquitin ligase HOS1 negatively regulates CONSTANS abundance in the photoperiodic control of flowering. Plant Cell 24:982–999.

Lee, C.M., and Thomashow, M.F. (2012). Photoperiodic regulation of the C-repeat binding factor (CBF) cold acclimation pathway and freezing tolerance in *Arabidopsis thaliana*. Proc. Natl. Acad. Sci. U S A 109:15054-15059.

Lee, D.H., and Goldberg, A.L. (1998). Proteasome inhibitors: valuable new tools for cell biologists. Trends Cell Biol. 8:397–403.

Lee, H., Gong, L.X., Ishitani, M., Stevenson, B., and Zhu, J.K. (2001). The *Arabidopsis HOS1* gene negatively regulates cold signal transduction and encodes a RING finger protein that displays cold-regulated nucleo-cytoplasmic partitioning. Genes Dev. 15:912–924.

Lee, H.J., Jung, J.H., Llorca, L.C., Kim, S.G., Lee, S.M., Baldwin, I.T., and Park, C.M. (2014). FCA mediates thermal adaptation of stem growth by attenuating auxin action in *Arabidopsis*. Nat. Commun. 5:5473.

Lee, H.J., Park, Y.J., Ha, J.H., Baldwin, I.T., and Park, C.M. (2017). Multiple routes of light signaling during root photomorphogenesis. Trends Plant Sci. 22:803-812.

Lee, S., Lee, H.J., Jung, J.H., and Park, C.M. (2015). The *Arabidopsis thaliana* RNA-binding protein FCA regulates thermotolerance by modulating the detoxification of reactive oxygen species. New Phytol. 205:555-569.

Lee, S., Seo, P.J., Lee, H.J., and Park, C.M. (2012). A NAC transcription factor NTL4 promotes reactive oxygen species production during drought-induced leaf senescence in *Arabidopsis*. Plant J. 70:831–844.

Legris, M., Klose, C., Burgie, E.S., Rojas, C.C., Neme, M., Hiltbrunner, A., Wiggie, P.A., Schafer, E., Vierstra, R.D., and Casal, J.J. (2016). Phytochrome B integrates light and temperature signals in *Arabidopsis*. Science 354:897-900.

Liu, H.C., Liao, H.T., and Charng, Y.Y. (2011). The role of class A1 heat shock factors (HSFA1s) in response to heat and other stresses in *Arabidopsis*. Plant Cell Environ. 34:738-751.

Liu, Z., Hong, S.W., Escobar, M., Vierling, E., Mitcell, D.L., Mount, D.W., and Hall, J.D. (2003). *Arabidopsis* UVH6, a homolog of human XPD and yeast RAD3 DNA repair genes, functions in DNA repair and is essential for plant growth. Plant Physiol. 132:1405–1414.

Ma, D., Li, X., Guo, Y., Chu, J., Fang, S., Yan, C., Noel, J.P., and Liu, H. (2016). Cryptochrome 1 interacts with PIF4 to regulate high temperature-mediated hypocotyl elongation in response to blue light. Proc. Natl. Acad. Sci. U S A 113:224-229.

MacGregor, D. R., and Penfield, S. (2015). Exploring the pleiotropy of *hos1*. J. Exp. Bot. 66:1661–1671.

Manova, V., and Gruszka, D. (2015) DNA damage and repair in plants from models to crops. Front. Plant Sci. 23:885.

Martín, G., Leivar, P., Ludevid, D., Tepperman, J.M., Quail, P.H., and Monte, E. (2016). Phytochrome and retrograde signalling pathways converge to antagonistically regulate a light-induced transcriptional network. Nat. Commun. 7:11431.

Mauch-Mani, B., Baccelli, I., Luna, E., and Flors, V. (2017). Defense priming: an adaptive part of induced resistance. Annu. Rev. Plant Biol. 68:485-512.

Menke, M., Chen, I., Angelis, K.J., and Schubert, I. (2001). DNA damage and repair in *Arabidopsis thaliana* as measured by the comet assay after treatment with different classes of genotoxins. Mutat. Res. 27:87–93.

Mittler, R., Vanderauwera, S., Gollery, M., and Van, B.F. (2004). Reactive oxygen gene network of plants. Trends Plant Sci. 9:490–498.

Morimoto, K., Ohama, N., Kidokoro, S., Mizoi, J., Takahashi, F., Todaka, D., Mogami, J., Sato, H., Qin, F., Kim, J.S. et al. (2017). BPM-CUL3 E3 ligase modulates thermotolerance by facilitating negative regulatory domain-mediated degradation of DREB2A in *Arabidopsis*. Proc. Natl. Acad. Sci. U S A 114:E8528-8536.

Mubarakshina, M.M., Ivanov, B.N., Naydov, L.A., Hillier, W., Badger, M.R. and Krieger-Liszkay, A. (2010). Production and diffusion of chloroplastic H_2O_2 and its implication to signaling. J. Exp. Bot. 61:3577-3587.

Noctor, G., and Foyer, C.H. (2016). Intracellular redox compartmentation and ROS-related communication in regulation and signaling. Plant Physiol. 171: 1581-1592.

Ochel, H.J., Eichhorn, K., and Gademann, G. (2011). Geldanamycin: the prototype of a class of antitumor drugs targeting the heat shock protein 90 family of molecular chaperones. Cell Stress Chaperon. 6:105–112.

Panchuk, I.I., Volkov, R.A., and Schöffl, F. (2002). Heat stress- and heat shock transcription factor-dependent expression and activity of ascorbate peroxidase

in *Arabidopsis*. Plant Physiol. 129:838-853.

Panchuk, I.I., Zentgraf, U., and Volkov, R.A. (2005). Expression of the Apx gene family during leaf senescence of *Arabidopsis thaliana*. Planta 222:926–932.

Park, Y.J., Lee, H.J., Ha, J.H., Kim, J.Y., and Park, C.M. (2017). COP1 conveys warm temperature information to hypocotyl thermomorphogenesis. New Phytol. 215:269-280.

Park, Y.J., and Park, C.M. (2018). External coincidence model for hypocotyl thermomorphogenesis. Plant Signal Behav. 13:e1327498.

Perez, D.E., Hoyer, J.S., Johnson, A.I., Moody, Z.R., Lopez, J., and Kaplinsky, N.J. (2009). BOBBER1 is a noncanonical *Arabidopsis* small heat shock protein required for both development and thermotolerance. Plant Physiol. 151:241-252.

Queitsch, C., Hong, S.W., Vierling, E., and Lindquist, S. (2000). Heat shock protein 101 plays a crucial role in thermotolerance in *Arabidopsis*. Plant Cell 12:479-492.

Quint, M., Delker, C., Franklin, K.A., Wigge, P.A., Halliday, K.J., and van, Zanten, M. (2016). Molecular and genetic control of plant thermomorphogenesis. Nat. Plants 2:15190.

Ramírez, L., Bartoli, C.G., and Lamattina, L. (2013). Glutathione and ascorbic acid protect *Arabidopsis* plants against detrimental effects of iron deficiency. J. Exp. Bot. 64:3169-3178.

Röhrig, S., Dorn, A., Enderle, J., Schindele, A., Herrmann, N.J., Knoll, A., and

Puchta, H. (2018). The RecQ-like helicase HRQ1 is involved in DNA crosslink repair in *Arabidopsis* in a common pathway with the Fanconi anemia-associated nuclease FAN1 and the postreplicative repair ATPase RAD5A. New Phytol. 218:1478–1490.

Schaffer, R., Landgraf, J., Accerbi, M., Simon, V., Larson, M., and Wisman, E. (2001). Microarray analysis of diurnal and circadian-regulated genes in *Arabidopsis*. Plant Cell 13:113-123.

Seo, P.J., Kim, M.J., Ryu, J.Y., Jeong, E.Y., and Park, C.M. (2011). Two splice variants of the IDD14 transcription factor competitively form nonfunctional heterodimers which may regulate starch metabolism. Nat. Commun. 2:303.

Seo, P.J., Kim, M.J., Park, J.Y., Kim, S.Y., Jeon, J., Lee, Y.H., Kim, J., and Park, C.M. (2010). Cold activation of a plasma membrane-tethered NAC transcription factor induces a pathogen resistance response in *Arabidopsis*. Plant J. 61:661–671.

Sharma, S.V., Agatsuma, T., and Nakano, H. (1998). Targeting of the protein chaperone, HSP90, by the transformation suppressing agent, radicicol. Oncogene 16:2639–2645.

Sherameti, I., Sopory, S.K., Trebicka, A., Pfannschmidt, T., and Oelmuller, R. (2002). Photosynthetic electron transport determines nitrate reductase gene expression and activity in higher plants. J. Biol. Chem. 277:46594-46600.

Su, P.H., and Li, H.M. (2008). *Arabidopsis* stromal 70-kD heat shock proteins

are essential for plant development and important for thermotolerance of germinating seeds. Plant Physiol. 146:1231-1241.

Swindell, W.R., Huebner, M., and Weber, A.P. (2007). Transcriptional profiling of *Arabidopsis* heat shock proteins and transcription factors reveals extensive overlap between heat and non-heat stress response pathways. BMC Genomics 8:125.

Tessadori, F., van, Zanten, M., Pavlova, P., Clifton, R., Pontvianne, F., Snoek, L.B., Millenaar, F.F., Schulkes, R.K., Driel, R.V., Voesenek, L.A. et al. (2009). Phytochrome B and histone deacetylase 6 control light-induced chromatin compaction in *Arabidopsis thaliana*. PLoS Genet. 5:e1000638.

Toivola, D.M., Strnad, P., Habtezion, A., and Omary, M.B. (2010). Intermediate filaments take the heat as stress proteins. Trends Cell Biol. 20:79–91.

Udvardi, M.K., Czechowski, T., and Scheible, W.R. (2008). Eleven golden rules of quantitative RT-PCR. Plant Cell 20:1736-1737.

Verma, S., and Dubey, R.S. (2003). Lead toxicity induces lipid peroxidation and alters the activities of antioxidant enzymes in growing rice plants. Plant Sci. 164:645-655.

Wahid, A., Gelani, S., Ashraf, M., and Foolad, M.R. (2007). Heat tolerance in plants: An overview. Environ. Exp. Bot. 61:199–223.

Wang, B., Duan, C.G., Wang, X., Hou, Y.J., Yan, J., Gao, C., Kim, J.H., Zhang, H., and Zhu, J.K. (2015). HOS1 regulates Argonaute1 by promoting transcription

of the microRNA gene *MIR168b* in *Arabidopsis*. Plant J. 81:861–870.

Wang, F.F., Lian, H.L., Kang, C.Y., and Yang, H.Q. (2010). Phytochrome B is involved in mediating red light-induced stomatal opening in *Arabidopsis thaliana*. Mol. Plant 3:246-259.

Wanner, L.A., and Junttila, O. (1999). Cold-induced freezing tolerance in *Arabidopsis*. Plant Physiol. 120:391–400.

Welch, W.J., and Suhan, J.P. (1986). Cellular and biochemical events in mammalian cells during and after recovery from physiological stress. J. Cell Biol. 103:2035–2052.

Xu, X., Paik, I., Zhu, L., and Huq, E. (2015). Illuminating progress in phytochrome-mediated light Signaling pathways. Trends Plant Sci. 20:641-650.

You, J., and Chan, Z. (2015). ROS Regulation during abiotic stress responses in crop plants. Front. Plant Sci. 6:1092.

Yu, L., Serrano, N., Gao, G., Atia, M., Mokhtar, M., Woo, Y.H., Bazin, J., Veluchamy, A., Benhamed, M., Crespi, M. et al. (2018). Thermopriming triggers splicing memory in *Arabidopsis*. J. Exp. Bot. 69:2659–2675.

Zhao, C., Liu, B., Piao, S., Wang, X., Lobell, D.B., Huang, Y., Huang, M., Yao, Y., Bassu, S., Ciais, P. et al. (2017). Temperature increase reduces global yields of major crops in four independent estimates. Proc. Natl. Acad. Sci. U S A 114:9326-9331.

Zhao, X., Wang, Y.L., Qiao, X.R., Wang, J., Wang, L.D., Xu, C.S., and Zhang, X. (2013). Phototropins function in high-intensity blue light-induced hypocotyl phototropism in *Arabidopsis* by altering cytosolic calcium. Plant Physiol. 162:1539-1551.

Zhang, Y., Mayba, O., Pfeiffer, A., Shi, H., Tepperman, JM., Speed, T.P., and Quail, P.H. (2013). A quartet of PIF bHLH factors provides a transcriptionally centered signaling hub that regulates seedling morphogenesis through differential expression-patterning of shared target genes in *Arabidopsis*. PLOS Genet. 9:e1003244.

Zhao, J., Missihoun, T.D., and Bartels, D. (2017). The role of *Arabidopsis* aldehyde dehydrogenase genes in response to high temperature and stress combinations. J. Exp. Bot. 68:4295-4308.

Zhong, S., Zhao, M., Shi, T., Shi, H., An, F., Zhao, Q., and Guo, H. (2009). EIN3/EIL1 cooperate with PIF1 to prevent photo-oxidation and to promote greening of *Arabidopsis* seedlings. Proc. Natl. Acad. Sci. U S A 106:21431-21436.

Zhu, J.Y., Oh, E., Wang, T., and Wang, Z.Y. (2016). TOC1-PIF4 interaction mediates the circadian gating of thermoresponsive growth in *Arabidopsis*. Nat. Commun. 7:13692.

ABSTRACT IN KOREAN (국문 초록)

자연적으로 식물은 불리한 조건에 지속적으로 노출된다. 열은 식물의 성장과 발달에 영향을 미치는 주요 스트레스 중 하나이다. 특히 최근 수십 년 동안 지구 온난화가 가속화되고 작물 생산성에 크게 영향을 미친다는 연구가 널리 보고되었다. 이러한 의미에서 고온 저항성의 분자 메커니즘에 대한 이해를 넓히는 것이 필수적이다.

고온 스트레스는 단백질 비접힘와 비특이적 응집에 의해 세포에 해로운 영향을 미친다. 또한 고온 스트레스는 세포 골격의 파괴를 통해 세포 기관 위치 조정 방해와 세포 내 수송 과정의 붕괴를 유발한다. 식물에서 고온 스트레스로 인한 산화 스트레스의 해로운 영향 중 하나는 DNA 손상 유도와 DNA 복구 활동의 억제로 인한 유전적 장애이다.

따라서 식물은 고온 스트레스로 인한 세포 손상에 대처할 수 있는 다양한 메커니즘을 가지고 있다. 고온 스트레스에 의해 식물에서 고온 반응 유전자의 전사 수준이 증가한다고 이전에 보고 된 바 있다. 열충격 단백질 (HSP) 및 열충격 전사인자 (HSF)는 단백질 항상성을 제어하여 식물의 고온 스트레스 조절 시스템의 주요 구성 요소이다. 2차 대사 산물은 활성산소 (ROS) 제거 효소를 활성화 또는 안정화시키고 ROS 생성을 억제한다. 이 연구에서 나는 고온 저항성이 빛의 전처리에 의해 어떻게 영향을 받는지, 식물의 DNA 온정성이 식물의 고온 저항성에 얼마나 중요한지 연구하였다.

제 1 장에서는 고온 스트레스가 오기 전 빛의 존재 유무에 따라 식물의 고온 저항성에 끼치는 영향에 대해서 연구하였다. 활성산소는 환경 자극에 대한 식물 적응 반응에서 중요한 신호 매개체 역할을 한다. 한편, 활성산소

생합성과 신진 대사는 종종 DNA 및 단백질과 같은 생물학적 분자 및 세포 구조에 산화 손상을 가하기 때문에 정확하게 조절되어야한다. 고온에서 활성산소는 식물 조직에 빠르게 축적되는 것으로 알려져 있다. 따라서 고온에 적응하기 위해 활성산소를 제거하는 시스템의 빠른 활성화가 필요하다. 그러나 고온에 의해 발생하는 활성산소를 제거하는 메커니즘이 외부의 환경 요인에 의해 어떻게 작동되는지는 거의 알려지지 않았다. 본 연구에서, 나는 외부 환경요소인 빛이 애기 장대의 고온 저항성을 위해 고온에 의해 발생한 활성산소를 제거하는 과정을 미리 대비한다는 것을 보여주었다. 활성산소를 제거하는 능력은 고온 스트레스가 오기 전 빛을 미리 처리 한 식물에서 현저하게 향상되었지만, 빛을 미리 처리하지 않고 암전시킨 식물에서는 그 향상이 분명하지 않았다. ASCORBATE PEROXIDASE 2 (APX2)는 열 스트레스 조건에서 활성화되는 대표적인 활성산소 제거 효소이다. APX2 유전자의 발현은 어두운 전처리 식물보다 빛을 전처리 한 식물에서 더 두드러지게 증가한 것으로 관찰되었다. 특히, 빛의 전처리로 인한 APX2 유전자 발현의 증가는 적색광 광 수용체 피토크롬 B (phyB)가 망가진 돌연변이 식물에서 감소해있었다. 더욱이, 항산화제인 아스코르베이트를 처리를 했을 때, phyB 돌연변이체는 열에 민감한 표현형을 회복시켰다. 이러한 관찰은 빛의 전처리로 인한 활성산소 제거 능력이 고온 저항성의 증가와 밀접한 관련이 있음을 나타낸다. 나는 활성산소 제거를 위한 피토크롬 B를 통한 빛의 전처리 과정이 식물의 고온 저항성의 핵심 구성 요소라고 제안한다.

제 2 장에서는 식물의 DNA 온정성이 식물의 고온 저항성에 어떤 영향을 미치는지 알아보았다. 고온 스트레스는 식물의 세포수준에서 단백질의 접힘을 방해하거나 세포의 세포벽이나 세포외골격을 붕괴시킨다. 뿐만 아니라

뉴클레오타이드 변형이나 DNA 가닥을 파손시켜 DNA 온전성을 감소시킨다. 하지만 이러한 DNA 온전성이 식물의 고온저항성에 어떻게 영향을 끼치는지 전혀 알려져 있지 않다. 본 연구에서는 HIGH EXPRESSION OF OSMOTICALLY RESPONSE GENES 1 (HOS1) 단백질에 의해서 고온에 의해 감소한 DNA 온전성을 수선하는 메커니즘을 활성화 시켜 식물의 고온저항성을 증가시킨다는 것을 증명하였다. HOS1 단백질은 표적 단백질을 분해하거나 크로마틴을 리모델링 하여, 식물의 저온 저항성 조절, 개화시기 조절, 일주기 조절 등을 하는 조절 단백질로 알려져 있다. 본 연구에서는 HOS1이 망가진 식물의 고온 저항성이 야생형 식물보다 현저하게 감소해 있는 것을 관찰했다. 이 표현형을 바탕으로 고온에서 HOS1이 DNA 수선과 관련된 유전자들을 조절 하는 것을 확인했다. 그 중에서도 DNA의 이중가닥을 풀어주는 RECQ2 헬리케이즈 효소가 망가진 돌연변이 식물에서 고온 저항성이 감소해 있는 것을 관찰했다. 뿐만 아니라 HOS1이 망가진 돌연변이 식물과 RECQ2가 망가진 돌연변이 식물에서 고온에 의해서 DNA가 망가진 것을 확인했다. 이를 통해서 고온에서 HOS1 단백질이 RECQ2의 발현을 증가시켜 망가진 DNA 수선을 하여 식물의 고온 저항성을 증가시킨다는 것을 알 수 있다. 추가적으로 고온에 의해서 HOS1 단백질의 안정성이 증가하며, HEAT SHOCK FACTOR A1 (HSFA1)-HEAT SHOCK PROTEIN90 (HSP90) 모듈이 HOS1 단백질의 안정성 증가에 필요하다는 것을 증명하였다. 나는 본 연구를 통해서 식물의 고온 저항성을 조절 하는 새로운 메커니즘을 제안하며, 식물의 DNA의 온전성을 유지하는 것이 식물의 고온 저항성에 얼마나 중요한지 주장한다.

주요어: 고온 스트레스, 활성산소, APX2, 프라이밍 효과, phytochrome B, 고온

저항성, HOS1, RECQ2, DNA 온전성, DNA 수선, HSFA1, HSP90

학번: 2016-23460